

# Exact $SO(8)$ Symmetry in the Weakly-Interacting Two-Leg Ladder

Hsiu-Hau Lin<sup>1</sup>, Leon Balents<sup>2</sup> and Matthew P. A. Fisher<sup>2</sup>

<sup>1</sup> *Department of Physics, University of California, Santa Barbara, CA 93106-9530*

<sup>2</sup> *Institute for Theoretical Physics, University of California, Santa Barbara, CA 93106-4030*  
(October 17, 2018)

We revisit the problem of interacting electrons hopping on a two-leg ladder. A perturbative renormalization group analysis reveals that at half-filling the model scales onto an exactly soluble Gross-Neveu model for *arbitrary* finite-ranged interactions, provided they are sufficiently weak. The Gross-Neveu model has an enormous global  $SO(8)$  symmetry, manifest in terms of eight real Fermion fields which, however, are highly non-local in terms of the electron operators. For generic repulsive interactions, the two-leg ladder exhibits a Mott insulating phase at half-filling with d-wave pairing correlations. Integrability of the Gross-Neveu model is employed to extract the *exact* energies, degeneracies and quantum numbers of *all* the low energy excited states, which fall into degenerate  $SO(8)$  multiplets. One  $SO(8)$  vector includes two charged Cooper pair excitations, a neutral  $s = 1$  triplet of magnons, and three other neutral  $s = 0$  particle-hole excitations. A *triality* symmetry relates these eight two-particle excitations to *two* other degenerate octets which are comprised of *single*-electron like excitations. In addition to these 24 degenerate “particle” states costing an energy (mass)  $m$  to create, there is a 28 dimensional antisymmetric tensor multiplet of “bound” states with energy  $\sqrt{3}m$ . Doping away from half-filling liberates the Cooper pairs leading to quasi-long-range d-wave pair field correlations, but maintaining a gap to spin and single-electron excitations. For very low doping levels, integrability allows one to extract *exact* values for these energy gaps. Enlarging the space of interactions to include attractive interactions reveals that there are *four* robust phases possible for the weak coupling two-leg ladder. While each of the four phases has a (different)  $SO(8)$  symmetry, they are shown to all share a common  $SO(5)$  symmetry - the one recently proposed by Zhang as a unifying feature of magnetism and superconductivity in the cuprates.

## I. INTRODUCTION

Since the discovery of the cuprate superconductors<sup>1</sup> there has been renewed interest in the behavior of weakly doped Mott insulators.<sup>2-4</sup> There are two broad classes of Mott insulators, distinguished by the presence or absence of magnetic order. More commonly spin rotational invariance is spontaneously broken, and long-range magnetic order, typically antiferromagnetic, is realized.<sup>5</sup> There are then low energy spin excitations, the spin 1 magnons. Alternatively, in a spin-liquid Mott insulator there are no broken symmetries, the magnetic order is short-ranged and there is a gap to all spin excitations : a spin-gap.

In the cuprates the Mott insulator is antiferromagnetically ordered, but upon doping with holes the antiferromagnetism is rapidly destroyed, and above a certain level superconductivity occurs. Below optimal doping levels, there are experimental signs of a spin gap opening at temperatures well above the transition into the superconducting phase.<sup>6-8</sup> The apparent connection between a spin-gap and superconductivity has been a source of motivation to search for Mott insulators of the spin-liquid variety.

Although spin-liquids are notoriously difficult to achieve in two-dimensions,<sup>9</sup> it was realized that quasi-one-dimensional ladders would be more promising. Particular attention has focussed on the two-leg ladder.<sup>10</sup> At half-filling in the Mott insulator, the spin excitations can be described by a Heisenberg antiferromagnet, and due to

the tendency for singlet bond formation across the rungs of the ladder, spin-liquid behavior is expected.<sup>3,4,11,12</sup> In the past several years there have been extensive analyses of two-leg ladders, particularly the Hubbard<sup>13,14</sup> and t-J models,<sup>3,15-17</sup> both at half-filling and with doping. Based on numerical methods, including Monte Carlo and density matrix renormalization group,<sup>3,4</sup> as well as analytic approaches at weak coupling,<sup>18-25</sup> the basic behavior is established. At half-filling there is a spin-liquid phase with a spin-gap. Upon doping, the spin-gap survives, although smaller in magnitude, and the system exhibits quasi-long-range superconducting pairing correlations, with approximate d-wave symmetry. This behavior is reminiscent of that seen in the underdoped cuprate superconductors.

There are a number of experimental systems which can be described in terms of coupled two-leg ladders, which exhibit a spin-gap in the insulating compound.<sup>26-28</sup> These materials are often very difficult to dope. In one case, doping has apparently been achieved, and under a pressure of 3GPa superconductivity is observed below 12K.<sup>29,30</sup> Carbon nanotubes<sup>31</sup> constitute another novel material which can be modelled in terms of a two-leg ladder.<sup>32-34</sup> Specifically, the low energy electronic excitations propagating down a single-walled nanotube can be mapped onto a two-leg ladder model with very *weak* interactions, inversely proportional to the tube radius.

An obvious advantage of such low-dimensional correlated electron systems is (relative) theoretical simplicity. Indeed, in one-dimension many correlated elec-

tron models, including the Hubbard model, are exactly soluble.<sup>35</sup> Unfortunately, the Mott insulating phases of these one-dimensional models typically have gapless spin-excitations, and upon doping do not exhibit pairing. To date, we are unaware of any exactly soluble two-leg ladder models which exhibit a gapped spin-liquid ground state.

In this paper, we revisit models of interacting electron hopping on a two-leg ladder, focusing on the behavior near half-filling. For *generic* short-range potentials, we derive a perturbative renormalization group valid for weak interactions, much smaller than the bandwidth.<sup>18,19</sup> Remarkably, at half-filling the renormalization group transformation scales the system towards a special model with enormous symmetry - the  $SO(8)$  Gross-Neveu (GN) model.<sup>36</sup> Scaling onto the GN model occurs *independent* of the initial interaction parameters, provided they are weak and predominantly repulsive. Thus, for weakly interacting two-leg ladders at half-filling *universal* low energy properties are expected. Specifically, all properties on energy scales of order a characteristic GN mass (gap)  $m$  and distance scales longer than or of order  $v/m$  (where  $v$  is the Fermi velocity) are universal and determined by the GN model. In terms of microscopic parameters, the GN mass is of order  $m \sim te^{-t/U}$ , where  $t$  is the 1d bandwidth and  $U$  is a typical interaction strength, but is more profitably treated, along with  $v$ , as a phenomenological parameter. The universality predicted by the renormalization group can be profitably exploited because the  $SO(8)$  GN model is *integrable*,<sup>37-39</sup> so that many of these universal properties can be computed exactly. To our knowledge, this is the first integrable model for a Mott-insulating spin liquid. It describes a state we call the *D-Mott* phase, because the Mott-insulator has short-range pairing correlations with approximate d-wave symmetry. We now summarize the results obtained from the  $SO(8)$  GN field theory.

The primary input from integrability is the complete excitation spectrum.<sup>37-40</sup> The excitations of the GN model are comprised of “particles” (i.e. sharp excitations with a single-valued energy-momentum relation) organized into  $SO(8)$  multiplets, as well as continuum scattering states of these particles. As expected for a Mott-insulating spin-liquid with no broken symmetries, each of these excitations is separated from the ground state by a non-zero gap. The lowest-lying particles come in three octets, all with mass  $m$ , i.e. dispersing as  $\epsilon_1(q) = \sqrt{m^2 + q^2}$ , where  $q$  is the deviation of the particle’s momentum from its minimum energy value. One *vector* multiplet (conveniently denoted formally by a vector of Majorana fermions  $\eta_A$ ,  $A = 1 \dots 8$ ) consists entirely of collective two-particle excitations: two charge  $\pm 2e$  “Cooper pairs” around zero momentum, a triplet of spin-one “magnons” around momentum  $(\pi, \pi)$ , and three neutral spin-zero “charge-density-wave” (or particle-hole pair) excitations.  $SO(8)$  transformations rotate the components of the vector into one another,

unifying the pair, magnon, and charge-density-wave excitations. Indeed, the  $SO(5)$  subgroup rotating only the first five components of this vector is exactly the symmetry proposed recently by Zhang<sup>41</sup> to unify antiferromagnetism and superconductivity in the cuprates. This vector octet, referred to as “fundamental” fermions in the field-theory literature, is related by a remarkable *triatlity* symmetry<sup>42,43</sup> (present in the  $SO(N)$  GN model only for  $N = 8$ ) to two other mass  $m$  octets: spinor and isospinor multiplets, called the even and odd kinks. These sixteen particles have the quantum numbers of individual quasi-electrons and quasi-holes. The triatlity symmetry thus goes beyond the  $SO(8)$  algebra to relate single-particle and two-particle properties in a fundamental way.<sup>42,43</sup> This relation also implies that pairing is present even in the Mott-insulator: the minimum energy to add a pair of electrons (as a member of the  $SO(8)$  vector multiplet) is  $m$ , reduced by a *binding energy* of  $m$  from the cost of  $2m$  needed to add two quasi-electrons far apart. At energies above the 24 mass  $m$  states, there exists an antisymmetric tensor multiplet of 28 particles with mass  $\sqrt{3}m$ . Each can be viewed as bound states of two different fundamental fermions (or equivalently, two even or two odd kinks). In this way their quantum numbers can be easily deduced by simple addition. The tensor states contribute additional sharp (delta-function) peaks to various spectral functions, providing, for instance, the continuation of the magnon branch near momentum  $(0, 0)$ . For convenience, the quantum numbers (charge, spin, and momentum) of the vector and tensor excitations are tabulated in Tables 1 and 2. Finally, continuum scattering states enter the spectrum above the energy  $2m$ .

Combining the excitation spectrum of the GN model with the non-interacting spectrum and some additional arguments, we have also constructed schematic forms for several correlation functions of interest. In particular, in Sec. V we give detailed predictions and plots of the single particle spectral function (measurable by photoemission), the spin spectral function (measurable by inelastic neutron scattering), and the optical conductivity. Integrability implies, for instance, sharp magnon peaks in the spin structure factor at  $\mathbf{k} = (\pi, \pi)$ ,  $(0, 0)$ , and  $(\pm(k_{F1} - k_{F2}), \pi)$  with minimum energy  $m$ ,  $\sqrt{3}m$  and  $\sqrt{3}m$  respectively (here  $k_{F1}$  and  $k_{F2}$  are the Fermi momenta of the non-interacting system). Complete details can be found in Sec. V. The optical conductivity has three principal features: a Drude peak around zero frequency, with exponentially small weight ( $\sim e^{-m/T}$ ) at low temperature; an “exciton” peak around  $\omega = \sqrt{3}m$ , exponentially narrow at low temperatures; and a continuum for  $\omega \gtrsim 2m$ , due to unbound quasi-particle quasi-hole pairs. See Sec. V for more details and a figure.

Our next calculations concern the relation of these results to a recent study of microscopically  $SO(5)$  invariant ladder models by Scalapino, Zhang and Hanke (SZH).<sup>44</sup> These authors consider the strong coupling limit of a certain locally-interacting two-leg ladder model designed

to exhibit exact  $SO(5)$  symmetry. Their model has an on-site interaction  $|U| \gg t$ , an intra-rung interaction  $|V| \gg t$ , and a magnetic rung-exchange interaction  $J$ , related to one another by the  $SO(5)$  symmetry. In the  $U$ - $V$  plane they derive a strong-coupling phase diagram, including the case of attractive interactions with  $U$  and  $V$  negative. We have analyzed general  $SO(5)$  invariant two-leg ladder models in the opposite limit of *weak interactions*, deriving as a special case the corresponding weak-coupling phase diagram for their model. In fact, although we have not explored the full 9-dimensional space completely, for all bare couplings we have considered, including attractive interactions that *break*  $SO(5)$  symmetry explicitly, the RG scales the system into the  $SO(5)$  subspace. When the interactions are predominantly repulsive, the  $SO(5)$  system falls into the basin of attraction of the D-Mott phase, and the above results apply. As negative interactions are introduced, four other phases emerge: an *S-Mott* spin-liquid, with short-range approximate s-wave pairing symmetry, a charge-density-wave (CDW) state with long-range positional order at  $(\pi, \pi)$ , a spin-Peierls phase with kinetic energy modulated at  $(\pi, \pi)$ , and a Luttinger liquid (C2S2, in the nomenclature of Ref. 18) phase continuously connected to the non-interacting system. The first two of these also occur in the strong-coupling limit, though their positions in the phase diagram (Fig. 10) are modified. The phase diagrams at weak and strong coupling differ in non-trivial ways, implying a rather complex evolution of the system with increasing  $U$  and  $V$ . In weak coupling, all four non-trivial phases have distinct asymptotic  $SO(8)$  symmetries, enhanced from the common bare  $SO(5)$ . Furthermore, critical points describing the transitions between the various phases can also be identified. In particular, the D-Mott to S-Mott and CDW to spin-Peierls critical points are  $c = 1$  conformal field theories (single mode Luttinger liquids), which in weak-coupling are accompanied by a decoupled massive  $SO(6)$  sector. The S-Mott to CDW and D-Mott to spin-Peierls transitions are Ising critical theories ( $c = 1/2$ ), with decoupled massive  $SO(7)$  sectors in weak-coupling. There is also a multi-critical point describing a direct transition from the D-Mott to CDW or from the S-Mott to spin-Peierls phases, which is simply a product of the  $c = 1$  and  $c = 1/2$  critical points.

Our final results concern the effects of doping a small density of holes (or electrons) into the D-Mott spin-liquid phase at half-filling. For very small hole concentrations, the modifications of the Fermi velocities by band curvature effects can be ignored, and the doping incorporated simply by including a chemical potential term coupled to the total charge  $Q$  in the GN model;  $H_\mu = H - \mu Q$ . An analogous procedure is employed by Zhang<sup>41</sup> in his study of the  $SO(5)$  non-linear sigma model. Because the charge  $Q$  is a global  $SO(8)$  generator, integrability of the GN model is preserved, and furthermore many of the  $SO(8)$  quantum numbers can still be employed to label the states. We find that doping occurs only for  $2\mu > m$ , at which point Cooper pair “fundamental fermions” en-

ter the system and effectively form a Luttinger liquid with a single gapless charge mode (with central charge  $c = 1$ ). This phase (often denoted “C1S0”) still has a gap to spin excitations. Previous work<sup>18,20,21</sup> has approached this phase via controlled perturbative calculations in the interaction strength, at fixed doping  $x$  away from half-filling. Here, we are considering a different order of limits, with fixed (albeit weak) interactions in the small doping limit,  $x \rightarrow 0$ . In this limit, the Cooper-pairs being dilute behave as hard-core bosons or free fermions. Although the spin-gap is preserved in the doped state, it is *discontinuous* as  $x \rightarrow 0^+$ . The discontinuity can be understood as the binding of an inserted spin-one magnon to a Cooper pair in the system to form a mass  $\sqrt{3}m$  tensor particle, reduced by the binding energy  $(2 - \sqrt{3})m$  from its bare energy. The spin-gap thus jumps from  $\Delta_s(x = 0) = m$  to  $\Delta_s(x = 0^+) = (\sqrt{3} - 1)m$  upon doping. Such binding of a pair to a magnon has been observed numerically in both Hubbard and t-J ladders by Scalapino and White.<sup>45</sup> Similarly, the energy to add an *electron* (for the hole-doped system) jumps from  $\Delta_{1-}(x = 0) = 3m/2$  to  $\Delta_{1-}(x = 0^+) = m/2$ , the same as the energy to add a single hole. When many pairs are present, we have not succeeded in obtaining exact expressions for the spin and single-particle gaps, but argue that the spin gap should decrease with increasing doping, since the added magnon is attracted to an increasing density of Cooper pairs. It seems likely, however, that integrability could be exploited even in this case to obtain exact results, and hope that some experts may explore this possibility in the future.

Finally, we briefly address the behavior of the spin-spectral function for the doped ladder at energies above the spin-gap. In a recent preprint SZH<sup>44</sup> have argued that in this regime the spin-spectral function for a model with exact  $SO(5)$  symmetry should exhibit a sharp resonance at energy  $2\mu$  and momentum  $(\pi, \pi)$ , the so-called  $\pi$ -resonance (introduced originally by Zhang to explain the 42meV neutron scattering peak in the superconducting Cuprates). We show that a delta-function  $\pi$ -resonance requires, in addition to  $SO(5)$  symmetry, the existence of a non-zero condensate density in the superconducting phase. Since condensation is not possible in one-dimension, this precludes a delta-function  $\pi$ -resonance. Following a recent suggestion by Zhang,<sup>46</sup> we address briefly the possibility of a weaker algebraic singularity in the spin spectral function. Regardless of the nature of the behavior in the vicinity of  $\omega = 2\mu$ , we expect spectral weight at energies below  $2\mu$  but above the spin-gap  $\Delta_s$  discussed above.

The remainder of the paper is organized as follows. In Sec. II we describe the model Hamiltonian for the interacting ladder, reduce it to the continuum limit, bosonize the nine distinct interaction channels, and apply the renormalization group (RG) transformation. Sec. III details the simplifications that occur upon RG scaling, presents the bosonized form of the Hamiltonian in the

D-Mott phase, and for completeness demonstrates the short-range d-wave correlations found in Ref. 18. The bulk of the field-theoretic analysis is contained in Sec. IV. By refermionizing the bosonized hamiltonian, we obtain the GN model exposing the exact  $SO(8)$  symmetry, and describe why this symmetry is hidden in the original variables. The triality symmetry is identified, and used to understand the degeneracy between the three mass  $m$  octets. To help in developing an intuition for the GN model, several approximate pictures are presented to understand the excitations: a mean field theory which is asymptotically exact for  $N \rightarrow \infty$  in a generalized  $SO(N)$  GN model, and a semi-classical theory based on the bosonized (sine-Gordon-like) form of the Hamiltonian. We conclude Sec. IV by proving the uniqueness of the ground-state in the D-Mott phase and determining the quantum numbers of the  $24 + 28 = 52$  particles. The latter task is complicated by the necessity of introducing Jordan-Wigner *strings*, which are required to preserve gauge-invariance under an unphysical gauge symmetry introduced in bosonization. The string operators modify the momenta of the certain excitations by a shift of  $(\pi, \pi)$  from their naive values determined from the GN fermion operators. With the field-theoretic analysis complete, we go on to discuss correlation functions in Sec. V, giving detailed predictions for the single-particle spectral function, spin spectral function, optical conductivity, and various equal-time spatial correlators. Sec. VI describes the construction of general  $SO(5)$  invariant models in weak-coupling, their phases, and the phase-diagram of the Scalapino-Zhang-Hanke model in weak-coupling. Finally, Sec. VII describes the behavior of the D-Mott phase upon doping, including the behavior of various gaps, and a discussion of the status of the  $SO(5)$  “ $\pi$  resonance” in one dimension. Various technical points and long equations are placed in the appendices. Appendix A gives the full set of nine RG equations at half-filling, Appendix B discusses gauge redundancy and the multiplicity of the ground state in different phases, Appendix C constructs spinor and vector representations of  $SO(5)$ , Appendix D relates  $SO(5)$  and  $SO(8)$  currents, and Appendix E gives the five RG equations in the reduced  $SO(5)$  subspace.

## II. MODEL

We consider electrons hopping on a two-leg ladder as shown in Fig. 1. In the absence of interactions, the Hamiltonian consists of the kinetic energy, which we assume contains only near-neighbor hopping,

$$H_0 = \sum_{x,\alpha} \left\{ -ta_{1\alpha}^\dagger(x+1)a_{1\alpha}(x) + (1 \rightarrow 2) -t_\perp a_{1\alpha}^\dagger(x)a_{2\alpha}(x) + h.c. \right\}, \quad (2.1)$$

where  $a_\ell(a_\ell^\dagger)$  is an electron annihilation (creation) operator on leg  $\ell$  of the ladder ( $\ell = 1, 2$ ),  $x$  is a discrete co-

ordinate running along the ladder and  $\alpha = \uparrow, \downarrow$  is a spin index. The parameters  $t$  and  $t_\perp$  are hopping amplitudes along and between the leg’s of the ladder.

Being interested in weak interactions, we first diagonalize the kinetic energy in terms of bonding and anti-bonding operators:  $c_{i,\alpha} = (a_{1,\alpha} + (-1)^i a_{2,\alpha})/\sqrt{2}$ , with  $i = 1, 2$ . The Hamiltonian is then diagonalized in momentum space along the ladder, describing two decoupled (bonding and anti-bonding) bands. Focussing on the case at half-filling with one electron per site, both bands intersect the Fermi energy (at zero energy) provided  $t_\perp < 2t$ . Moreover, due to a particle/hole symmetry present with near neighbor hopping only, the Fermi velocity  $v_i$  in each band is the same, denoted hereafter as  $v$ . It is convenient to linearize the spectrum around the Fermi points at  $\pm k_{Fi}$  (see Fig. 1), which at half-filling satisfy  $k_{F1} + k_{F2} = \pi$ . Upon expanding the electron operators as,

$$c_{i\alpha} \sim c_{Ri\alpha} e^{ik_{Fi}x} + c_{Li\alpha} e^{-ik_{Fi}x}, \quad (2.2)$$

the effective low energy expression for the kinetic energy takes the form,  $H_0 = \int dx \mathcal{H}_0$ , with Hamiltonian density,

$$\mathcal{H}_0 = v \sum_{i,\alpha} [c_{Ri\alpha}^\dagger i\partial_x c_{Ri\alpha} - c_{Li\alpha}^\dagger i\partial_x c_{Li\alpha}]. \quad (2.3)$$

This Hamiltonian describes Dirac Fermions, with four flavors labelled by band and spin indices. Since all flavors propagate both to the right and left with the *same* velocity, the model exhibits an enlarged symmetry. Specifically, if the four right (and left) moving Dirac Fermions are decomposed into real and imaginary parts,  $\psi_{Pi\alpha} = (\xi_{Pi\alpha}^1 + i\xi_{Pi\alpha}^2)/\sqrt{2}$  where  $P = R/L$  and  $\xi^1, \xi^2$  are Majorana fields, the eight right (and left) moving Majorana fields, denoted  $\xi_{PA}$  with  $A = 1, 2, \dots, 8$  form an eight component vector. The Hamiltonian density, when re-expressed in terms of these eight component vectors takes the simple form

$$\mathcal{H}_0 = \frac{v}{2} \sum_{A=1}^8 [\xi_{RA} i\partial_x \xi_{RA} - \xi_{LA} i\partial_x \xi_{LA}], \quad (2.4)$$

which is invariant under *independent* global  $SO(8)$  rotations among *either* the right or left vector of Majorana fields. This enlarged  $O(8)_R \times O(8)_L$  symmetry is only present at half-filling with particle/hole symmetry.

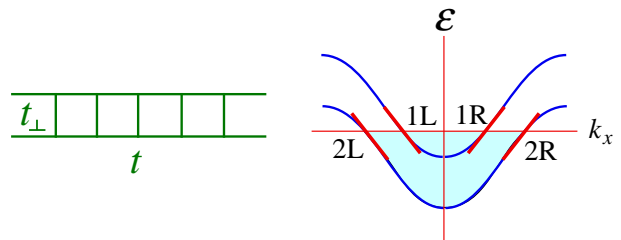


FIG. 1: A two-leg ladder and its band structure. In the low-energy limit, the energy dispersion is linearized near the Fermi points. The two resulting relativistic Dirac Fermions are distinguished by pseudospin indices  $i = 1, 2$  for the anti-bonding and bonding bands, respectively.

Electron-electron interactions scatter right-moving electrons into left-moving electrons and vice-versa, destroying this large symmetry. For general spin-independent interactions the symmetry will be broken down to  $U(1) \times SU(2)$ , corresponding to total charge and spin conservation. In the following we consider general finite-ranged spin-independent interactions between the electrons hopping on the two-leg ladder. We assume the typical interaction strength,  $U$ , is weak – much smaller than the bandwidth. We focus on the effects of the interactions to *leading* non-vanishing order in  $U$ . In this limit it is legitimate to keep only those pieces of the interactions which scatter the low energy Dirac Fermions. Of these, only those involving four-Fermions are marginal, the rest scaling rapidly to zero under renormalization. Moreover, four-Fermion interactions which are chiral, say only scattering right movers, only renormalize Fermi velocities and can be neglected at leading order in small  $U$ .<sup>18,19</sup> All of the remaining four-Fermion interactions can be conveniently expressed in terms of currents, defined as

$$J_{ij} = c_{i\alpha}^\dagger c_{j\alpha}, \quad \mathbf{J}_{ij} = \frac{1}{2} c_{i\alpha}^\dagger \boldsymbol{\sigma}_{\alpha\beta} c_{j\beta}; \quad (2.5)$$

$$I_{ij} = c_{i\alpha} \epsilon_{\alpha\beta} c_{j\beta}, \quad \mathbf{I}_{ij} = \frac{1}{2} c_{i\alpha} (\epsilon \boldsymbol{\sigma})_{\alpha\beta} c_{j\beta}, \quad (2.6)$$

where the  $R, L$  subscript has been suppressed. Both  $J$  and  $I$  are invariant under global  $SU(2)$  spin rotations, whereas  $\mathbf{J}$  and  $\mathbf{I}$  rotate as  $SU(2)$  vectors. Due to Fermi statistics, some of the currents are (anti-)symmetrical

$$I_{ij} = I_{ji} \quad \mathbf{I}_{ij} = -\mathbf{I}_{ji}, \quad (2.7)$$

so that  $\mathbf{I}_{ii} = 0$  (no sum on  $i$ ).

The full set of marginal momentum-conserving four-Fermion interactions can be written

$$\begin{aligned} \mathcal{H}_I^{(1)} = & b_{ij}^\rho J_{Rij} J_{Lij} - b_{ij}^\sigma \mathbf{J}_{Rij} \cdot \mathbf{J}_{Lij}, \\ & + f_{ij}^\rho J_{Rii} J_{Ljj} - f_{ij}^\sigma \mathbf{J}_{Rii} \cdot \mathbf{J}_{Ljj}. \end{aligned} \quad (2.8)$$

Here  $f_{ij}$  and  $b_{ij}$  denote the forward and backward (Cooper) scattering amplitudes, respectively, between bands  $i$  and  $j$ . Summation on  $i, j = 1, 2$  is implied. To avoid double counting, we set  $f_{ii} = 0$  (no sum on  $i$ ). Hermiticity implies  $b_{12} = b_{21}$  and parity symmetry ( $R \leftrightarrow L$ ) gives  $f_{12} = f_{21}$ , so that there are generally eight independent couplings  $b_{11}^\rho, b_{22}^\rho, b_{12}^\rho, b_{11}^\sigma, b_{22}^\sigma, b_{12}^\sigma$ , and  $f_{12}^\rho, f_{12}^\sigma$ . At half-filling with particle/hole symmetry  $b_{11} = b_{22}$ . Additional momentum non-conserving Umklapp interactions of the form

$$\mathcal{H}_I^{(2)} = u_{ij}^\rho I_{Rij}^\dagger I_{L\hat{i}\hat{j}} - u_{ij}^\sigma \mathbf{I}_{Rij}^\dagger \cdot \mathbf{I}_{L\hat{i}\hat{j}} + \text{h.c.} \quad (2.9)$$

are also allowed, (here  $\hat{1} = 2, \hat{2} = 1$ ). Because the currents  $(\mathbf{I}_{ij}), I_{ij}$  are (anti-)symmetric, one can always choose  $u_{12} = u_{21}$  for convenience. We also take  $u_{ii}^\sigma = 0$  since  $\mathbf{I}_{ii} = 0$ . With particle/hole symmetry there are thus just three independent Umklapp vertices,  $u_{11}^\rho, u_{12}^\rho$ , and  $u_{12}^\sigma$ . Together with the six forward and backward vertices, nine independent couplings are required to describe the most general set of marginal non-chiral four-Fermion interactions for a two-leg ladder with particle/hole symmetry at half-filling.

Since our analysis below makes heavy use of abelian Bosonization,<sup>47,35</sup> it is convenient at this stage to consider the Bosonized form of the general interacting theory. To this end, the Dirac fermion fields are expressed in terms of Boson fields as

$$c_{P i \alpha} = \kappa_{i \alpha} e^{i \phi_{P i \alpha}}, \quad (2.10)$$

where  $P = R/L = \pm$ . To ensure that the Fermionic operators anti-commute the Boson fields are taken to satisfy

$$[\phi_{P i \alpha}(x), \phi_{P j \beta}(x')] = iP\pi\delta_{ij}\delta_{\alpha\beta}\text{sgn}(x-x'), \quad (2.11)$$

$$[\phi_{R i \alpha}(x), \phi_{L j \beta}(x')] = i\pi\delta_{ij}\delta_{\alpha\beta}. \quad (2.12)$$

Klein factors, satisfying

$$\{\kappa_{i \alpha}, \kappa_{j \beta}\} = 2\delta_{ij}\delta_{\alpha\beta}, \quad (2.13)$$

have been introduced so that the Fermionic operators in different bands or with different spins anticommute with one another.

It will also be convenient to define a pair of conjugate non-chiral Boson fields for each flavor,

$$\varphi_{i \alpha} \equiv \phi_{R i \alpha} + \phi_{L i \alpha}, \quad (2.14)$$

$$\theta_{i \alpha} \equiv \phi_{R i \alpha} - \phi_{L i \alpha}, \quad (2.15)$$

which satisfy

$$[\varphi(x), \theta(x')] = -i4\pi\Theta(x' - x). \quad (2.16)$$

Here, and in the remainder of the paper, we denote by  $\Theta(x)$  the heavyside step function to avoid confusion with the  $\theta$  fields defined in Eq. 2.15 above. The field  $\theta_{i \alpha}$  is a displacement (or phonon) field and  $\varphi_{i \alpha}$  is a phase field.

The Bosonized form for the kinetic energy Eq. 2.3 is

$$\mathcal{H}_0 = \frac{v}{8\pi} \sum_{i, \alpha} [(\partial_x \theta_{i \alpha})^2 + (\partial_x \varphi_{i \alpha})^2], \quad (2.17)$$

which describes density waves propagating in band  $i$  and with spin  $\alpha$ .

This expression can be conveniently separated into charge and spin modes, by defining

$$\theta_{i \rho} = (\theta_{i \uparrow} + \theta_{i \downarrow})/\sqrt{2} \quad (2.18)$$

$$\theta_{i \sigma} = (\theta_{i \uparrow} - \theta_{i \downarrow})/\sqrt{2}, \quad (2.19)$$

and similarly for  $\varphi$ . The  $\sqrt{2}$  ensures that these new fields satisfy the same commutators, Eq. (2.16). It is also convenient to combine the fields in the two bands into a  $\pm$  combination, by defining

$$\theta_{\mu\pm} = (\theta_{1\mu} \pm \theta_{2\mu})/\sqrt{2}, \quad (2.20)$$

where  $\mu = \rho, \sigma$ , and similarly for  $\varphi$ . It will sometimes be convenient to employ charge/spin and flavor decoupled *chiral* fields, defined as

$$\phi_{P\mu\pm} = (\varphi_{\mu\pm} + P\theta_{\mu\pm})/2, \quad (2.21)$$

with  $P = R/L = \pm$ .

The Hamiltonian density  $\mathcal{H}_0$  can now be re-expressed in a charge/spin and flavor decoupled form,

$$\mathcal{H}_0 = \frac{v}{8\pi} \sum_{\mu,\pm} [(\partial_x \theta_{\mu\pm})^2 + (\partial_x \varphi_{\mu\pm})^2]. \quad (2.22)$$

The fields  $\theta_{\rho+}$  and  $\varphi_{\rho+}$  describe the total charge and current fluctuations, since under Bosonization,  $c_{P_i\alpha}^\dagger c_{P_i\alpha} = \partial_x \theta_{\rho+}/\pi$  and  $vPc_{P_i\alpha}^\dagger c_{P_i\alpha} = \partial_x \varphi_{\rho+}/\pi$ .

The interaction Hamiltonians can also be readily expressed in terms of the Boson fields. The momentum conserving terms in Eq. 2.8 can be decomposed into two contributions,  $\mathcal{H}_I^{(1)} = \mathcal{H}_I^{(1a)} + \mathcal{H}_I^{(1b)}$ , the first 2 involving gradients of the Boson fields,

$$\mathcal{H}_I^{(1a)} = \frac{1}{16\pi^2} \sum_{\mu\pm} A_{\mu\pm} [(\partial_x \theta_{\mu\pm})^2 - (\partial_x \varphi_{\mu\pm})^2], \quad (2.23)$$

with coefficient  $A_{\rho\pm} = 2(c_{11}^\rho \pm f_{12}^\rho)$  and  $A_{\sigma\pm} = -(c_{11}^\sigma \pm f_{12}^\sigma)/2$ , whereas the second contribution involves cosines of the Boson fields:

$$\begin{aligned} \mathcal{H}_I^{(1b)} = & -2\Gamma b_{12}^\sigma \cos \varphi_{\rho-} \cos \theta_{\sigma+} \\ & + \cos \theta_{\sigma+} (2b_{11}^\sigma \cos \theta_{\sigma-} + 2\Gamma f_{12}^\sigma \cos \varphi_{\sigma-}) \\ & - \cos \varphi_{\rho-} (\Gamma b_{12}^+ \cos \theta_{\sigma-} + b_{12}^- \cos \varphi_{\sigma-}), \end{aligned} \quad (2.24)$$

with  $b_{12}^\pm = b_{12}^\sigma \pm 4b_{12}^\rho$ . Similarly, the Umklapp interactions can be Bosonized as,

$$\begin{aligned} \mathcal{H}_I^{(2)} = & -16\Gamma u_{11}^\rho \cos \theta_{\rho+} \cos \varphi_{\rho-} - 4u_{12}^\sigma \cos \theta_{\rho+} \cos \theta_{\sigma+} \\ & - \cos \theta_{\rho+} (2u_{12}^+ \cos \theta_{\sigma-} + 2\Gamma u_{12}^- \cos \varphi_{\sigma-}), \end{aligned} \quad (2.25)$$

with  $u^\pm = u_{12}^\sigma \pm 4u_{12}^\rho$ . Here  $\Gamma = \kappa_{1\uparrow}\kappa_{1\downarrow}\kappa_{2\uparrow}\kappa_{2\downarrow}$  is a product of Klein factors. Since  $\Gamma^2 = 1$ , we can take  $\Gamma = \pm 1$ . Hereafter, we will put  $\Gamma = 1$ .

In the absence of electron-electron interactions, the Hamiltonian is invariant under spatially constant shifts of any of the eight non-chiral Boson fields,  $\theta_{\mu\pm}$  and  $\varphi_{\mu\pm}$ . With interactions *five* of the eight Boson fields enter as arguments of cosines, but for the remaining three –  $\varphi_{\rho+}$ ,  $\varphi_{\sigma+}$  and  $\theta_{\rho-}$  – this continuous shift symmetry is still present. For the first two fields, the conservation law responsible for this symmetry is readily apparent. Specifically, the operators  $\exp(iaQ)$  and  $\exp(iaS_z)$ , with  $Q$  the

total electric charge and  $S_z$  the total z-component of spin, generate “translations” proportional to  $a$  in the two fields  $\varphi_{\rho+}$  and  $\varphi_{\sigma+}$ . To see this, we note that  $Q = \int dx \rho(x)$  with  $\rho(x) = \partial_x \theta_{\rho+}/\pi$  the momentum conjugate to  $\varphi_{\rho+}$ , whereas  $S_z$  can be expressed as an integral of the momentum conjugate to  $\varphi_{\sigma+}$ . Since the total charge is conserved,  $[Q, H] = 0$ , the full Hamiltonian must therefore be invariant under  $\varphi_{\rho+} \rightarrow \varphi_{\rho+} + a$  for arbitrary constant  $a$ , precluding a cosine term for this field. Similarly, conservation of  $S_z$  implies invariance under  $\varphi_{\sigma+} \rightarrow \varphi_{\sigma+} + a$ . The conservation law responsible for the symmetry under shifts of the third field,  $\theta_{\sigma-}$ , is present only in the weak coupling limit. To see this, consider the operator,  $\mathcal{P} = k_{F1}J_1 + k_{F2}J_2$ , with  $J_i = \sum_\alpha (N_{Ri\alpha} - N_{Li\alpha})$ , where  $N_{Pi\alpha}$  is the total number of electrons in band  $i$  with spin  $\alpha$  and chirality  $P$ . At weak coupling with Fermi fields restricted to the vicinity of  $k_{Fi}$ , this operator is essentially the total momentum. Since the total momentum is conserved up to multiples of  $2\pi$ , one has  $\Delta\mathcal{P} = \pm 2\pi n = \pm 2n(k_{F1} + k_{F2})$  for integer  $n$ . Moreover, since the Fermi momenta  $k_{Fi}$  are in general unequal and incommensurate, this implies that  $\Delta J_1 = \Delta J_2 = \pm 2n$ , or equivalently that  $J_1 - J_2$  is conserved at weak coupling. Since  $J_1 - J_2 = \int dx j(x)$  with  $j(x) = \partial_x \varphi_{\rho-}/\pi$  the momentum conjugate to  $\theta_{\rho-}$ , this conservation law implies invariance under  $\theta_{\rho-} \rightarrow \theta_{\rho-} + a$ .

The remaining 5 Boson fields, entering as arguments of various cosine terms, will tend to be pinned at the minima of these potentials. Two of these 5 fields,  $\theta_{\sigma-}$  and  $\varphi_{\sigma-}$ , are dual to one another so that the uncertainty principle precludes pinning both fields. Since there are various competing terms in the potential seen by these 5 fields, minimization for a given set of bare interaction strengths is generally complicated. For this reason we employ the weak coupling perturbative renormalization group transformation, derived in earlier work.<sup>18,19</sup> Upon systematically integrating out high-energy modes away from the Fermi points and then rescaling the spatial coordinate and Fermi fields, a set of renormalization group (RG) transformations can be derived for the interaction strengths. Denoting the nine interaction strengths as  $g_i$ , the leading order RG flow equations take the general form,  $\partial_\ell g_i = A_{ijk} g_j g_k$ , valid up to order  $g^3$ . For completeness the RG flow equations are given explicitly in Appendix A. Our approach is to integrate the RG flow equations, numerically if necessary, to determine which of the nine coupling constants are growing large.

Under a numerical integration of these nine flow equations it is found that some of the couplings remain small, while others tend to increase, sometimes after a sign change, and then eventually diverge. Quite surprisingly, though, the ratios of the growing couplings tend to approach fixed constants, which are *independent* of the initial coupling strengths, at least over a wide range in the nine dimensional parameter space. These constants can be determined by inserting the Ansatz,

$$g_i(\ell) = \frac{g_{i0}}{(\ell_d - \ell)}, \quad (2.26)$$

into the RG flow equations, to obtain nine *algebraic* equations quadratic in the constants  $g_{i0}$ . There are various distinct solutions of these algebraic equations, or rays in the nine-dimensional space, which correspond to different possible phases. But for generic *repulsive* interactions between the electrons on the two-leg ladder, a numerical integration reveals that the flows are essentially always attracted to one particular ray. In the next sections we shall consider the properties of this phase, which, for reasons which will become apparent, we denote by *D-Mott*.

### III. D-MOTT PHASE

In the phase of interest, two of the nine coupling constants,  $b_{11}^\rho$  and  $f_{12}^\sigma$ , remain small, while the other seven grow large with fixed ratios:

$$b_{12}^\rho = \frac{1}{4}b_{12}^\sigma = f_{12}^\rho = -\frac{1}{4}b_{11}^\sigma = \quad (3.1)$$

$$2u_{11}^\rho = 2u_{12}^\rho = \frac{1}{2}u_{12}^\sigma = g > 0. \quad (3.2)$$

Once the ratio's are fixed, there is a single remaining coupling constant, denoted  $g$ , which measures the distance from the origin along a very special direction (or “ray”) in the nine dimensional space of couplings. The RG equations reveal that as the flows scale towards strong coupling, they are *attracted* to this special direction. If the initial bare interaction parameters are sufficiently weak, the RG flows have sufficient “time” to renormalize onto this special “ray”, before scaling out of the regime of perturbative validity. In this case, the low energy physics, on the scale of energy gaps which open in the spectrum, is *universal*, depending only on the properties of the physics along this special ray, and independent of the precise values of the bare interaction strengths.

To expose this universal weak coupling physics, we use Eq. 3.2 to replace the nine independent coupling constants in the most general Hamiltonian with the *single* parameter  $g$ , measuring the distance along the special ray. Doing so reveals a remarkable symmetry, which is most readily exposed in terms of a new set of Boson fields, defined by,

$$\begin{aligned} (\theta, \varphi)_1 &= (\theta, \varphi)_{\rho+}, & (\theta, \varphi)_2 &= (\theta, \varphi)_{\sigma+}, \\ (\theta, \varphi)_3 &= (\theta, \varphi)_{\sigma-}, & (\theta, \varphi)_4 &= (\varphi, \theta)_{\rho-}. \end{aligned} \quad (3.3)$$

The first three are simply the charge/spin and flavor fields defined earlier. However, in the fourth pair of fields,  $\theta$  and  $\varphi$  have been interchanged. It will also be useful to consider *chiral* boson fields for this new set, defined in the usual way,

$$\phi_{Pa} = (\varphi_a + P\theta_a)/2, \quad (3.4)$$

with  $a = 1, \dots, 4$ , and  $P = R/L = \pm$  as before. The first three of these chiral fields satisfy the commutators Eq. (2.11) and (2.12). But for the fourth field, since  $\phi_{P4} = P\phi_{P\rho-}$ , the second commutator is modified to  $[\phi_{R4}, \phi_{L4}] = -i\pi$ .

In terms of these new fields, the full interacting Hamiltonian density along the special ray takes an exceedingly simple form:  $\mathcal{H} = \mathcal{H}_0 + \mathcal{H}_I$ , with

$$\mathcal{H}_0 = \frac{v}{8\pi} \sum_a [(\partial_x \theta_a)^2 + (\partial_x \varphi_a)^2], \quad (3.5)$$

$$\begin{aligned} \mathcal{H}_I &= -\frac{g}{2\pi^2} \sum_a \partial_x \phi_{Ra} \partial_x \phi_{La} \\ &\quad -4g \sum_{a \neq b} \cos \theta_a \cos \theta_b. \end{aligned} \quad (3.6)$$

We now briefly discuss some of the general physical properties which follow from this Hamiltonian. In the next sections we will explore in detail the symmetries present in the model, and the resulting implications.

Ground state properties of the above Hamiltonian can be inferred by employing semi-classical considerations. Since the fields  $\varphi_a$  enter quadratically, they can be integrated out, leaving an effective action in terms of the four fields  $\theta_a$ . Since the single coupling constant  $g$  is marginally relevant and flowing off to strong coupling, these fields will be pinned in the minima of the cosine potentials. Specifically, there are two sets of semiclassical ground states with all  $\theta_a = 2n_a\pi$  or all  $\theta_a = (2n_a + 1)\pi$ , where  $n_a$  are integers. Excitations will be separated from the ground state by a finite energy gap, since the fields are harmonically confined, and instanton excitations connecting different minima are also costly in energy.

Since both  $\theta_{\sigma\pm}$  fields are pinned, so are the spin-fields in each band,  $\theta_{i\sigma}$  ( $i = 1, 2$ ). Since  $\partial_x \theta_{i\sigma}$  is proportional to the z-component of spin in band  $i$ , a pinning of these fields implies that the spin in each band vanishes, and excitations with non-zero spin are expected to cost finite energy: the spin gap. This can equivalently be interpreted as singlet pairing of electron pairs in each band. It is instructive to consider the pair field operator in band  $i$ :

$$\Delta_i = c_{Ri\uparrow} c_{Li\downarrow} = \kappa_{i\uparrow} \kappa_{i\downarrow} e^{\frac{i}{\sqrt{2}}(\varphi_{i\rho} + \theta_{i\sigma})}. \quad (3.7)$$

With  $\theta_{i\sigma} \approx 0$ ,  $\varphi_{i\rho}$  can be interpreted as the phase of the pair field in band  $i$ . The relative phase of the pair field in the two bands follows by considering the product

$$\Delta_1 \Delta_2^\dagger = -\Gamma e^{i\theta_{\sigma-}} e^{i\varphi_{\rho-}}, \quad (3.8)$$

with  $\Gamma = \kappa_{1\uparrow} \kappa_{1\downarrow} \kappa_{2\uparrow} \kappa_{2\downarrow} = 1$ . Since  $\theta_4 = \varphi_{\rho-}$  the relative phase is also pinned by the cosine potential, with a sign change in the relative pair field,  $\Delta_1 \Delta_2^\dagger < 0$ , corresponding to a D-wave symmetry. Being at half-filling, the overall charge mode,  $\theta_{\rho+}$  is also pinned – there is a charge gap – and the two-point pair field correlation

function falls off exponentially with separation. We refer to this phase as a ‘‘D-Mott’’ phase, having D-wave pairing correlations coincident with a charge gap. Upon doping the D-Mott phase away from half-filling, gapless charge fluctuations are expected in the  $(\rho+)$  sector, and power-law D-wave pairing correlations develop.

It is worth noting that the fully gapped D-Mott phase has a very simple interpretation in the strong coupling limit. Two electrons across each of the rungs of the two-legged ladder form singlets, of the usual form  $|\uparrow, \downarrow\rangle - |\downarrow, \uparrow\rangle$ , where the two states refer to electrons on leg 1 or 2, respectively. This two-electron state can be re-written in the bonding anti-bonding basis, and takes the form,  $|\uparrow\downarrow, -\rangle - |-\rangle, \uparrow\downarrow\rangle$ , where the two states now refer to bonding and anti-bonding orbitals. This resembles a local Cooper pair, with a relative sign change between bonding and anti-bonding pairs: an approximate D-wave symmetry.

#### IV. $SO(8)$ GROSS-NEVEU MODEL

As shown above, the bosonized effective Hamiltonian on energy scales of order the gap is exceptionally simple in the D-Mott phase. In this section, we show that this simplicity is indicative of a higher symmetry, and explore its ramifications upon the spectrum.

##### A. Gross-Neveu Model

An obvious symmetry of the bosonic action, Eqs. 3.5-3.6, is permutation of the fields  $\theta_a \rightarrow P_{ab}\theta_b$ , where  $P_{ab}$  is a permutation matrix. In fact, this is only a small subset of the true invariances of the model. As is often the case, abelian bosonization masks the full symmetry group. It can be brought out, however, by a refermionization procedure. We define ‘‘fundamental’’ (Dirac) fermion operators  $\psi_{Pa}$  with  $a = 1, 2, 3, 4$  via

$$\begin{aligned}\psi_{Pa} &= \kappa_a e^{i\phi_{Pa}}, & a = 1 \dots 3 \\ \psi_{P4} &= P\kappa_4 e^{i\phi_{P4}},\end{aligned}\quad (4.1)$$

and  $P = R, L = \pm 1$ , as before. The Klein factors are given by

$$\kappa_1 = \kappa_{2\uparrow} \quad \kappa_2 = \kappa_{1\uparrow}, \quad (4.2)$$

$$\kappa_3 = \kappa_{1\downarrow} \quad \kappa_4 = \kappa_{2\downarrow}. \quad (4.3)$$

In the re-Fermionization of the fourth field we have chosen to include a minus sign for the left mover. This is convenient, due to the modified commutators between the left and right fields:  $[\phi_{R4}, \phi_{L4}] = -i\pi$ , in contrast to the ‘‘standard’’ form in Eq. 2.12.

In these variables, the effective Hamiltonian density becomes

$$\mathcal{H} = \psi_a^\dagger i\tau^z \partial_x \psi_a - g \left( \psi_a^\dagger \tau^y \psi_a \right)^2, \quad (4.4)$$

where  $\psi_a = (\psi_{Ra}, \psi_{La})$ , and  $\tau$  is a vector of Pauli matrices acting in the  $R, L$  space. Here, summation over repeated indices,  $a = 1, 2, \dots, 4$  is implicit. It is remarkable that the Hamiltonian can be written locally in the ‘‘fundamental’’ fermion variables, which are themselves highly *non-locally* related to the ‘‘bare’’ electron operators.

A further simplification arises upon changing to Majorana fields,

$$\psi_{Pa} = \frac{1}{\sqrt{2}} (\eta_{R2a} + i\eta_{R2a-1}). \quad (4.5)$$

The Hamiltonian density then takes the manifestly invariant form

$$\mathcal{H} = \frac{1}{2} \eta_{RA} i\partial_x \eta_{RA} - \frac{1}{2} \eta_{LA} i\partial_x \eta_{LA} + g G_R^{AB} G_L^{AB}, \quad (4.6)$$

where the currents are

$$G_P^{AB} = i\eta_{PA}\eta_{PB}, \quad A \neq B, \quad (4.7)$$

and  $A, B = 1 \dots 8$ .

##### B. $SO(8)$ Symmetry

Eq. 4.6 is the standard form for the  $SO(8)$  Gross-Neveu model, which has been intensively studied in the literature.<sup>36–40,42,43</sup> We first discuss its manifest symmetry properties.

The 28 currents  $G_P^{AB}$  generate chiral  $SO(8)$  transformations. For  $g = 0$ , Eq. 4.6 has two independent symmetries under separate rotations of the left- and right-moving fields. For  $g \neq 0$ , however, only simultaneous rotations of both chiralities are allowed. More precisely, the unitary operators

$$U(\chi_{AB}) = e^{i\chi_{AB} \int dx (G_R^{AB} + G_L^{AB})}, \quad (4.8)$$

generate global orthogonal transformations of the Majorana fields,

$$U^\dagger(\chi)\eta_{PA}U(\chi) = \mathcal{O}_{AB}(\chi)\eta_{PB}, \quad (4.9)$$

where the orthogonal matrix  $\mathcal{O}(\chi)$  is given by

$$\mathcal{O}(\chi) = e^{i\chi_{AB} T_{AB}}. \quad (4.10)$$

Here the  $T_{AB}$  ( $A > B$ ) are the 28 generators of  $SO(8)$  in the fundamental representation, with matrix elements  $[T_{AB}]_{CD} = i(\delta_{AC}\delta_{BD} - \delta_{AD}\delta_{BC})/2$ . Eq. 4.9 indicates that the  $\eta_{PA}$  transform as  $SO(8)$  vectors. Similarly, the currents  $G_P^{AB}$  are rank 2  $SO(8)$  tensors.

It is worth noting that despite the non-local relation between the fundamental and bare fermion operators, the  $SO(8)$  symmetry remains local in the bare electron basis.



This follows from the fact that the chiral  $SO(8)$  currents in the two bases are actually linearly related, i.e.

$$G_P^{AB} = M_P^{ABCD} \tilde{G}_P^{CD}, \quad (4.11)$$

where  $\tilde{G}_P^{AB} = i\xi_{PA}\xi_{PB}$ , and the bare Majorana operators are defined by

$$c_{P1\uparrow} = \frac{1}{\sqrt{2}} (\xi_{P2} + i\xi_{P1}), \quad (4.12)$$

$$c_{P1\downarrow} = \frac{1}{\sqrt{2}} (\xi_{P4} + i\xi_{P3}), \quad (4.13)$$

$$c_{P2\uparrow} = \frac{1}{\sqrt{2}} (\xi_{P6} + i\xi_{P5}), \quad (4.14)$$

$$c_{P2\downarrow} = \frac{1}{\sqrt{2}} (\xi_{P8} + i\xi_{P7}). \quad (4.15)$$

The precise forms of the tensors  $M_P$  are complicated and not particularly enlightening. Nevertheless, the *existence* of the linear relation between currents implies that the unitary operator  $U(\chi)$  also generates local rotations of the bare electron fields. In these variables, however, the  $SO(8)$  symmetry is *hidden*, because  $M_R \neq M_L$ , which implies different rotations must be performed amongst right- and left-moving electron operators.

Finally, it is instructive to see how the conservation of total charge and spin, corresponding to a global  $U(1) \times SU(2)$  symmetry, is embedded in the larger  $SO(8)$  symmetry. To this end, consider the total electron charge operator,  $Q$ , which in terms of the low energy fields can be written,

$$Q = 2 \int dx \sum_P \psi_{P1}^\dagger \psi_{P1} = 2 \int dx (G_R^{21} + G_L^{21}), \quad (4.16)$$

where  $\psi_{P1}$  is a fundamental Gross-Neveu fermion. The  $U(1)$  charge symmetry is thus seen to be equivalent to the  $SO(2)$  symmetry of rotations in the 1 – 2 plane of the eight-dimensional vector space. Similarly, the total spin operator

$$\mathbf{S} = \int dx [\mathbf{J}_R(x) + \mathbf{J}_L(x)], \quad (4.17)$$

with  $\mathbf{J}_P(x) = \mathbf{J}_{Pii}(x)$ , can be re-expressed in terms of  $SO(8)$  generators by using,

$$J_P^a(x) = \epsilon^{abc} G_P^{bc}, \quad (4.18)$$

with  $a, b, c = 3, 4, 5 = x, y, z$ . Thus we see the equivalence between the  $SU(2)$  spin rotations and  $SO(3)$  rotations in the 3-dimensional sub-space 3 – 4 – 5 of the eight dimensional vector space. Rotations in the five-dimensional subspace 1 – 2 – 3 – 4 – 5, correspond to global  $SO(5)$  rotations which unify the charge and spin degrees of freedom.

In the absence of interactions in the Gross-Neveu model, all of the excitations including spin remain massless. In this case there is an independent  $SU(2)$  spin

symmetry in the right and left moving sectors. The spin currents  $\mathbf{J}_P$  can then be shown to satisfy,

$$[J_P^a(x), J_P^b(x')] = \delta(x - x') i\epsilon^{abc} J_P^c(x) + \quad (4.19)$$

$$i \frac{P}{2\pi} k \delta_{ab} \delta'(x - x'), \quad (4.20)$$

with  $a, b, c = x, y, z$  and  $k = 2$ . This is referred to as an  $SU(2)$  current algebra at level ( $k$ ) two.

We conclude this subsection by answering a question which may have occurred to the alert reader: why is the symmetry of the model  $SO(8)$  rather than  $O(8)$ ? Based on Eq. 4.6, it would appear that *any* transformation of the form  $\eta_{PA} \rightarrow \mathcal{O}_{AB} \eta_{PB}$  would leave the Hamiltonian invariant, including *improper* rotations with  $\det \mathcal{O} = -1$ . The presence of such improper rotations means  $O(8) = SO(8) \times \mathcal{Z}_2$ , since any orthogonal matrix can be factored into a product of matrix with determinant one and a *particular* (reflection) matrix, e.g.  $\mathcal{O}_{AB}^r = \delta_{AB} - 2\delta_{A1}\delta_{B1}$ . We have already shown above that the  $SO(8)$  symmetry is physical – i.e. the symmetry generators act within the Hilbert space of the physical electrons. It is straightforward to show that the  $\mathcal{Z}_2$  reflection is however, *unphysical*. To see this, imagine performing the  $\mathcal{Z}_2$  reflection effected by  $\mathcal{O}^r$  above, which takes  $\eta_{P1} \rightarrow -\eta_{P1}$ . Using the bosonization rules, this corresponds to  $\theta_1 \rightarrow -\theta_1$  and  $\varphi_1 \rightarrow -\varphi_1$ . Returning to the physical fields, one finds that the bare electron operators transform much more non-trivially:

$$c_{Pi\alpha} \xrightarrow{\mathcal{Z}_2} c_{Pi\alpha} \psi_{P1}^\dagger. \quad (4.21)$$

As we shall show in Sec. IV.E.3, a single GN fermion operator, such as  $\psi_{P1}^\dagger$ , is unphysical. The  $\mathcal{Z}_2$  reflection thus takes a physical electron operator into an unphysical one, which implies that the symmetry cannot be effected by a unitary operator within the Hilbert space of the electrons. For this reason, the true symmetry group of the ladder model is  $SO(8)$ .

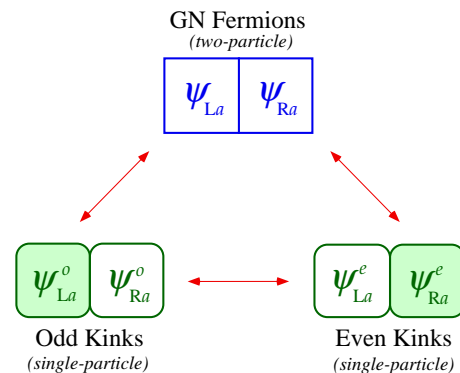


FIG. 2: Triality between GN fermions, even kinks and odd kinks. The  $SO(8)$  GN Hamiltonian is identical in terms of these three sets of fermionic operators. Operators in the gray areas are physical and gauge independent (see Sec. IV.E), while the other fermion operators must be “dressed” by an appropriate Jordan-Wigner string to remain in the physical Hilbert space.

### C. Triality

Most of the above properties hold more generally for the  $SO(N)$  GN model, even for  $N \neq 8$ . However, the case  $N = 8$  is extremely special, and in fact possesses an additional *triality* symmetry not found for other  $N$ . A useful reference is Ref. 42,43.

To expose the additional symmetry, we return to the sine-Gordon formulation. Essentially, the triality operation trades the original basis  $\{\theta_a\}$  in the four-dimensional space of boson fields for either one of two other orthogonal bases. Explicitly, the two alternate choices are the even and odd fields  $\theta_a^{e/o}$ , where

$$\theta_1^{e/o} = (\theta_1 + \theta_2 + \theta_3 \pm \theta_4)/2, \quad (4.22)$$

$$\theta_2^{e/o} = (\theta_1 + \theta_2 - \theta_3 \mp \theta_4)/2, \quad (4.23)$$

$$\theta_3^{e/o} = (\theta_1 - \theta_2 + \theta_3 \mp \theta_4)/2, \quad (4.24)$$

$$\theta_4^{e/o} = (\theta_1 - \theta_2 - \theta_3 \pm \theta_4)/2. \quad (4.25)$$

Here the upper and lower signs apply to the even and odd fields, respectively, and identical definitions hold for the dual  $\varphi_a^{e/o}$  and chiral  $\phi_{Pa}^{e/o}$  bosons. The bosonized Hamiltonian in Eqs. 3.5, 3.6 is invariant under either change of variables, i.e.

$$H[\theta_a] = H[\theta_a^e] = H[\theta_a^o]. \quad (4.26)$$

For each of these bases, an inequivalent refermionization is possible, analogous to the introduction of the fundamental fermions in Eq. 4.1. In particular, the Hamiltonian is unchanged in form when rewritten in terms of either the even or odd fermion operators,

$$\psi_{Pa}^{e/o} = \kappa_a^{e/o} e^{i\phi_{Pa}^{e/o}}. \quad (4.27)$$

It should be noted that the set of even and odd fermion operators contains all the bare electron fields. In particular,

$$\psi_{R1}^e = c_{R1\uparrow}, \quad \psi_{L1}^o = c_{L1\uparrow}, \quad (4.28)$$

$$\psi_{R2}^e = c_{R2\uparrow}, \quad \psi_{L2}^o = c_{L2\uparrow}, \quad (4.29)$$

$$\psi_{R3}^e = c_{R2\downarrow}, \quad \psi_{L3}^o = c_{L2\downarrow}, \quad (4.30)$$

$$\psi_{R4}^e = c_{R1\downarrow}, \quad \psi_{L4}^o = c_{L1\downarrow}. \quad (4.31)$$

The other eight even and odd fields ( $\psi_{La}^e$  and  $\psi_{Ra}^o$ ) are not simply related, however, to the electron fields.

### D. Conventional Gross-Neveu Excitation spectrum

The  $SO(N)$  GN model is integrable, and the excitation spectrum is known exactly. To organize the presentation, we divide the discussion of the excitation spectrum into two parts. In this subsection, we summarize known results for the conventional GN model. The precise nature of the excitations for the two-leg ladder model, however,

differs from those in the conventional GN model. This difference arises from the non-local relation between the electron and GN fields. Excitations within the GN model must be slightly modified to satisfy gauge invariance with respect to some unphysical degrees of freedom introduced in the mapping. These modifications and the resulting spectrum in the D-Mott phase are described in the subsequent subsection.

Within the GN model, the excitations are of course organized into  $SO(N)$  multiplets, but are further constrained for the case of interest,  $N = 8$ , by triality. In this subsection, we discuss the lowest-lying states, their multiplet structures and quantum numbers, and give some useful physical pictures to aid in understanding their properties.

#### 1. Results from integrability

The lowest-lying excitations are organized into three  $SO(8)$  vector multiplets, which are degenerate due to triality, for a total of 24 particles. Four of the 28 global  $SO(8)$  generators may be chosen diagonal (to form the Cartan subalgebra). We will label the particles by the values of the four associated charges, denoted by the ordered quadruplet  $(N_1, N_2, N_3, N_4)$ , and defined by

$$N_a = \int dx \psi_a^\dagger \psi_a, \quad (4.32)$$

(no sum on  $a$ ). In this notation, one  $SO(8)$  multiplet contains the states (known as *fundamental fermions*) with only one of the four  $N_a = \pm 1$ , and all others equal to zero. The remaining 16 degenerate states have  $N_a = \pm 1/2$  for  $a = 1, 2, 3, 4$ , which are divided into those with an even number of  $N_a = +1/2$  (the *even kinks*) and the remainder with an odd number of  $N_a = +1/2$  (the *odd kinks*). The reasons for this terminology will become apparent later in this section. Each particle has a mass  $m$  and disperses (due to Lorentz invariance) as  $\epsilon_1(q) = \sqrt{m^2 + q^2}$ , with momentum  $q$ . Since the electron band operators  $c_{Pi\alpha}$  are defined relative to their Fermi momenta  $k_{Fi}$ , the actual momenta of each particle is offset from the GN model momentum,  $q$ , by some amount. We will return to these “base” momenta later in this subsection, as well as to the other physical quantum numbers of the excitations.

At somewhat higher energies there is another multiplet of 28 “particles”, which transform as an antisymmetric second rank  $SO(8)$  tensor. This multiplet can be viewed as two-particle bound states of the fundamental Gross-Neveu fermions, or equivalently under triality as bound even-even or odd-odd kinks. Indeed, of these 28 states, 24 have two zero charges and two  $N_a = \pm 1$ . The other four are bound states of a fundamental fermion with its anti-particle (an excitation in the semiconductor picture, below), so they do not carry any of the four quantum numbers. Each of the 28 “particle” states has a mass  $m_2 = \sqrt{3}m$ . Finally, for energies

$\epsilon > \epsilon_c(q) = 2\sqrt{m^2 + q^2}/4$ , a two-particle continuum of (unbound) scattering states exists.

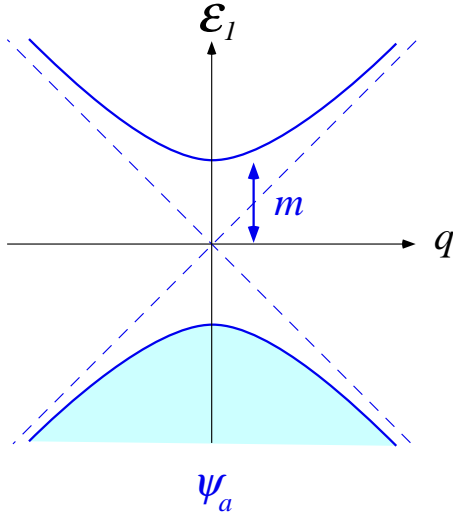


FIG. 3: The mean field picture of the  $SO(N)$  GN model. There are four flavors of relativistic massive fermions  $\psi_a$ , with dispersion  $\epsilon_1(q) = \pm\sqrt{m^2 + q^2}$ . The negative energy bands are filled, while the positive energy bands are empty. As in a semi-conductor, the positive and negative energy bands are separated by a finite gap  $2m$ .

## 2. Mean-field picture

It is instructive to see how these excitations arise in a mean-field treatment of the GN interaction. The mean-field treatment becomes exact for the  $SO(N)$  generalization of the GN model for large even  $N$ . To carry it out, we employ the Dirac fermion version of the Hamiltonian, Eq. 4.4. In the mean-field approximation, the bilinear  $\psi_a^\dagger \tau^y \psi_a$  acquires an expectation value, and the “quasi-particle” Hamiltonian density becomes

$$\mathcal{H}_{\text{MF}} = \psi_a^\dagger i\tau^z \partial_x \psi_a - \Delta \psi_a^\dagger \tau^y \psi_a, \quad (4.33)$$

where  $\Delta = 2g\langle\psi_a^\dagger \tau^y \psi_a\rangle$  is a mean-field gap parameter. The mean-field Hamiltonian is simply that of four massive Dirac equations. It is easily diagonalized in momentum space, using  $\psi_a(q) = \exp(i\Omega(q)\tau^x/2)\tilde{\psi}_a$ , where  $\Omega(q) = \cot^{-1}(vq/\Delta)$ , which gives

$$H_{\text{MF}} = \int \frac{dq}{2\pi} \epsilon_1(q) \tilde{\psi}_a^\dagger \tau^z \tilde{\psi}_a, \quad (4.34)$$

with  $\epsilon_1(q) = \sqrt{m^2 + q^2}$  and the mass  $m = \Delta$ . From the diagonalized form it is straightforward to determine the MF estimate,

$$m_{\text{MF}} = 2\Lambda e^{-\pi/Ng}, \quad (4.35)$$

for the general  $SO(N)$  case, where  $\Lambda \sim t$  is a momentum cut-off. The exponential dependence on  $g$  can be

understood from the marginality of the interactions under the RG scaling transformation. The picture is that of a “semi-conductor”, as indicated schematically in Fig. 3. These massive Dirac particles and their antiparticles may be identified with the fundamental fermion  $SO(8)$  vector multiplet. The even and odd kinks likewise arise from applying the same decoupling to the even and odd fermion representations of the Hamiltonian.

While Eq. 4.33 is correct for  $SO(\infty)$ , it requires corrections otherwise. For finite  $N$ , the chiral “order parameter”  $\Delta$  fluctuates around its vacuum value, and these fluctuations generate *attractive* interactions between the GN fermions. The attractive interactions lead to the formation of two-particle bound states, whose mass  $m_2 = 2m[1 - (\pi^2/2N^2) + O(N^{-4})]$  approaches twice the fermion mass for  $N \gg 1$ , due to the weakness of the interactions in this limit. For  $SO(8)$ , however, the inter-fermion interactions are not weak, and the bound states have the strongly reduced mass  $m_2 = \sqrt{3}m$ . The 28 bound states of two fermions form the abovementioned rank 2 tensor multiplet. A priori, one might expect three such multiplets, arising from bound states of the three sets of fermions. We will see, however, in the next section that this does not lead to any new particle content. Indeed, the particles in the tensor multiplet can be equally well viewed as bound states of fundamental, even, or odd fermions.

## 3. Semi-classical picture

These excitations can be readily understood in the semi-classical limit of the Bosonized Hamiltonian. In this language, particles correspond to classical solitons, in which the phase fields  $\theta_a$  connect different vacuum (classical minimum energy) values at  $x = \pm\infty$ . The winding numbers of these solitons have a direct connection to the  $SO(8)$  charges, since by bosonization

$$\begin{aligned} \Delta\theta_a &= \theta(\infty) - \theta(-\infty) = \int_{-\infty}^{\infty} dx \partial_x \theta_a \\ &= 2\pi N_a. \end{aligned} \quad (4.36)$$

Thus each of the GN particles labelled by the four quantum numbers  $(N_1, N_2, N_3, N_4)$  can be readily transcribed into a semi-classical soliton. The fundamental fermions are those configurations in which *one* of the four phase fields  $\theta_a$  changes by  $\pm 2\pi$ . The second type of soliton changes all four  $\theta_a$  fields by  $\pm\pi$ , which changes  $\cos\theta_a \rightarrow -\cos\theta_a$ , but leaves the vacuum energy unchanged. The  $2^4 = 16$  possible “kinks” form the semi-classical analog of the even and odd kink  $SO(8)$  octets.

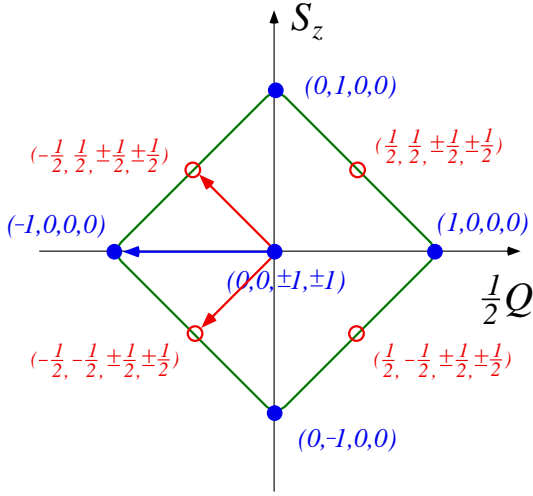


FIG. 4: The 24 mass  $m$  excitations of the  $SO(8)$  GN model, projected into the  $(N_1, N_2) = (Q/2, S_z)$  plane. Full and open circles indicate the “fundamental” fermions and kinks, respectively. All 24 excitations lie on the unit sphere in the full four-dimensional Cartan space. The equivalence of a fundamental fermion and an even and odd kink can be seen graphically by simple vectorial addition, e.g. the odd kink  $(-1, 1, 1, 1)/2$  and the even kink  $(-1, 1, 1, 1)/2$  add to form the GN fermion  $(-1, 0, 0, 0)$ .

While the even and odd kinks exist for general  $N$ , for the special case of  $SO(8)$ , triality implies that the kinks and fundamental solitons are on an equal footing. This is most easily seen using a simple graphical construction. Construct an  $N/2$ -dimensional space (for  $N$  even) with axes  $\theta_a$ . In this space, draw a lattice consisting of a point for each vacuum configuration of the fields. All possible solitons can be represented on this lattice as lines connecting different points to the origin (see Fig. 4). The fundamental fermions are then the line segments to the neighboring points along the axes. For  $N = 8$ , however, there are another 16 points equidistant to the origin, which represent the even and odd kinks (for  $N > 8$ , these are further from the origin, while for  $N < 8$  they are in fact closer). In this case, the even or odd kink segments form equally good orthonormal axes in this space, and viewed in this basis, the three sets of particles cyclically exchange their roles.

One can also compose these particles by vectorial addition. For instance, an even and an odd kink can be added to form a fundamental fermion. The 2-particle bound states may also be visualized in this way, by adding e.g. two different fundamental fermion vectors. From this construction it is easy to see that any such 2-particle state can be equally well composed from two even or two odd kinks. There is thus only a single 28-fold tensor multiplet of 2-particle bound states.

## E. Consequences for the D-Mott phase

We are now in a position to discuss the nature of the ground state and excitation spectrum in the D-Mott phase, using the technology of the GN model.

### 1. Gauge redundancy

To proceed, we must first describe the boundary conditions and gauge-redundancy needed to fully specify the model. Since the phase fields were originally introduced to bosonize the (physical) electron operators, the chiral electron phases are defined only moduli  $2\pi$ ,

$$\phi_{P_i\alpha}(x, \tau) \leftrightarrow \phi_{P_i\alpha}(x, \tau) + 2\pi\mathcal{A}_{P_i\alpha}(x, \tau), \quad (4.37)$$

where the  $\mathcal{A}_{P_i\alpha}$  are integers. These integers describe a sort of gauge redundancy in the description: semiclassical phase configurations which differ only by a different choice of  $\mathcal{A}_{P_i\alpha}$  are to be treated as identical quantum states. Furthermore, as for any gauge theory, physical operators must be gauge-invariant, i.e. unchanged under the operation in Eq. 4.37, which can be performed *locally*.

### 2. Uniqueness of the ground state

From both the standpoint of the fermionic GN Hamiltonian and its bosonized sine-Gordon form, the system appears to exhibit broken symmetry. The conventional GN model has a spontaneously broken “chiral” symmetry: the hamiltonian is invariant under the chiral transformation  $\psi_a \rightarrow \tau^z \psi_a$ , however, the chiral order parameter  $\Delta = 2g\langle\psi_a^\dagger \tau^y \psi_a\rangle \neq 0$  and changes sign under this transformation. In the bosonization language, this transformation corresponds to  $\theta_a \rightarrow \theta_a + \pi$  (for all  $a$ ), which takes  $\cos \theta_a \rightarrow -\cos \theta_a$ . The bosonic model appears to have even more broken symmetries, i.e. there is a countably infinite set of semiclassical vacua, related by the additional transformations  $\theta_a \rightarrow \theta_a + 2\pi n_a$ , for integer  $n_a$ .

On physical grounds, however, we expect that the D-Mott phase has no broken symmetry, and consequently a unique ground state. To reconcile this apparent discrepancy, we must account for the fact that the phases  $\theta_a$  are not gauge invariant. Indeed apparently different vacua may represent the same physical state in a different gauge. To establish the physical equivalence between different vacua is a rather tedious and technical exercise, although straightforward. In Appendix B we carry through this exercise and demonstrate that *all* of the semi-classical vacua do indeed correspond to the same physical state. Thus, as expected, there are no broken symmetries in the D-Mott phase and the ground state is unique.

### 3. Quantum numbers

To connect the GN results with the physical two-leg ladder system, we now consider the quantum numbers of the various excitations. Each quantum number corresponds to some conserved quantity in the system. The most physically interesting are the charge, spin, momentum along the  $x$  direction, and parity (or equivalently, momentum in the  $y$  direction). The charge and spin are conserved quantities corresponding to continuous global symmetries, so we can work directly with the Hermitian generators

$$Q = \int dx c_{Pj\alpha}^\dagger c_{Pj\alpha}, \quad (4.38)$$

$$S = \int dx c_{Pj\alpha}^\dagger \frac{\sigma_{\alpha\beta}}{2} c_{Pj\beta}. \quad (4.39)$$

Since the translational and leg-interchange symmetries are discrete, we should really speak of the unitary operators themselves. Since right- and left-moving particles in band  $j$  carry quasi-momentum  $\pm k_{Fj}$ , respectively, the translation operator is simply

$$\hat{T}_x = e^{i \sum_j k_{Fj} (N_{Rj} - N_{Lj})}, \quad (4.40)$$

where  $N_{Pj} = \int dx \sum_\alpha c_{Pj\alpha}^\dagger c_{Pj\alpha}$  is the total number of electrons in band  $j$  with chirality  $P$ . The quasi-momentum  $P_x$  is defined by  $\hat{T}_x = \exp(iP_x)$ . Because the anti-bonding (band 1) operators have  $k_y = \pi$ , the parity or translation operator in the  $y$  direction is

$$\hat{T}_y = e^{i\pi N_1}, \quad (4.41)$$

where  $N_1 = N_{R1} + N_{L1}$ .

In the weak-coupling limit,  $U \ll t, t_\perp$ , there are two additional conserved quantities, the band spin difference  $S_{12}^z = S_1^z - S_2^z$  and the relative band chirality  $P_{12} = (N_{R1} - N_{L1} - N_{R2} + N_{L2})/2$ .

It is useful to rewrite these expressions in terms of the bosonized phase variables. Because the symmetry generators involve spatial integrals of fermionic bilinears, they can be expressed in terms of the winding numbers  $\Delta\theta_a$  and their conjugates

$$\Delta\varphi_a = \int_{-\infty}^{\infty} dx \partial_x \varphi_a(x) = \varphi_a(\infty) - \varphi_a(-\infty). \quad (4.42)$$

Using Eqs. 2.18-2.21, we find

$$Q = \frac{\Delta\theta_1}{\pi}, \quad (4.43)$$

$$S^z = \frac{\Delta\theta_2}{2\pi}, \quad (4.44)$$

$$S_{12}^z = \frac{\Delta\theta_3}{2\pi}, \quad (4.45)$$

$$P_{12} = \frac{\Delta\theta_4}{2\pi}, \quad (4.46)$$

$$\hat{T}_x = \exp \left[ \frac{i}{2} \left( \Delta\varphi_1 + \frac{(k_{F1} - k_{F2})}{\pi} \Delta\theta_4 \right) \right], \quad (4.47)$$

$$\hat{T}_y = \exp \left[ \frac{i}{2} (\Delta\theta_1 + \Delta\varphi_4) \right]. \quad (4.48)$$

As discussed in the previous section, the winding numbers of the  $\theta_a$  are just the  $SO(8)$  conserved charges. Thus the first four conserved quantities can be directly transcribed for all the GN excitations, i.e.  $(Q, S^z, S_{12}^z, P_{12}) = (2N_1, N_2, N_3, N_4)$ . These are tabulated in the first three columns in Table 1.

The momentum and parity of the particles are more complicated, however, because Eqs. 4.47–4.48 contain the conjugate fields  $\Delta\varphi_1, \Delta\varphi_4$ . As such,  $P_x$  and  $P_y$  are not simply determined from the  $SO(8)$  charges  $N_a$ . The additional physics required is the operator content of the original electron problem.

To see how this comes in, let us imagine a local operator  $\mathcal{O}^\dagger(\{N_a\}; x)$ , which creates the particle with charges  $\{N_a\}$  when acting on the ground state, i.e.

$$\mathcal{O}^\dagger(\{N_a\}; x)|0\rangle = |\{N_a\}; x\rangle, \quad (4.49)$$

where  $|\{N_a\}\rangle$  is the quantum state with one excited  $\{N_a\}$  particle localized at  $x$ . Now consider the exponential of a phase field  $\varphi_a$ . It can be rewritten as the line integral of the momentum conjugate to  $\theta_a$ , i.e.

$$e^{-iN_a\varphi_a(x)/2} = e^{i2\pi N_a \int_x^\infty dx \Pi_a(x)}, \quad (4.50)$$

where  $\Pi_a(x) = \partial_x \varphi_a / (4\pi)$  is the momentum conjugate to  $\theta_a$ , i.e.  $[\theta_a(x), \Pi_b(x')] = i\delta_{ab}\delta(x - x')$ . Since the momentum  $\Pi_a$  generates translations of the phase  $\theta_a$ , the exponential operator creates a soliton of size  $2\pi N_a$  located at the point  $x$ . In order to have the correct winding numbers, the desired quantum operator must thus have the form

$$\mathcal{O}^\dagger(\{N_a\}; x) = \Lambda[\{\theta_a\}; \{N_a\}] e^{-iN_a\varphi_a/2}. \quad (4.51)$$

Here we have included an arbitrary function  $\Lambda$  of the  $\theta_a$  fields, which does not wind the phase and thus does not affect the  $SO(8)$  charges.

To determine  $\Lambda$ , we next impose gauge invariance. Consider first the operators which create the fundamental fermions, with only one non-zero  $N_a = \pm 1$ . The creation operator takes the form

$$\mathcal{O}_a^\pm = \tilde{\Lambda}_a[\{\theta_a\}] e^{\mp i(\varphi_a + \theta_a)/2}, \quad (4.52)$$

where we have removed a factor  $e^{\mp i\theta_a/2}$  from  $\Lambda$  to define  $\tilde{\Lambda}_a^\pm$ . This is desirable because the last factor (up to a Klein factor  $\kappa_a$ ) is simply the GN fermion operator  $\psi_{Ra}^\dagger$  ( $\psi_{Ra}$  for the lower sign). Now  $\mathcal{O}_a^\pm$  must be invariant under all possible gauge transformations, Eq. 4.37. It is a straightforward exercise to show that the most general form for  $\tilde{\Lambda}_a^\pm$  is the same for all the fundamental fermions, and is given by

$$\tilde{\Lambda} = \mathcal{O}_s \sum'_{\{k_a\}} \lambda_{\{k_a\}} e^{i \sum_a k_a \theta_a}, \quad (4.53)$$

where  $\sum'$  indicates a sum over all quadruplets of integers with  $\sum_a k_a$  even, and

$$\mathcal{O}_s = e^{\frac{i}{2}(\theta_1 + \theta_2 + \theta_3 - \theta_4)}. \quad (4.54)$$

Note that  $\tilde{\Lambda}$  *does not* include a term proportional to unity, which implies that a single GN fermion is by itself not gauge-invariant and hence unphysical. Instead, physical particles have an attached operator  $\mathcal{O}_s$  (or its counterparts with extra factors from the  $\sum'$  term).  $\mathcal{O}_s$  represents a Jordan-Wigner “string”, and can be rewritten only non-locally in terms of the fermion fields. It modifies the momentum and statistics of the fundamental fermions to those of the physical excitations.

It is now straightforward to determine the quasi-momentum and parity of the fundamental fermions using the translation operators in Eqs. 4.47–4.48. In particular, we must have

$$\hat{T}_x \mathcal{O}_a^\pm \hat{T}_x^{-1} = e^{iP_x(a)} \mathcal{O}_a^\pm, \quad (4.55)$$

$$\hat{T}_y \mathcal{O}_a^\pm \hat{T}_y^{-1} = e^{iP_y(a)} \mathcal{O}_a^\pm. \quad (4.56)$$

The left-hand sides of Eqs. 4.55–4.56 can be evaluated by employing the commutators of the Bose fields to obtain:

$$\hat{T}_x \theta_a \hat{T}_x^{-1} = \theta_a + 2\pi\delta_{a1}, \quad (4.57)$$

$$\hat{T}_x \varphi_a \hat{T}_x^{-1} = \varphi_a + 2(k_{F1} - k_{F2})\delta_{a4}, \quad (4.58)$$

and

$$\hat{T}_y \theta_a \hat{T}_y^{-1} = \theta_a + 2\pi\delta_{a4}, \quad (4.59)$$

$$\hat{T}_y \varphi_a \hat{T}_y^{-1} = \varphi_a + 2\pi\delta_{a1}. \quad (4.60)$$

Eq. 4.55 can be written as a product of three terms:

$$\begin{aligned} \hat{T}_x \mathcal{O}_a^\pm \hat{T}_x^{-1} &= \hat{T}_x \left( \sum' \right) \hat{T}_x^{-1} \times \hat{T}_x \mathcal{O}_s \hat{T}_x^{-1} \\ &\times \hat{T}_x e^{\mp i(\varphi_a + \theta_a)/2} \hat{T}_x^{-1}. \end{aligned} \quad (4.61)$$

Consider the first term. Using the above commutators one can readily show that the sum in Eq. 4.53 is invariant under  $x$ -translations. The string, however, carries momentum  $P_x = \pi$ :

$$\hat{T}_x \mathcal{O}_s \hat{T}_x^{-1} = -\mathcal{O}_s = e^{i\pi} \mathcal{O}_s. \quad (4.62)$$

This momentum must be added to the “bare” momentum of the GN fermion, given by the last term in Eq. 4.61. A similar calculation for  $\hat{T}_y$  shows that  $\sum'$  is again invariant, but  $\mathcal{O}_s$  carries transverse momentum  $\pi$ . The resulting net momenta of the fundamental solitons are summarized in the last two columns of Table 1.

Similar manipulations hold for the kink excitations. In particular, the even kink creation operators must obey

$$\mathcal{O}_a^{e\pm} = \sum'_{\{k_a\}} \lambda_{\{k_a\}} e^{i \sum_a k_a \theta_a} \times e^{\mp i(\varphi_a^e + \theta_a^e)/2}, \quad (4.63)$$

and similarly for the odd kinks,

$$\mathcal{O}_a^{o\pm} = \sum'_{\{k_a\}} \lambda_{\{k_a\}} e^{i \sum_a k_a \theta_a} \times e^{\mp i(\varphi_a^o - \theta_a^o)/2}. \quad (4.64)$$

Note that the choice to factor out the right-moving even and GN fermions in Eqs. 4.52, 4.63 and left-moving odd fermions in Eq. 4.64 is arbitrary. A right-mover can always be converted to a left-mover and vice-versa by absorption of an  $e^{\pm i\theta}$  factor into a redefinition of the “string” part of the soliton creation operator. For the even and odd kinks, the above choice is particularly convenient, since the right-moving even fields and left-moving odd fields are *exactly* bare electron operators, and hence manifestly physical. We see from Eqs. 4.63–4.64 that the kinks have the quantum numbers of bare electrons. A remarkable consequence of this result is that the number of single-electron degrees of freedom has effectively *doubled* relative to the free fermi gas, since each of the 16 kinks can be created with arbitrary momentum (relative to its base momentum of  $\pm k_{Fi}$ ), including particles *below* the former fermi sea and holes *above* it. The momenta calculated from Eqs. 4.63–4.64 complete the last two columns of Table 1.

$(N_1, N_2, N_3, N_4)$	$Q$	$S^z$	$P_x$	$P_y$
$(1, 0, 0, 0)$	2	0	0	0
$(0, 1, 0, 0)$	0	1	$\pi$	$\pi$
$(0, 0, 1, 0)$	0	0	$\pi$	$\pi$
$(0, 0, 0, 1)$	0	0	$2k_{F1}$	0
$(1, 1, 1, 1)/2$	1	$\frac{1}{2}$	$k_{F1}$	$\pi$
$(1, -1, -1, 1)/2$	1	$-\frac{1}{2}$	$k_{F1}$	$\pi$
$(1, 1, -1, -1)/2$	1	$\frac{1}{2}$	$k_{F2}$	0
$(1, -1, 1, -1)/2$	1	$-\frac{1}{2}$	$k_{F2}$	0
$(1, 1, 1, -1)/2$	1	$\frac{1}{2}$	$-k_{F1}$	$\pi$
$(1, -1, -1, -1)/2$	1	$-\frac{1}{2}$	$-k_{F1}$	$\pi$
$(1, 1, -1, 1)/2$	1	$\frac{1}{2}$	$-k_{F2}$	0
$(1, -1, 1, 1)/2$	1	$-\frac{1}{2}$	$-k_{F2}$	0

Table 1: Physical quantum numbers of the mass  $m$  particles labelled by their four  $U(1)$  charges. The antiparticles are obtained by changing the sign of all the quantum numbers.

## F. $SU(2)$ invariance and spin multiplets

We conclude this section with a remark on  $SU(2)$  invariance and the excitations with spin. In Table 1, we have classified the mass  $m$  excitations in the D-Mott phase by the four  $U(1)$  charges ( $SO(8)$  Cartan generators)  $N_a$ . Another almost equivalent choice is to label the particles by their charge, momentum, *total spin*  $S^2 = s(s+1)$  and spin projection  $S^z$ . It is fairly trivial to relabel the kinks in this way, reflecting their natural

correspondence with single-particle spin-1/2 excitations. They may be grouped into doublets with  $s = 1/2$  and  $S^z = \pm 1/2$ , e.g. the  $(1, 1, 1, 1)/2$  and  $(1, -1, -1, 1)/2$  kinks form a spin-1/2 doublet with  $Q = 1e$  and  $\mathbf{P} = (k_{F1}, \pi)$ . For the GN fermions, this is less trivial. The  $(\pm 1, 0, 0, 0)$  solitons are spin zero, and correspond to charge  $\pm 2e$  Cooper pairs with zero momentum. Similarly, the  $(0, 0, 0, \pm 1)$  fermions carry neither charge nor spin, and may be regarded as dressed particle-hole pairs carrying only momentum. The remaining four solitons are more nontrivial, however. Their spin content may be brought out by re-fermionizing the total spin operator, as in Eq. 4.17,

$$\mathbf{S} = \int dx [\mathbf{J}_R(x) + \mathbf{J}_L(x)], \quad (4.65)$$

with chiral currents,

$$J_P^A(x) = i\epsilon^{ABC} \eta_{PB} \eta_{PC}, \quad (4.66)$$

with  $A, B, C = 3, 4, 5$ . Thus the three Majorana fields  $\eta_{PA}$ , with  $A = 3, 4, 5$ , transform as a triplet of spin  $s = 1$  operators, i.e.

$$[S^A, \eta_{PB}] = -i\epsilon^{ABC} \eta_{PC}. \quad (4.67)$$

The other 5 GN Majorana fields commute with  $\mathbf{S}$ , and hence represent spin-singlet operators.

As was shown in the previous subsection, the physical GN excitations consist not of GN fermions but rather required an attached string  $\mathcal{O}_s$ . Fortunately, the string does not carry any spin, i.e.

$$\mathcal{O}_s \mathbf{S} \mathcal{O}_s^\dagger = \mathbf{S}. \quad (4.68)$$

Thus the true soliton excitations (GN fermions+strings) satisfy the same transformation rules with respect to spin as the bare Majorana fermions. The four remaining solitons  $(0, \pm 1, 0, 0)$  and  $(0, 0, \pm 1, 0)$ , which involve the four Majorana Fermions  $\eta_A$  with  $A = 3, 4, 5, 6$ , can therefore be decomposed into an  $s = 1$  triplet and a spin-zero singlet (both with  $Q = 0$  and  $\mathbf{P} = (\pi, \pi)$ ). The triplet can be regarded as a minimum energy magnon, while the singlet can be grouped with the  $(0, 0, 0, \pm 1)$  solitons as another particle-hole excitation.

With the  $SU(2)$  invariance realized, we can tabulate the particles in the GN model in a slightly different way, classifying them by their  $SU(2)$  multiplet (i.e.  $s = 0, 1/2$  or  $1$ ), charge, and momentum. To label the particles classified in this way, the abelian  $(N_1, N_2, N_3, N_4)$  notation is no longer convenient, since it does not respect the  $SU(2)$  invariance. Instead, we can schematically indicate the 8 particles in the vector multiplet by  $\eta_A$  and the 28 in the tensor multiplet by  $\eta_A \eta_B$  (remembering that  $\eta_B \eta_A = -\eta_A \eta_B$ ). For convenience, we list the 8 GN fermions and the 28 mass  $\sqrt{3}m$  bound states in this way in Table 2 (we do not list the remaining 16 particles, since they have the quantum numbers of electrons and are easily remembered in this way).

Label	$Q$	$s$	$P_x$	$P_y$
$\eta_1, \eta_2$	$\pm 2$	0	0	0
$\eta_3, \eta_4, \eta_5$	0	1	$\pi$	$\pi$
$\eta_6$	0	0	$\pi$	$\pi$
$\eta_7, \eta_8$	0	0	$\pm 2k_{F1}$	0
$\eta_1 \eta_2$	0	0	0	0
$\eta_7 \eta_8$	0	0	0	0
$\eta_A \eta_B, A = 1, 2; B = 7, 8$	$\pm 2$	0	$\pm 2k_{F1}$	0
$\eta_A \eta_6, A = 1, 2$	$\pm 2$	0	$\pi$	$\pi$
$\eta_6 \eta_A, A = 7, 8$	0	0	$\pm(k_{F1} - k_{F2})$	$\pi$
$\eta_A \eta_B, A \neq B = 3, 4, 5$	0	1	0	0
$\eta_A \eta_6, A = 3, 4, 5$	0	1	0	0
$\eta_A \eta_B, A = 1, 2; B = 3, 4, 5$	$\pm 2$	1	$\pi$	$\pi$
$\eta_A \eta_B, A = 3, 4, 5; B = 7, 8$	0	1	$\pm(k_{F1} - k_{F2})$	$\pi$

Table 2: Physical quantum numbers of the mass  $m$  (above horizontal line) and mass  $\sqrt{3}m$  (below horizontal line) particles.

## V. CORRELATION FUNCTIONS AND PHYSICAL PROPERTIES

We have seen that in the weak-coupling limit, the two-leg ladder possesses an enhanced symmetry. The effective theory in this limit is the  $SO(8)$  GN model, which is both exactly integrable and exhibits a remarkable “triviality”. In this section we will discuss a variety of the resulting physical consequences.

The most remarkable consequence of triality is the equality of the single-particle and two-particle gaps.<sup>42,43</sup> The 16 kinks have the same quantum numbers as the bare electrons at the former Fermi surface. The single-particle gap, defined as the minimum energy needed to add an electron or hole to the system, is thus simply  $\Delta_1 = m$ . The 8 GN fermions, however, have charge  $Q = \pm 2$  or  $Q = 0$ , and thus represent excitations corresponding to an even number of electrons and/or holes. For instance, electron or hole pairs can be added with zero net momentum via the  $(\pm 1, 0, 0, 0)$  solitons, while spin-1 excitations may be added with momentum  $(\pi, \pi)$  via the  $(0, \pm 1, 0, 0)$  and  $(0, 0, \pm 1, 0)$  solitons (more precisely the  $\eta_5$  state). The gap for all 8 minimal energy 2-particle excitations is also  $\Delta_2 = m$ .

The equality of the single-particle and two-particle gaps is in marked contrast to the behavior of other more conventional insulators. In a band insulator (such as the two-leg ladder at half-filling with  $t_\perp \gg t$ ), the single-particle gap is just the band gap, while the two-particle gaps are twice as large:  $\Delta_2 = 2\Delta_1$ . Another familiar case is the strong-interaction limit  $U \gg t$ . In this case, the single particle gap is huge  $\Delta_1 \sim U$ , while the lowest two-particle (e.g. spin) gaps are much smaller  $\Delta_2 \sim t^2/U \ll \Delta_1$  or indeed vanishing ( $\Delta_2 = 0$ ) for ordered or quasi-long-range ordered antiferromagnets (e.g.  $d = 2$  or single-chain Hubbard models). The detailed



mathematical mapping between the GN, odd, and even fermion fields allows us to extend the relationship between the single-particle and two-particle properties beyond the values of the gaps, as we detail below.

First, we will discuss several correlation functions which characterize the spin and charge dynamics of the system. The most interesting of these are the single-particle spectral function, measurable by electron photoemission, and the dynamic spin structure factor, which is probed by inelastic neutron scattering. Other interesting correlators include the current-current correlation function, which determines the conductivity, the density-density correlation function and pairing correlation function, which can be measured in numerical simulations.

### A. Single-particle spectral function

First consider the single-particle Greens function,

$$G_1(\mathbf{k}, \tau) = \sum_{\ell x} e^{-ik_y \ell - ik_x x} T_\tau \langle 0 | a_{1+\ell\alpha}(x, \tau) a_{1\alpha}^\dagger(0, 0) | 0 \rangle, \quad (5.1)$$

where  $T_\tau$  is the (Euclidean) time-ordering symbol and  $\mathbf{k} = (k_x, k_y)$ . The right-hand side is independent of  $\alpha$  by spin-rotational invariance; however, we choose to define the spectral function for fixed  $\alpha$ , i.e. no sum is implied above. In general, the single-particle spectral functions can be extracted from  $G_1$  by Fourier transformation. Defining  $G_1(\mathbf{k}, i\omega) = \int d\tau G_1(\mathbf{k}, \tau) \exp(i\omega\tau)$ , one finds

$$\frac{1}{\pi} \text{Im} G_1(\mathbf{k}, i\omega \rightarrow \omega + i\delta) \rightarrow A_{1p}(\mathbf{k}, \omega) + A_{1h}(-\mathbf{k}, -\omega), \quad (5.2)$$

where the particle and hole spectral functions are

$$A_{1p}(\mathbf{k}, \omega) = \sum_n \left| \langle n | a_{1\alpha}^\dagger | 0 \rangle \right|^2 \delta(\mathbf{k} - \mathbf{k}_n) \delta(\omega - E_n), \quad (5.3)$$

$$A_{1h}(\mathbf{k}, \omega) = \sum_n \left| \langle n | a_{1\alpha} | 0 \rangle \right|^2 \delta(\mathbf{k} - \mathbf{k}_n) \delta(\omega - E_n). \quad (5.4)$$

Here we have abbreviated  $\delta(\mathbf{k}) \equiv 2\pi\delta(k_x)\delta(k_y)$ . The task is then to evaluate  $G_1(\mathbf{k}, \tau)$ . In the weak-coupling limit studied here, this is obtained in two stages. We first integrate out the electron fields  $c_{i\alpha}^\dagger(k), c_{i\alpha}(k)$ , for  $|k - k_{Fi}| > \Lambda$ , which can be accomplished perturbatively in the interactions, since the energy denominators are finite away from the Fermi momenta. The perturbative corrections to the free-electron  $G_1(k, \tau)$  are therefore small in these regions. Within the cut-off region of width  $2\Lambda$ , we must employ the full RG treatment. The RG scales the problem onto the GN model, which thus applies at the lowest energies.

For the electron spectral function, the non-interacting result  $A_{1p/h}^0$  is trivial, since single electron states are exact eigenexcitations. The result is

$$A_{1p}^0(\mathbf{k}, \omega) = \delta(\omega - \varepsilon_1(\mathbf{k}))\theta(\omega), \quad (5.5)$$

$$A_{1h}^0(\mathbf{k}, \omega) = \delta(\omega + \varepsilon_1(\mathbf{k}))\theta(\omega), \quad (5.6)$$

where  $\varepsilon_1(\mathbf{k}) = -t \cos k_x - \frac{t}{2} \cos k_y$ . Interactions of course modify this form somewhat, leading to some spectral weight away from  $\omega = \varepsilon_1(\mathbf{k})$ , and a broadening of the delta-function peak in  $A_{1p/h}$  for some momenta. In weak-coupling, away from small  $\omega$ , however, both effects are small. We will return to them after we consider the behavior of the spectral function for small frequencies.

The low-frequency limit of  $A_{1p}$  is dominated by momentum near the Fermi points. Transforming to the slowly-varying Luttinger fields, we have

$$G_1(Pk_{Fi} + q, k_{yi}; \tau) \approx \int dx e^{-iqx} \langle c_{Pi\alpha}(x, \tau) c_{Pi\alpha}^\dagger(0, 0) \rangle, \quad (5.7)$$

for  $q \ll 1$ , where  $k_{yi} = (2 - i)\pi$ . Unfortunately, integrability does *not* give exact forms for the time-dependent correlation functions in Eq. 5.7. A considerable amount can be learned, however, from the exact excitation spectrum and from approximate methods.

The spectrum determines the *support* of  $A_{1p/h}(\mathbf{k}, \omega)$ . From Eq. 5.3, it is clear that  $A_{1p/h}(\mathbf{k}, \omega)$  is non-zero only when there exists an excitation (or more than one) with momentum  $\mathbf{k}$ , spin  $s = 1/2$ , charge  $\pm e$  and energy  $\omega$ . From Table 1, we see that the sixteen kinks have exactly the appropriate quantum numbers for all possible momenta near the four (i.e. two pairs) fermi points with either  $S^z = \pm 1/2$  and charge  $\pm e$ . We therefore expect that  $A_{1p/h}(\mathbf{k}, \omega)$  first becomes non-zero for  $\omega = \sqrt{(k_x - k_{Fi})^2 + (k_y - k_{yi})^2} + m^2$ . Since the kinks are isolated particles with a fixed energy-momentum relation, these excitations give a sharp delta-function peak in  $A_{p/h}$ . It is natural to identify this peak as the continuation of the non-interacting delta-function in Eqs. 5.5-5.6 to the region near the Fermi points. At higher energies other states should contribute to the spectral weight. A quick consideration of the quantum numbers is sufficient to conclude that none of the mass  $\sqrt{3}m$  bound states have the appropriate quantum numbers (e.g. all have charge zero or  $\pm 2e$ ). The next lowest-lying excitations with the quantum numbers of individual electrons are in fact scattering (unbound) states of a kink and a GN fermion. For instance, a  $(1, 1, 1, -1)/2$  kink and a  $(0, 0, 0, 1)$  fermion can form a scattering state with the quantum numbers of a spin up electron with momentum  $(k_{F1} + q, \pi)$ , with  $q \ll 1$ . Similarly, other combinations of kinks with the  $(0, 0, 0, \pm 1)$  GN fermions contribute to the single-particle spectral weight at  $(\pm 3k_{F1} + q, \pi)$ ,  $(\pm k_{F2} + q, 0)$ , and  $(\pm 3k_{F2} + q, 0)$ . All these form continua with  $\omega > \epsilon_c(q) = 2\sqrt{m^2 + (q/2)^2}$  at each momenta, since



the energy at a particular momenta can always be increased continuously by shifting the kink and the bound-state momenta in opposite directions. Further excitation of more than one  $(0, 0, 0, \pm 1)$  quanta leads to spectral weight at all momenta separated by an even multiple of  $2k_{F1}$ , i.e.  $\mathbf{k} = ((2n + 1)k_{F1}, \pi)$ . The excitation gap for such a point increases, however, by an additional factor of  $m$  as each GN fermion (i.e. factor of  $(2k_{F1}, 0)$  away from the Fermi points) is added. Furthermore, the higher harmonic contributions to the spectral function are expected to have small amplitudes, as they involve multiple scatterings of the original injected electron (see below).

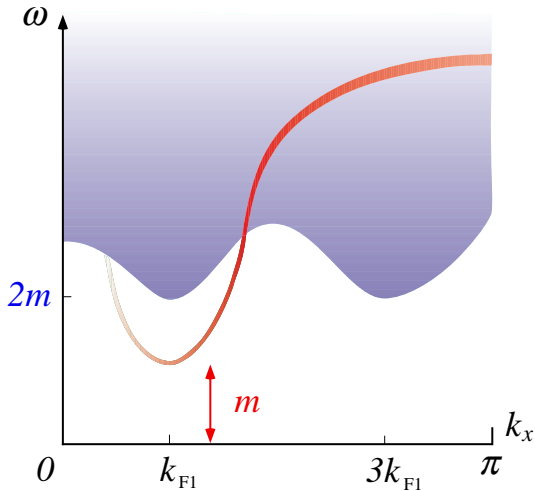


FIG. 5: Schematic plot of the single-particle electron spectral function  $A_{1p}(k_x, k_y = \pi, \omega)$ . The curve below the continuum indicates a sharp resonance, i.e. a delta-function peak in  $A_{1p}$ , which acquires a finite width once it passes inside the continuum due to the onset of decay processes. The continuum above energy  $2m$  coincides with the creation of (unbound) scattering states of a single kink and a GN fermion.

To understand the magnitude of  $A_{1p/h}(\mathbf{k}, \omega)$  in the allowed regions requires a knowledge of the matrix elements in Eq. 5.3, or of the full Green’s function in Eq. 5.7. Since exact results are unavailable for these quantities, we consider instead the mean-field approximation. Without loss of generality, let us consider momenta near the particular Fermi point  $\mathbf{k} \approx (k_{F1}, \pi)$  and spin  $S^z = +1/2$ . Using Eq. 5.7 and Eqs. 4.28-4.31, the bare electron operators can be rewritten exactly in terms of even Fermion fields,

$$\langle c_{R1\alpha}(x, \tau) c_{R1\alpha}^\dagger(0, 0) \rangle = \langle \psi_{R1}^e(x, \tau) \psi_{R1}^{e\dagger}(0, 0) \rangle. \quad (5.8)$$

In the mean-field approximation, the exact eigenstates are created by the rotated operators for particles  $\tilde{\psi}_{Ra}^{e\dagger}(k)$  and holes  $\tilde{\psi}_{La}^e(k)$  (see Sec. IV.D.2), so that the above expectation value can be computed by a simple rotation. One finds

$$A_{1p}^{\text{MF}}(k_{F1} + q, \pi, \omega) =$$

$$\frac{1}{2} \left( 1 + \frac{q}{\sqrt{q^2 + m^2}} \right) \delta(\omega - \sqrt{q^2 + m^2}). \quad (5.9)$$

The  $q$ -dependent factor out front arises from the rotation to the  $\tilde{\psi}$  spinor, and is analogous to a “coherence factor” in superconductivity. Eq. 5.9 captures a simple and appealing physical effect. Although single-kink states exist for all momenta, their contribution to the spectral weight is suppressed for  $q \ll -m$  by the “coherence factor” above. Such a negative momentum corresponds to the addition of an electron at a momentum *inside* the Fermi sea. Interactions deplete the Fermi sea slightly near the Fermi points, allowing electrons to be added, but with a weight that vanishes as  $q \rightarrow -\infty$ , i.e. deep within the sea. Similarly, the hole spectral function has weight *outside* the Fermi sea, since some excited particles exist as part of the ground state. Unfortunately, the mean-field approximation is not sophisticated enough to capture the continuum at  $\omega > \epsilon_c(q)$ , since the  $\tilde{\psi}$  fields create exact eigenstates in this limit. Thus the continuum is not present in Eq. 5.9. On physical grounds, however, we expect that it will be similarly suppressed for momenta inside the former Fermi sea.

Having determined the behavior of  $A_{1p/h}$  near the Fermi points and momenta separated from them by even multiples of  $(2k_{F1}, 0)$ , we return to the question of the spectral weight away from these points, at energies away from the non-interacting single-particle energy  $\epsilon_1(\mathbf{k})$ . In the non-interacting system, states with one added electron *plus* additional neutral electron-hole pairs in fact form a continuum away from the single-particle energy. Consider, for instance,  $k_y = \pi$ . The lowest energy continuum of states with a single added particle-hole pair (plus one electron) consists of those states in which both electrons are infinitesimally above the Fermi surface ( $k_1 = k_2 = k_{F1}$ ) and the hole makes up the missing momentum ( $k_3 = 2k_{F1} - k$ ). This begins at  $\epsilon_2(k_x, \pi) = \cos(2k_{F1} - k_x) - t_\perp/2$ , which is *below* the single-particle energy (i.e.  $\epsilon_2 < \epsilon_1$ ) for  $k_{F1} < k_x < 3k_{F1}$ , crossing zero again at  $k_x = 3k_{F1}$ . It does not contribute to the single-particle spectral function, however, due to orthogonality. In an interacting Fermi liquid, we would expect that an added electron can scatter into these states (i.e. emit a low energy particle-hole pair), and some weight would appear in  $A_{1p/h}$  associated with the continuum states.

In the weakly-interacting ladder, an added electron away from the Fermi points can also scatter to create neutral excitations, and some weight will appear in the regions near the non-interacting continuum for  $\omega \gtrsim \epsilon_2(\mathbf{k})$ . This continuum away from the Fermi points should merge smoothly into the continuum above  $\omega = 2m$  at the Fermi points (and the higher harmonics, e.g.  $(\pm 3k_{F1}, \pi)$ ). Clearly, since the single-particle energy begins *below* the continuum near the Fermi momenta and it is above the continuum far away, it must cross into the continuum at some point. Where it is below the continuum, we

expect that the spectral function retains a sharp delta-function peak. Once it passes above, however, the single-particle mode can decay into the continuum states, and should acquire a small width. Putting this behavior together with the spectral function near the Fermi points and higher harmonics, we arrive at the schematic single-particle spectral function illustrated in Fig. 5. The most dramatic feature is the sharp delta-function peak near the Fermi points which crosses into the continuum and acquires a width at higher energies.

### B. Spin structure factor

The spin spectral function can be defined in a similar way to the single-particle one. Consider the structure function

$$S^{ij}(\mathbf{k}, i\omega) = \frac{1}{2} \sum_{\ell\ell'x} \int d\tau e^{-ik_x x - ik_y(\ell - \ell') + i\omega\tau} \times T_\tau \langle 0 | S_\ell^i(x, \tau) S_{\ell'}^j(0, 0) | 0 \rangle, \quad (5.10)$$

where the lattice spin operator is  $\mathbf{S}_\ell(x) = a_{\ell\alpha}^\dagger \frac{\boldsymbol{\sigma}_{\alpha\beta}}{2} a_{\ell\beta}$ . The spin spectral function  $A_s$  is obtained from this in the usual way

$$\frac{1}{\pi} \text{Im} S^{ij}(\mathbf{k}, i\omega \rightarrow \omega + i\delta) \rightarrow A_s(\mathbf{k}, \omega) \delta^{ij}, \quad \text{for } \omega > 0. \quad (5.11)$$

The spectral decomposition of  $A_s$  is

$$A_s(\mathbf{k}, \omega) = \frac{1}{3} \sum_n |\langle 0 | S^i | n \rangle|^2 \delta(\mathbf{k} - \mathbf{k}_n) \delta(\omega - E_n). \quad (5.12)$$

As for the single-particle case, we expect that the spin spectral function will be approximately equal to its non-interacting value for  $\omega \gg m$ . A straightforward calculation for the non-interacting problem gives

$$A_s^0(\mathbf{k}, \omega) = \frac{1}{8\pi} \sum_{a,b=\pm 1} \frac{\Theta(1 - |r|)}{\sin \frac{k_x}{2} \sqrt{1 - r^2}} \times \left\{ \Theta \left[ b \cos \frac{k_x}{2} \sqrt{1 - r^2} + r \sin \frac{k_x}{2} + a t_\perp / 2 \right] - \Theta \left[ b \cos \frac{k_x}{2} \sqrt{1 - r^2} - r \sin \frac{k_x}{2} + a \frac{t_\perp}{2} \cos k_y \right] \right\}, \quad (5.13)$$

where  $r = (\omega + a \frac{t_\perp}{2} (\cos k_y - 1)) / (2 \sin \frac{k_x}{2})$ . Clearly, the non-interacting spin spectral function is considerably more complex than its single-particle counterpart. This is because the neutral spin-one excitations in the non-interacting system are particle-hole pairs, and thus comprise a continuous spectrum. The result in Eq. 5.13 is plotted in Fig. 6.

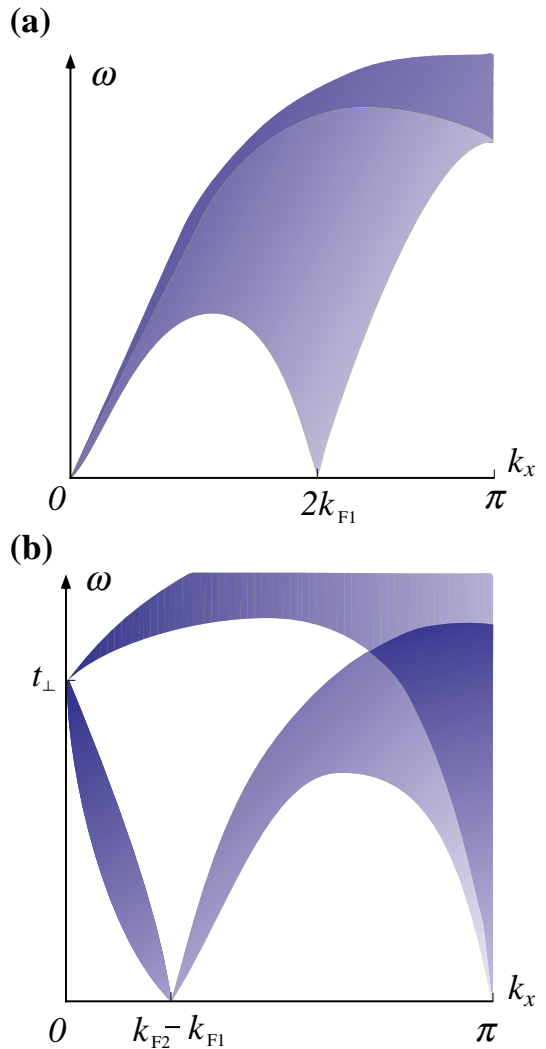


FIG. 6: Intensity plot of the non-interacting spin spectral function at (a)  $k_y = 0$ , (b)  $k_y = \pi$ . The darkness is proportional to the spectral weight, white indicating regions of phase space in which no particle-hole pairs exist.

For  $k_y = 0$ , the particle and hole must come from the same band. In this case low energy excitations exist near  $k_x = 0$ , when both are taken near the same Fermi point, and near  $k_x = \pm 2k_{F1}$  ( $k_x = \pm 2k_{F2}$  are equivalent to these values modulo  $2\pi$ ), when the particle and hole are taken from opposite Fermi points (still in the same band). Two branches of continua (from the bonding and anti-bonding bands) form as the momenta of the particles and holes are varied. For  $k_y = \pi$ , the particle and hole must come from opposite bands. In this case, the  $k_x = 0$  states have an energy of exactly  $t_\perp$ , since this requires a vertical transition. Low energy excitations exist near  $k_x = \pm(k_{F2} - k_{F1})$ , due to particle-hole pairs taken from two right-moving or two left-moving Fermi points. They also exist near  $k_x = \pi$ , when the particle and hole are taken from opposite sides of the Fermi surface. Extending these two branches of excitations gives the form shown in Fig. 6(b).

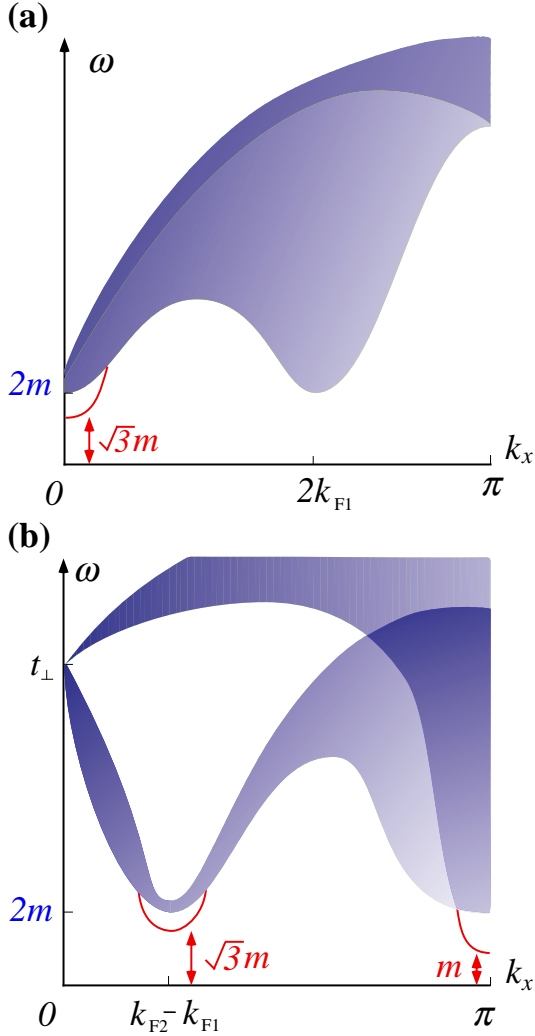


FIG. 7: Intensity plot of the interacting spin spectral function at (a)  $k_y = 0$ , (b)  $k_y = \pi$  in the presence of interactions. In the low-energy portion, various gaps develop and excitations with sharp delta-function peaks are present (see Sec. V.B). Note that the minimum energy spin excitations occur at  $\mathbf{k} = (\pi, \pi)$ .

As for the single-particle spectral function, introducing interactions allows for additional structure, and the low-lying excitations are raised up to energies of order  $m$ . In particular, from Table. 2, we see that the lowest lying neutral triplet states are the mass  $m$  GN fermions  $\eta_{3,4,5}$  at  $\mathbf{k} = (\pi, \pi)$ . The next highest energy neutral triplets are the mass  $\sqrt{3}m$  bound states. The  $\eta_{3,4,5}\eta_{7,8}$  have momenta  $(\pm(k_{F1} - k_{F2}), \pi)$ , while the  $\eta_{3,4,5}\eta_{4,5,3}$  and  $\eta_{3,4,5}\eta_6$  have momentum  $(0, 0)$ . Above these exist continua dispersing like  $\epsilon_c(q) = 2\sqrt{m^2 + (q/2)^2}$  away from all the aforementioned points and  $(\pm 2k_{F1}, 0)$  (the excitations at these last points arise from certain pairs of unbound kinks). Since there are no sharp resonances (delta-function peaks) in the non-interacting limit, we expect that the mass  $m$  and  $\sqrt{3}m$  peaks must broaden at higher energies to merge into the continua found there. A schematic form is shown in

Fig. 7.

### C. Optical conductivity

Another quantity of considerable experimental relevance is the optical conductivity. We are interested in the real part of the conductivity, defined by

$$\text{Re } \sigma(\omega) = \text{Im} \left[ \frac{\Pi(i\omega \rightarrow \omega + i\delta)}{\omega} \right], \quad (5.14)$$

where the ( $\mathbf{k} = \mathbf{0}$ ) current-current correlator is

$$\Pi(i\omega) = \frac{1}{2} \sum_{\ell\ell'} \int dx d\tau e^{i\omega\tau} \langle T_\tau J_\ell(x, \tau) J_{\ell'}(0, 0) \rangle. \quad (5.15)$$

The electrical current operator is

$$J_\ell(x) = \frac{e}{2i} \left( a_\ell^\dagger(x) a_\ell(x+1) - a_\ell^\dagger(x+1) a_\ell(x) \right). \quad (5.16)$$

To evaluate Eq. 5.15, only the slowly varying ( $\mathbf{k} = \mathbf{0}$ ) component of the current is needed. Decomposing the lattice fields into their continuum components using Eq. 2.2 and then applying the bosonization and refermionization rules, one finds the long-wavelength form

$$J_\ell \sim \sin k_{F1} \partial_x \phi_1 \quad (5.17)$$

$$= \frac{\sin k_{F1}}{2\pi} \psi_1^\dagger \tau^z \psi_1 \quad (5.18)$$

$$= \frac{\sin k_{F1}}{2\pi} (G_R^{12} - G_L^{12}). \quad (5.19)$$

From this form, the current operator clearly excites the mass  $\sqrt{3}m$   $\eta_1\eta_2$  bound states, as well as higher energy continuum scattering states with energies above  $2m$ . Since Eq. 5.14 is nothing but  $1/\omega$  times the spectral function of  $J$ , the zero temperature optical conductivity is thus zero for  $\omega < \sqrt{3}m$ , has a sharp (delta-function) peak at  $\omega = \sqrt{3}m$ , and a threshold with continuous weight for  $\omega > 2m$ . Based on the mean-field picture, we expect the spectral weight in the two-particle continuum to have a square root singularity (due to the van Hove singularity at the bottom of the band – see, e.g. Ref. 48), i.e.

$$\sigma(\omega) \approx A\delta(\omega - \sqrt{3}m) + B\sqrt{\frac{m}{\omega - 2m}}\Theta(\omega - 2m). \quad (5.20)$$

At non-zero temperatures it is difficult to determine  $\sigma(\omega)$  from the Kubo formula, Eq. 5.14. Instead, the general features can be argued on more conventional transport grounds, borrowing heavily from recent results of Damle and Sachdev<sup>49</sup> for *spin* dynamics of gapped 2-leg ladders. The important physical effect for  $T > 0$  is the presence of a non-zero equilibrium concentration ( $\propto e^{-m/T}$ ) of activated excitations. In the semi-conductor

analogy, these are activated particles and holes. In principle, all 24 mass  $m$  states have identical equilibrium concentrations; for  $T \ll m$  we expect that we can neglect the much smaller activated densities ( $O(e^{-\sqrt{3}m/T})$ ) of bound states.

In this case the low-frequency conductivity can be estimated using a simple Drude argument. We focus on the charged species of mass  $m$ , i.e. the  $\eta_{1,2}$  fundamental fermions and the kinks. Each of these contributes in parallel to the conductivity a term of the Drude form,

$$\sigma(\omega) = \frac{\sigma_0}{1 + i\omega\tau}, \quad (5.21)$$

with  $\sigma_0 = n\tau/m$ ,  $\tau$  a scattering time, and  $n$  the density of thermally excited carriers. Using the Boltzmann distribution, we have  $n \sim \sqrt{mT}e^{-m/T}$  for  $T \ll m$ . The average separation between particles  $l(T) = 1/n$  is thus much larger than their typical wavelength  $\lambda(T) \sim 2\pi/p \sim 1/\sqrt{mT}$ , obtained by equipartition. The particles thus behave essentially classically except during a collision, when they scatter strongly (as known, e.g. from the exact S-matrices for the  $SO(N)$  GN model), and their scattering time is determined simply by the time between collisions:  $\tau \sim l(T)m/p \sim T^{-1}e^{m/T}$ . The exponential dependences in the dc conductivity thus cancel, and  $\sigma_0 \sim 1/\sqrt{mT}$  (the same result is obtained from the Einstein relation  $\sigma_0 = \frac{\partial n}{\partial \mu}D$ ). In principle, the dimensionless numerical prefactor in this relation could be obtained using the methods of Ref. 49, but we content ourselves here simply with the scaling form. Note that although the height of the Drude peak diverges as  $T \rightarrow 0$ , its width shrinks much more rapidly (exponentially), and the weight at  $\omega = 0$  is negligible at low temperatures.

Turning to the higher-frequency features (for  $\omega \approx \sqrt{3}m$  and  $\omega \gtrsim 2m$ ), we expect that scattering between the *injected* bound states or particle-hole pairs and the thermally excited carriers will occur on the same characteristic timescale,  $\tau$ . These peaks therefore also acquire exponentially small widths ( $O(1/\tau)$ ) for  $T \ll \Delta$ . Since the overall spectral weight in  $\text{Re } \sigma(\omega)$  must be conserved, we expect the heights of these features to diverge much more strongly than the Drude peak, i.e.  $\sigma(\omega = \sqrt{3}m, T) \sim \tau \sim e^{m/T}$  and  $\sigma(\omega = 2m, T) \sim \sqrt{\tau} \sim e^{m/2T}$ . Indeed, the optical conductivity presumably satisfies universal scaling forms near these points, i.e.

$$\text{Re } \sigma(\omega) \sim \begin{cases} \tau \Sigma_1[(\omega - \sqrt{3}m)\tau], & |\omega - \sqrt{3}m| \ll m \\ \sqrt{\tau} \Sigma_2[(\omega - 2m)\tau] & |\omega - 2m| \ll m \end{cases}, \quad (5.22)$$

for  $T \ll m$ , where  $\Sigma_1$  and  $\Sigma_2$  are universal scaling functions. A schematic illustration of the optical conductivity at finite temperature is given in Fig. 8.

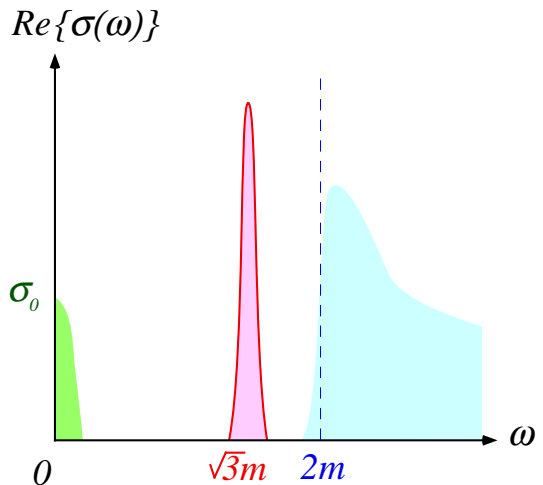


FIG. 8: Optical conductivity at finite temperature. At low temperatures, all the features become exponentially sharp, with a width  $\delta\omega \sim e^{-m/T}$ . In this limit, the “exciton” peak at  $\omega = \sqrt{3}m$  retains a non-zero weight, sharpening into a delta-function, and the peak near  $\omega = 2m$  is also exponentially high. By contrast, the Drude peak at  $\omega = 0$  has vanishing weight at low temperatures, its height diverging only as  $\sigma_0 \sim 1/\sqrt{mT}$ .

#### D. Equal-time spatial correlators

Numerous other correlators can be measured at equal times in numerical simulations, and sometimes experimentally (e.g. static structure factors). The properties of essentially any such correlator can be deduced from the GN spectrum, as summarized in Table 2. Due to the Lorentz invariance of the GN model, intermediate states with a finite energy  $\epsilon$  give rise to exponentially decaying *spatial* correlation functions with the corresponding length  $\xi_\epsilon = v/\epsilon$ .

For completeness, we quote two examples here. The pair-field correlator, defined by  $\Delta(x) = a_{1\uparrow}(x)a_{2\downarrow}(x)$  has the correlation function

$$\langle \Delta(x)\Delta^\dagger(0) \rangle \sim A_1 e^{-m|x|/v} + \left[ A_2 (-1)^x + A_3 e^{i2k_{F1}x} + A_4 e^{-i2k_{F1}x} \right] e^{-\sqrt{3}m|x|/v} + \dots, \quad (5.23)$$

for  $|x| \gg 1$ . Here the first term comes from the mass  $m$  “Cooper pairs” and the second from the corresponding bound states. In the prefactors to the exponentials,  $A_j$ , we have neglected sub-dominant spatial dependences, which generally will have power law forms. For example, due to the one-dimensional van-Hove singularity for adding a pair above the threshold energy  $m$ , one expects  $A_1(x) \sim x^{-1/2}$  for large  $x$ . Similarly, the real-space density-density correlation function is

$$\langle n_\ell(x)n_1(0) \rangle \sim [B_1(-1)^{x+\ell} + B_2 \cos(2k_{F1}x)]e^{-m|x|/v} + \left[ B_3 + B_4(-1)^\ell \cos(k_{F1} - k_{F2})x \right] e^{-\sqrt{3}m|x|/v} + \dots \quad (5.24)$$

Here  $n_\ell(x) = a_{\ell\alpha}^\dagger(x)a_{\ell\alpha}(x) - 1$ . The real-space spin-spin correlation function has an identical form, except with  $B_2 = 0$ .

## VI. GENERIC INTERACTIONS AND $SO(5)$ SYMMETRY

In the previous sections, we focused on the properties of the D-Mott phase which occurs with generic predominantly repulsive interactions in the two-leg ladder. In weak coupling this phase exhibits a remarkable  $SO(8)$  symmetry with dramatic physical consequences for both two-particle and single-particle properties. As remarked in the introduction, there exists an  $SO(5)$  subalgebra of the full  $SO(8)$  group whose vector representation ‘‘unifies’’ superconductivity and antiferromagnetism. Thus all the consequences of this  $SO(5)$  symmetry, proposed by Zhang as a phenomenological model for the cuprates, are shared by the D-Mott phase. A number of authors have proposed *exactly*  $SO(5)$ -invariant lattice models including, in a recent paper by Scalapino, Zhang and Hanke (SZH), a two-leg ladder model.<sup>44</sup> SZH derived a complex phase diagram for this model in the strong coupling limit in a space including both repulsive and attractive interactions. In this section, we will develop the necessary technology and study in weak-coupling both the SZH model and other generic  $SO(5)$ -invariant two-leg ladder systems.<sup>50,51</sup>

In fact, the focus on  $SO(5)$ -invariant models is less restrictive than might be naively expected. Indeed, in our numerical studies of the full RG equations at half-filling, *all* weak coupling two-leg ladder models we have studied (including those with attractive interactions) scale under the RG onto the  $SO(5)$ -invariant manifold. *Within* this manifold, we have observed five attractors, including the D-Mott phase and a Luttinger liquid (C2S2) phase continuously connected to the non-interacting Fermi liquid, in which all the elementary excitations remain gapless. The remaining three attractors are all massive phases, and comprise an *S-Mott* phase similar to the D-Mott phase but with approximate ‘‘s-wave’’ pair correlations, a *charge-density-wave* (CDW) phase with a density-wave at  $\mathbf{k} = (\pi, \pi)$ , and a *spin-Peierls* (SP) phase without a density wave but with kinetic energy modulated at the same wavevector. We group the D-Mott with the latter three to form four *dominant phases*. We will see that (in weak coupling) while all of these dominant phases share Zhang’s  $SO(5)$  symmetry, each one possesses a *distinct* higher  $SO(8)$  symmetry. The different  $SO(8)$  symmetries are related in rather simple ways which have ramifications for the critical points between the different dominant phases.

## A. $SO(5)$ Symmetry

We begin by reviewing some basic properties of the  $SO(5)$  symmetry, demonstrating in the process the relation to the  $SO(8)$  symmetry already discussed. The  $SO(5)$  algebra was originally designed to rotate the five-component *vector* containing the real and imaginary parts of the D-wave pair field and the three components of the staggered magnetization. A set of operators which performs this function was introduced by Zhang<sup>41</sup> – these are the 10 generators of  $SO(5)$ , which are conveniently grouped into the antisymmetric matrix

$$K_{AB} = \begin{bmatrix} 0 & & & & \\ Q_p & 0 & & & \\ \text{Re}\Pi_x & -\text{Im}\Pi_x & 0 & & \\ \text{Re}\Pi_y & -\text{Im}\Pi_y & S_z & 0 & \\ \text{Re}\Pi_z & -\text{Im}\Pi_z & -S_y & S_x & 0 \end{bmatrix}, \quad (6.1)$$

where  $A, B = 1 \dots 5$  spans the matrix of generators and  $K_{AB} = -K_{BA}$ . The various components are defined as bi-linears in electron operators,

$$Q_p = \frac{1}{2} \sum_{\mathbf{k}} (a_\alpha^\dagger(\mathbf{k})a_\alpha(\mathbf{k}) - 1), \quad (6.2)$$

$$\mathbf{S} = \frac{1}{2} \sum_{\mathbf{k}} a_\alpha^\dagger(\mathbf{k})\boldsymbol{\sigma}_{\alpha\beta}a_\beta(\mathbf{k}), \quad (6.3)$$

$$\boldsymbol{\Pi} = \frac{1}{2} \sum_{\mathbf{k}} \phi_{\mathbf{k}}a_\alpha(-\mathbf{k} + \mathbf{N})(\boldsymbol{\sigma}_y\boldsymbol{\sigma})_{\alpha\beta}a_\beta(\mathbf{k}), \quad (6.4)$$

where  $\mathbf{N} = (\pi, \pi)$  is the ‘‘nesting’’ vector and  $Q_p$  is the charge measured in the number of *pairs* of electrons relative to half-filling. Here  $a_\alpha(\mathbf{k})$  is the Fourier transform of the lattice electron operator and a spin sum is implicit. To see that the  $SO(5)$  symmetry is just the first subgroup of  $SO(8)$ , we need simply take the continuum limit of Eq. 6.1. Straightforward but lengthy decomposition of the lattice electron fields into their slowly varying components (as in Section II) and consequent bosonization and refermionization (as in Section IV) gives the exceedingly simple result

$$K_{AB} = \int dx (G_R^{AB} + G_L^{AB}), \quad (6.5)$$

where the  $G_P^{AB}$  are precisely the  $SO(8)$  generators introduced in Section IV. Since only the five-dimensional upper-left block of the full matrix of  $SO(8)$  generators enter in Eq. 6.5, the  $SO(5)$  symmetry rotates the first five Majorana fermions  $\eta_A$ ,  $A = 1 \dots 5$ . As discussed in Section IV, the first five components of this vector representation contain both the pair field ( $\sim \eta_{1,2}$ ) and the staggered magnetization ( $\sim \eta_{3,4,5}$ ).



## B. Microscopically $SO(5)$ -invariant models and $SO(5)$ spinors

We now turn to a discussion of *microscopically*  $SO(5)$ -invariant ladder Hamiltonians. A particular example is the SZH model, which is the most general  $SO(5)$ -symmetric two-leg ladder Hamiltonian with nearest-neighbor hopping and only intra-rung two-body interactions. The interaction terms on each rung of the ladder take the form

$$H_{int} = U \sum_{\ell} \left\{ (n_{\ell\uparrow} - \frac{1}{2})(n_{\ell\downarrow} - \frac{1}{2}) \right\} + V(n_1 - 1)(n_2 - 1) + JS_1 \cdot S_2, \quad (6.6)$$

where  $\ell = 1, 2$  refer to the two legs.  $SO(5)$  symmetry requires a single constraint on the three couplings:  $J = 4(U + V)$ . For  $U, V \gg t, t_{\perp}$  the hopping  $t$  can be treated perturbatively, and SZH have determined the (quite complex) phase diagram in the  $U - V$  plane. With the weak-coupling RG, we can attempt to complete the phase diagram by exploring the opposite limit,  $U, V \ll t, t_{\perp}$ . (One can hope to determine the behavior at intermediate coupling  $U, V \sim t, t_{\perp}$  by interpolation.) Further, we can explore the generic behavior of other weakly-interacting  $SO(5)$ -invariant two-leg ladder systems which contain, for example, inter-rung interactions.

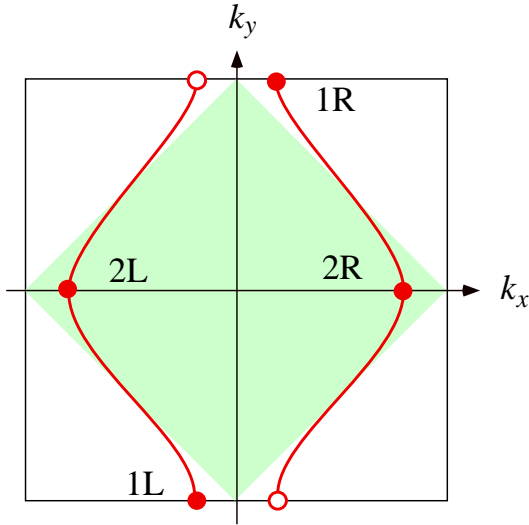


FIG. 9: The folded Brillouin zone for the  $SO(5)$  spinor. The allowed momenta are chosen to be in the grey area. For a two-leg model, the transverse momentum  $k_y$  takes two values  $0, \pi$ . In our convention, only  $k_y = 0$  excitations are inside the folded Brillouin zone.

To do so, we need a means of *constructing*  $SO(5)$ -invariant models in weak coupling. For lattice models, such constructions have been discussed by Henley<sup>52</sup> and Rabello et. al.,<sup>53</sup> and applied by SZH to the two-leg ladder. Here we generalize these methods to the *chiral*

fermions operators which appear in the linearized continuum model obtained in the weakly-interacting limit. Since the Hamiltonian is built from electron operators, we need to introduce *spinor* representations of  $SO(5)$ . We begin with the lattice construction of Rabello et. al.,<sup>53</sup> defining the four-component spinor as

$$\Psi(\mathbf{k}) = \begin{pmatrix} a_{\alpha}(\mathbf{k}) \\ \phi_{\mathbf{k}} a_{\alpha}^{\dagger}(-\mathbf{k} + \mathbf{N}) \end{pmatrix}, \quad (6.7)$$

where  $\mathbf{N} = (\pi, \pi)$  is the nesting vector of the Fermi surface. To avoid double-counting, the allowed momentum  $\mathbf{k}$  in the spinor only runs in the “folded” Brillouin zone, whose size is half of the original one, as shown in Fig. 9. For the two-leg ladder model, in which the only transverse momenta are  $k_y = 0, \pi$ , it is possible to specify the folded Brillouin zone by simply setting  $k_y = 0$  in the above spinor. The factor  $\phi_{\mathbf{k}}$  (which in the general two-dimensional case is a non-trivial function with absolute value one) can be taken to be unity with this convention. Re-expressing the spinor in terms of the band electron operators and Fourier transforming gives

$$\Psi(x) = \int dk_x \Psi(k_x, 0) e^{ik_x x} = \begin{pmatrix} c_{2\alpha}(x) \\ (-1)^x c_{1\alpha}^{\dagger}(x) \end{pmatrix}. \quad (6.8)$$

In the continuum limit valid for weak coupling at low energies, a chiral decomposition is possible:

$$\Psi(x) \approx \Psi_R e^{ik_{F2}x} + \Psi_L e^{-ik_{F2}x}, \quad (6.9)$$

with chiral spinors defined by

$$\Psi_P(x) = \begin{pmatrix} c_{P2\alpha}(x) \\ c_{P1\alpha}^{\dagger}(x) \end{pmatrix}. \quad (6.10)$$

To obtain Eq. 6.10, the  $(-1)^x$  factor in Eq. 6.8 was cancelled using the relation  $k_{F1} + k_{F2} = \pi$ .

The advantage of the spinor basis over the electron band operators  $c_{P\alpha}$  is that they transform simply under  $SO(5)$ . In particular, under a unitary transformation generated by the operator

$$U(\theta_{AB}) = \exp(i\theta_{AB}K_{AB}), \quad (6.11)$$

where  $A, B = 1 \dots 5$ , the spinors  $\Psi_P$  transform according to

$$\Psi'_{Pa} = U^{\dagger}(\theta)\Psi_{Pa}U(\theta) = [T(\theta)]_{ab}\Psi_{Pb}, \quad (6.12)$$

where the spinor indices  $a, b = 1 \dots 4$ , and  $T(\theta) = \exp(i\theta_{AB}\Gamma^{AB})$  is the rotational matrix for a spinor. Here  $\Gamma^{AB} = i[\Gamma^A, \Gamma^B]/4$  where the  $\Gamma^A$  are five generalized (4 by 4) Dirac matrices, discussed in detail in Appendix C. They satisfy the usual Clifford algebra

$$\{\Gamma^A, \Gamma^B\} = 2\delta_{AB}. \quad (6.13)$$

Using the spinors, we can break down all fermion bilinears into irreducible representations of  $SO(5)$ , i.e. generalized currents. Three “normal” sets, which involve one  $\Psi^{\dagger}$  and one  $\Psi$  spinor, carry net momentum zero or  $(\pi, \pi)$ :

$$\mathcal{J}_P \equiv \Psi_{Pa}^\dagger \Psi_{Pa}, \quad (6.14)$$

$$\mathcal{J}_P^A \equiv \Psi_{Pa}^\dagger (\Gamma^A)_{ab} \Psi_{Pb}, \quad (6.15)$$

$$\mathcal{J}_P^{AB} \equiv \Psi_{Pa}^\dagger (\Gamma^{AB})_{ab} \Psi_{Pb}. \quad (6.16)$$

The three currents in Eqs. 6.14-6.16 transform as an  $SO(5)$  scalar, vector, and rank 2 antisymmetric tensor, respectively. A second set of currents (and their hermitian conjugates) appear ‘‘anomalous’’, and carry net momentum  $(\pm 2k_{F2}, 0)$  or  $(\pi \pm 2k_{F2}, \pi)$ :

$$\mathcal{I}_P \equiv \Psi_{Pa} R_{ab} \Psi_{Pb}, \quad (6.17)$$

$$\mathcal{I}_P^A \equiv \Psi_{Pa} (R\Gamma^A)_{ab} \Psi_{Pb}. \quad (6.18)$$

These two currents, which transform as a scalar and a vector under  $SO(5)$ , require the introduction of the matrix

$$R = \begin{pmatrix} 0 & \mathbf{1} \\ -\mathbf{1} & 0 \end{pmatrix}, \quad (6.19)$$

where  $\mathbf{1}$  is the two by two identity matrix. Note that it is straightforward to show that the matrices  $R\Gamma^{AB}$  are symmetric, so that a non-vanishing anomalous tensor current cannot be defined. A simple counting verifies that the above set of currents completely spans the space of electron bilinears. There are  $1 + 5 + 10 = 16$  currents in Eqs. 6.14-6.16, and an additional  $2 \cdot (1 + 5) = 12$  currents in Eq. 6.17-6.18 and their complex conjugates, for a total of  $28 = 8 \cdot 7/2$  independent bilinears.

In weak coupling, we must generically consider all Hermitian products of two bilinears which are (1) invariant under  $SO(5)$  and (2) conserve quasi-momentum. Neglecting purely chiral terms (which, as in Sec. II, only renormalize velocities), there are then five allowed couplings. The interaction Hamiltonian density takes the form

$$\begin{aligned} \mathcal{H}_{int} = & g_s \mathcal{J}_R \mathcal{J}_L + g_v \mathcal{J}_R^A \mathcal{J}_L^A + g_t \mathcal{J}_R^{AB} \mathcal{J}_L^{AB} \\ & + h_s \left\{ \mathcal{I}_R \mathcal{I}_L + \text{h.c.} \right\} + h_v \left\{ \mathcal{I}_R^A \mathcal{I}_L^A + \text{h.c.} \right\}. \end{aligned} \quad (6.20)$$

Note that momentum conservation forbids forming a quartic interaction from one normal and one anomalous current.

The above Hamiltonian represents the most general  $SO(5)$  invariant ladder theory with weak interactions. The five coupling constants  $(g_s, g_v, g_t, h_s, h_v)$  specify a five-dimensional manifold within the more general nine-dimensional space of  $U(1) \times SU(2)$  symmetric theories. This manifold is determined explicitly by a set of linear equations, given in App. D, which relate the five  $SO(5)$  invariant couplings to the 9  $U(1) \times SU(2)$  couplings which were introduced in Sec. II. Because the  $SO(5)$  manifold possesses higher symmetry, it closes under an RG transformation. The five RG equations describing the flows *within* the  $SO(5)$  manifold are given explicitly in App. E.

### C. SZH Model and Four Dominant Phases

The weak coupling phase diagram for the SZH model can now be obtained, by numerical integration of the  $SO(5)$  invariant RG flow equations (Eqs. E1-E5). The initial (bare) values of the  $SO(5)$  coupling constants are obtained by taking the continuum limit of the SZH model. For *each* initial set of bare parameters, the phase is determined by bosonizing those couplings which grow large under the RG transformation, as described in Sec. II. The resulting weak coupling phase diagram is shown in Fig. 10.

Four new phases appear in addition to the D-Mott phase which occurs for predominantly repulsive interactions. In the ‘‘C2S2’’ region in Fig. 10, all five couplings scale to zero under the RG. This *Luttinger liquid* phase thus retains all the gapless modes (2 charge and 2 spin, hence C2S2) of the original non-interacting electron system, and thereby has (an approximate) chiral  $SO(8)$  symmetry.

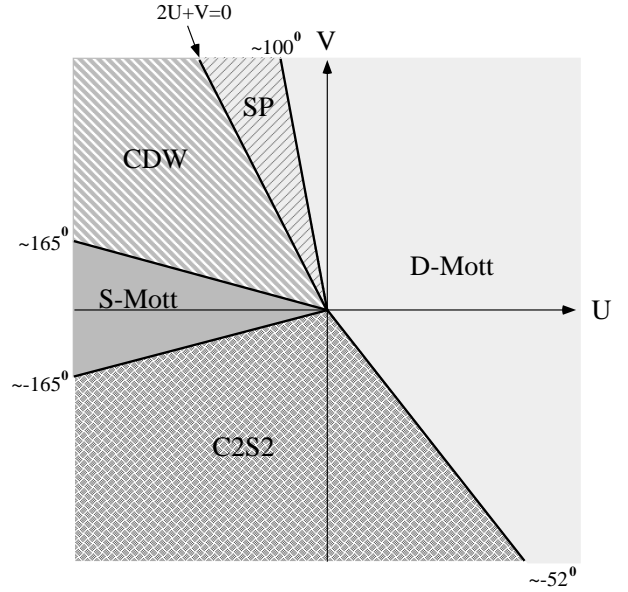


FIG. 10: Phase diagram of the  $SO(5)$  symmetric SZH model plotted in the  $U$ - $V$  plane with  $J = 4(U + V)$  and  $U, V \ll t = t_\perp$ .

We group the other three states together with the D-Mott as four *dominant phases*. In the S-Mott phase, the interactions diverge in the same way as in the D-Mott case, given by Eqs. 3.2, with the modification  $b_{12}^\rho, b_{12}^\sigma, u_{11}^\rho \rightarrow -b_{12}^\rho, -b_{12}^\sigma, -u_{11}^\rho$ . In the  $SO(5)$ -invariant notation, this corresponds to changing the sign of  $h_s$  and  $h_v$ . Semiclassically, the only change in the behavior is that  $\langle \varphi_{\rho-} \rangle_{\text{S-Mott}} = \langle \varphi_{\rho-} \rangle_{\text{D-Mott}} + \pi = \pi$ . The  $\theta_{\sigma\pm}$  and  $\theta_{\rho+}$  fields are unaffected, so that the S-Mott phase still has short-range pairing. It is, however, of approximate *s*-wave symmetry, with  $\Delta_1 \Delta_2^{\dagger} > 0$  due to the shift in  $\varphi_{\rho-}$ , as can be seen from Eq. 3.8. It is inter-

esting that the strong-coupling “s-wave” paired state on a rung,  $|\uparrow\downarrow, -\rangle + |-\rangle, \uparrow\downarrow\rangle$  is identical in the ladder leg and band bases, and corresponds to an *on-site* pairing or singlet state. In contrast, pairing in the strong-coupling D-Mott state is across the rung of the ladder, as depicted schematically in Fig. 11.

In the SP and CDW phases, the ratios of diverging couplings are somewhat different. In particular,  $b_{11}^\sigma, b_{11}^\rho$  are irrelevant and

$$f_{12}^\rho = -\frac{1}{4}f_{12}^\sigma = (\mp)b_{12}^\rho = (\pm)\frac{1}{4}b_{12}^\sigma = \quad (6.21)$$

$$\frac{1}{2}u_{12}^\sigma = -2u_{12}^\rho = (\pm)2u_{11}^\rho = g > 0, \quad (6.22)$$

where the upper and lower signs hold in the SP and CDW phases, respectively. These modifications imply a fairly dramatic change in the behavior relative to the D-Mott and S-Mott states. In fact, the SP and CDW are *dual* to the D-Mott and S-Mott, respectively, in the following sense: each is obtained from its dual counterpart by interchanging  $\varphi_{\sigma-}$  and  $\theta_{\sigma-}$ . Because of this interchange, the pair fields fluctuate wildly even locally, and  $\langle\Delta_1\Delta_2^\dagger\rangle_{\text{SP}} = \langle\Delta_1\Delta_2^\dagger\rangle_{\text{CDW}} = 0$ . Instead, these two phases break discrete  $\mathcal{Z}_2$  symmetries.

To explore this in detail, consider the order parameters

$$B_\ell(x) = \frac{1}{2}[a_{\ell\alpha}^\dagger(x+1)a_{\ell\alpha}(x) + \text{h.c.}], \quad (6.23)$$

$$n_\ell(x) = a_{\ell\alpha}^\dagger(x)a_{\ell\alpha}(x) - 1. \quad (6.24)$$

The field  $B_\ell(x)$  is the local kinetic energy, while  $n_\ell(x)$  is the local electron density relative to half filling. The two order parameters differ in symmetry since  $B_\ell(x)$  is even and  $n_\ell(x)$  is odd under a  $\mathcal{Z}_2$  particle-hole symmetry  $a_{\ell\alpha}(x) \rightarrow (-1)^{\ell+x}a_{\ell\alpha}^\dagger(x)$ . Using the usual relations to rewrite  $B_\ell$  and  $n_\ell$  in terms of chiral operators, bosonizing, and applying the semi-classical results (common to both the SP and CDW phases)  $\langle\theta_{\rho+}\rangle = \langle\theta_{\sigma+}\rangle = \langle\varphi_{\sigma-}\rangle = 0$ , one obtains

$$\langle B_\ell(x) \rangle \sim (-1)^{x+\ell} \langle \cos(\frac{1}{2}\varphi_{\rho-}) \rangle, \quad (6.25)$$

$$\langle n_\ell(x) \rangle \sim (-1)^{x+\ell} \langle \sin(\frac{1}{2}\varphi_{\rho-}) \rangle. \quad (6.26)$$

Since  $\langle\varphi_{\rho-}\rangle = 0, \pi$  in the SP and CDW phases, respectively, we find  $\langle B_\ell \rangle_{\text{SP}} \sim (-1)^{x+\ell}$ ,  $\langle n_\ell \rangle_{\text{SP}} = 0$  and  $\langle B_\ell \rangle_{\text{CDW}} = 0$ ,  $\langle n_\ell \rangle_{\text{CDW}} \sim (-1)^{x+\ell}$ . The SP phase thus breaks only the discrete symmetry under translations by one lattice spacing (the translation in the  $y$ -direction is, of course, equivalent to parity), while the CDW phase breaks *both* translational symmetry and the  $\mathcal{Z}_2$  particle-hole symmetry. These broken symmetries can be depicted easily in the strong coupling limit, as shown in Fig. 11.

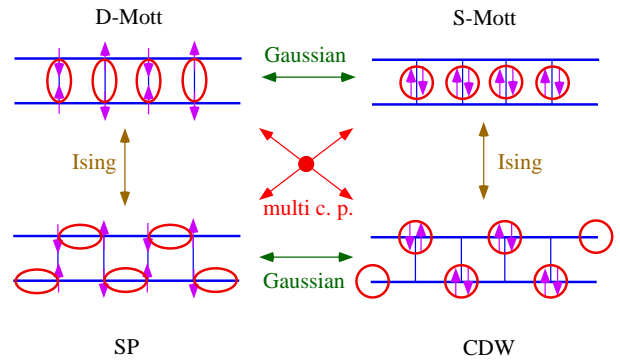


FIG. 11: Schematic illustration of the four dominant phases, drawn for simplicity in the strong-coupling limit. In the D-Mott and S-Mott phases, neighboring rungs contain essentially decoupled pairs. Adjacent rungs are highly correlated in the SP and CDW phases, which furthermore break parity symmetry.

#### D. $SO(8)$ Symmetries and Degeneracies of the S-Mott, SP, and CDW Phases

Since the four dominant phases appear on essentially equal footing, one might suspect that the S-Mott, SP, and CDW phases exhibit  $SO(8)$  symmetries similar to that of the D-Mott phase. We shall see that this is indeed the case, but that the  $SO(8)$  algebras are *different* in each state.

Consider first the S-Mott. In the previous subsection, it was shown that the S-Mott is related to the D-Mott by a  $\pi$  shift in  $\varphi_{\rho-}$ . It follows that if we define

$$\theta_a^S = \begin{cases} \theta_a & a = 1, 2, 3 \\ \varphi_{\rho-} + \pi & a = 4 \end{cases}, \quad (6.27)$$

and  $\varphi_a^S = \varphi_a$ , the bosonized Hamiltonian in the S-Mott phase takes the form of Eqs. 3.5-3.6 (with  $\theta_a, \varphi_a$  replaced by  $\theta_a^S, \varphi_a^S$ ). Consequently, a refermionization into the GN form is again possible. In particular, upon defining

$$\eta_{PA}^S = \begin{cases} \eta_{PA} & A = 1 \dots 6 \\ P\eta_{PA} & A = 7, 8 \end{cases}, \quad (6.28)$$

the S-Mott Hamiltonian takes the “canonical” GN form (Eq. 4.6) in terms of the  $\eta_{PA}^S$ . The sign changes in Eq. 6.28 imply that the generators of the  $SO(8)$  symmetry in the S-Mott phase (are different from those of the D-Mott phase. For instance,  $G_S^{71} = G_R^{71} - G_L^{71}$ , whose spatial integral is not an  $SO(8)$  generator in the D-Mott case. However, since the Majorana fermions for the two phases are equal for  $A = 1 \dots 6$ , the D-Mott and S-Mott do share a common  $SO(6)$  subalgebra.

Similar constructions can be performed for the SP and CDW phases. Recalling the duality of the previous subsection, we choose



$$\theta_a^{\text{SP}} = \begin{cases} \theta_a & a = 1, 2 \\ \varphi_{\sigma-} & a = 3 \\ \varphi_{\rho-} & a = 4 \end{cases} \quad \varphi_a^{\text{SP}} = \begin{cases} \varphi_a & a = 1, 2, 4 \\ \theta_{\sigma-} & a = 3 \end{cases} \quad (6.29)$$

for the SP phase. Similarly for the CDW, we take

$$\theta_a^{\text{CDW}} = \begin{cases} \theta_a & a = 1, 2 \\ \varphi_{\sigma-} & a = 3 \\ \varphi_{\rho-} + \pi & a = 4 \end{cases} \quad (6.30)$$

and  $\varphi_a^{\text{CDW}} = \varphi_a^{\text{SP}}$ . As before, the GN form can be retained. The appropriate Majorana fermions in these cases are

$$\eta_{PA}^{\text{SP}} = \begin{cases} \eta_{PA} & A = 1 \dots 5, 7, 8 \\ P\eta_{P6} & A = 6 \end{cases} \quad (6.31)$$

and

$$\eta_{PA}^{\text{CDW}} = \begin{cases} \eta_{PA} & A = 1 \dots 5 \\ P\eta_{PA} & A = 6, 7, 8 \end{cases} \quad (6.32)$$

Like the D-Mott and S-Mott, the SP and CDW phases share a common  $SO(6)$  symmetry. Moreover, the D-Mott and SP share an  $SO(7)$  symmetry, as do the S-Mott and CDW.

A final calculation is possible now that the appropriate bosonized variables have been established. In Sec. IV and App. B, the uniqueness of the D-Mott ground state was established. We also expect a unique ground state for the S-Mott phase, but have yet to establish it. In the SP and CDW phases, discrete symmetries are broken, and one expects at least a two-fold degeneracy in the thermodynamic limit. Using the techniques applied earlier (gauge equivalence of semiclassical solutions) to the D-Mott, we can determine these degeneracies. Details can be found in App. B. The result of such an analysis is that the S-Mott indeed has a unique ground state, while the SP and CDW ground states are each exactly two-fold degenerate.

### E. Full Set of $SO(5)$ Fixed Points

Because of the relative simplicity of the  $SO(5)$ -invariant manifold (5 coupling constants versus 9 for the general case), it is possible to perform an exhaustive determination of the possible asymptotic scaling trajectories under the RG. To do so, we insert the power-law ansatz of Eq. 2.26 into the  $SO(5)$  RG equations, Eqs. E1-E5. This set of five coupled algebraic equations can be solved exactly, in contrast to the corresponding set of nine  $U(1) \times SU(2)$  equations, which have proved intractable. One finds fourteen solutions, delineated in Table 3. Five represent the states discussed so far: the gapless C2S2 and four dominant  $SO(8)$ -symmetric phases.

$48g_s$	$48g_v$	$48g_t$	$48h_s$	$48h_v$	phase
0	0	0	0	0	C2S2
-2	2	4	1	-1	D-Mott
-2	2	4	-1	1	S-Mott
-2	-2	4	-1	-1	SP
-2	-2	4	1	1	CDW
0	3	6	0	0	D-Mott $\leftrightarrow$ S-Mott
0	-3	6	0	0	SP $\leftrightarrow$ CDW
$-(12/5)$	0	$(24/5)$	0	$-(6/5)$	D-Mott $\leftrightarrow$ SP
$-(12/5)$	0	$(24/5)$	0	$(6/5)$	S-Mott $\leftrightarrow$ CDW
0	0	8	0	0	multi-critical
-12	0	8	$\pm 6$	0	$SO(5) \times SO(3)$ GN
-12	0	0	$\pm 6$	0	$SO(5)$ WZW $\times$ $SO(3)$ GN

Table 3: Fourteen algebraic solutions of the  $SO(5)$  RG equations

Of the remainder, five represent critical points. Consider first the D-Mott $\leftrightarrow$ S-Mott transition. Taking the values in Table 3, one finds that semi-classically the fields  $\theta_{\rho+}$ ,  $\theta_{\sigma+}$ , and  $\theta_{\sigma-}$  are pinned as in the D-Mott and S-Mott states, but that neither the  $\theta_{\rho-}$  nor the  $\varphi_{\rho-}$  field appears in the interaction Hamiltonian. There is thus a single gapless (central charge  $c = 1$ ) bosonic mode at the critical point. That this is indeed the critical point between the D-Mott and S-Mott phases can be seen by perturbing slightly away from the scaling trajectory. If the perturbations are small, those terms involving the gapped degrees of freedom will have negligible effect, and we need only include the couplings involving the  $\rho-$  fields. As argued in Sec. II,  $\cos n\theta_{\rho-}$  terms are not allowed by translational invariance. The low-energy Hamiltonian density near the critical point (after integrating out the massive fields) thus has the form

$$\mathcal{H}_{\text{D}\leftrightarrow\text{S}}^{\text{eff.}} = \frac{1}{8\pi} [(\partial_x \varphi_{\rho-})^2 + (\partial_x \theta_{\rho-})^2] - \lambda \cos \varphi_{\rho-}. \quad (6.33)$$

For  $\lambda > 0$ , the semiclassical minimum occurs for  $\varphi_{\rho-} = 0$ , describing the D-Mott phase, while for  $\lambda < 0$ , the minimum shifts to  $\varphi_{\rho-} = \pi$ , yielding the S-Mott phase. We expect that the general form of this low-energy *critical* Hamiltonian will remain valid even in strong coupling, though the Luttinger stiffness and velocity of the critical  $\varphi_{\rho-}$  mode will shift in this case. What are the critical properties of this transition? The correlation length exponent is determined by the scaling dimension of  $\cos \varphi_{\rho-}$ . In a general strong-coupling situation, this is a *continuously variable* exponent. In weak-coupling, however, it is determined. In particular, refermionization implies  $\cos \varphi_{\rho-} \sim \psi_4^\dagger \tau^y \psi_4$ , which acts as a Dirac mass and has scaling dimension one. In this limit then, the correlation length  $\xi \sim |\lambda|^{-\nu}$ , with  $\nu = 1$ . Both in strong and weak coupling, the dynamical exponent  $z = 1$ , as determined by the quadratic bosonic kinetic energy. This type of  $c = 1$  continuously-variable critical point is known as a Gaussian model, as shown in Fig. 11. Of course, in neglecting the massive modes, we have thrown out ad-

ditional universal physics in the weak-coupling limit. In particular, these massive modes have a large  $SO(6)$  symmetry, which can be seen by rewriting the critical interaction Hamiltonian density using Table 3 and Eqs. D11-D12,

$$\mathcal{H}_{\text{D}\leftrightarrow\text{S}}^{\text{int.}}(\lambda = 0) = g \sum_{A,B=1}^6 G_R^{AB} G_L^{AB}. \quad (6.34)$$

The full weak-coupling critical symmetry is thus  $U(1)_R \times U(1)_L \times SO(6)$ . It may seem surprising that this critical point has *lower* symmetry than the massive dominant phases, which enjoy  $SO(8)$ -invariance. This is a result unique to the weak-coupling limit. With stronger interactions, corrections to the weak-coupling scaling will break the  $SO(8)$  symmetry, while leaving the  $U(1)_R \times U(1)_L$  critical symmetry (which results from truly infinite-wavelength physics) intact.

Having understood the D-Mott $\leftrightarrow$ S-Mott transition, it is clear that the SP $\leftrightarrow$ CDW transition is essentially identical. The Hamiltonian in this case differs only via the interchange of  $\theta_{\sigma-}$  and  $\varphi_{\sigma-}$ , which in any case are massive at this critical point.

The next two critical points are somewhat different. For concreteness, consider the D-Mott $\leftrightarrow$ SP transition. As before, three of the bosonic fields are massive, in this case  $\theta_{\rho+}, \theta_{\sigma+}, \theta_{\rho-}$ . These can be integrated out, leaving the  $\sigma-$  fields critical. However, here *both*  $\theta_{\sigma-}$  and the dual  $\varphi_{\sigma-}$  appear, so a semi-classical analysis is not tenable. Instead, we refermionize this single remaining bosonic field and its interactions *after* integrating out the three massive bosons (i.e. setting them to their semi-classical minima). The reduced Hamiltonian density in this case is

$$\mathcal{H}_{\text{D}\leftrightarrow\text{SP}}^{\text{int.,eff.}} = g i \eta_{R5} \eta_{L5} + \tilde{\lambda} i \eta_{R6} \eta_{L6}. \quad (6.35)$$

Here  $g$  is the finite coupling along the scaled RG trajectory, and  $\tilde{\lambda}$  is a deviation from the critical trajectory similar to  $\lambda$  in the Gaussian model above. Since  $g$  is non-zero, the  $\eta_{P5}$  Majorana fermion acquires a gap, and only the single  $\eta_{P6}$  Majorana fermion is gapless at the critical point. This is a central charge  $c = 1/2$  critical point, which uniquely identifies it as an Ising transition. Indeed, the Ising nature of this transition is very physical, given the discrete  $\mathcal{Z}_2$  parity symmetry broken in the SP phase. This also explains the duality between the D-Mott and SP phases found earlier: this duality is nothing but the usual Kramers–Wannier duality of the Ising model. As before, we expect the Ising critical behavior to be robust to corrections to the weak-coupling RG, so these transitions should be in the same universality class even with strong interactions. In the weak-coupling limit, the massive degrees of freedom again have higher symmetry, in this case including the  $\eta_{P5}$  Majorana fermion coming from the  $\sigma-$  fields. The full weak-coupling critical theory is thus  $\mathcal{Z}_2 \times SO(7)$ , where the  $\mathcal{Z}_2$  theory is the conformally-invariant Ising model, as indicated in Fig. 11.

Not surprisingly, the S-Mott $\leftrightarrow$ CDW transition is also of the Ising variety. The “multi-critical point” in Table 3 describes the case when all four phases come together at a point, i.e. when two transition lines cross. It is simply a direct product of the two critical theories above, i.e. a Gaussian model and an Ising theory. It is possible that these theories actually become coupled if one re-introduces interactions that were irrelevant at the non-interacting Fermi fixed point, but we do not explore this possibility here.

The remaining four “fixed points” of the  $SO(5)$ -invariant RG describe more exotic situations. We have not observed any microscopic Hamiltonians attracted to these phases, but some of these may perhaps occur for some choices of bare interactions. We suspect that these “phases” are unstable, and hence spurious for physically relevant situations. Nevertheless, we discuss them briefly for completeness. They are most easily understood by using the representations in Eqs. D10-D14. The form of the  $SO(5) \times SO(3)$  case is then easily seen from the interaction Hamiltonian density (taking the positive sign for  $h_s$  for simplicity)

$$\mathcal{H}_{SO(5) \times SO(3)\text{GN}}^{\text{int.}} \sim g \left[ \sum_{A,B=1}^5 G_R^{AB} G_L^{AB} + 3 \sum_{A,B=6}^8 G_R^{AB} G_L^{AB} \right]. \quad (6.36)$$

These interactions are precisely those of an  $SO(5) \times SO(3)$  GN model. Both of the constituent GN models are massive, so this represents another gapped phase. The solution with the opposite sign for  $h_s$  can be converted into the same form by the canonical transformation  $\eta_{R6} \rightarrow -\eta_{R6}$ , so it is also a gapped phase of this sort. The remaining two phases can be understood similarly. Note that in these cases only the scalar interactions  $g_s$  and  $h_s$  are non-zero. This implies that the first five and last three Majoranas are decoupled. Furthermore, in this case since  $g_v = g_t = 0$ , the first five Majorana fermions are non-interacting. They comprise a gapless  $SO(5)$  Wess-Zumino-Witten (WZW) model with central charge  $c = 5/2$ , while the last three Majorana fermions combine to form an  $SO(3)$  GN model. The interaction Hamiltonian density is thus simply

$$\mathcal{H}_{SO(5)\text{WZW} \times SO(3)\text{GN}}^{\text{int.}} \sim g \sum_{A,B=6}^8 G_R^{AB} G_L^{AB}. \quad (6.37)$$

## VII. DOPING THE D-MOTT PHASE

In this Section we briefly consider the effects of doping away from half-filling in the two-leg ladder. In the weak coupling limit of interest and with nearest neighbor hopping in the kinetic energy, the ladder at half-filling was argued to scale onto the soluble Gross-Neveu

model which possesses an exact global  $SO(8)$  symmetry. Generally, doping away from half-filling will break down this large symmetry, leaving only charge and spin conservation, with the much smaller  $U(1) \times SU(2)$  symmetry. This can already be anticipated for the non-interacting problem: When the Fermi energy moves away from zero (half-filling) the Fermi velocities in the bonding and antibonding bands will in general become unequal due to curvature in the energy/wavevector dispersion. For weak doping, however, this effect is small. Indeed, in the relativistic model derived in Section II where the dispersion was linearized about the Fermi points, the small curvature is ignored entirely. In the following we focus on this very low doping limit ( $x = 1 - n \ll 1$ ), where the difference between the two Fermi velocities can be safely ignored. We thus continue to employ the linearized relativistic model. Nevertheless, as we shall see, even within this limit doping away from half-filling breaks down the global  $SO(8)$  symmetry of the Gross-Neveu model, although in a rather straightforward manner.

To dope we consider adding a chemical potential term to the Gross-Neveu Hamiltonian,  $H$ , with  $H_\mu = H - \mu Q$ , where  $Q$  is the *total* electron charge. This charge can be written

$$Q = 2 \int dx (\psi_{R1}^\dagger \psi_{R1} + \psi_{L1}^\dagger \psi_{L1}) = 2 \int dx (G_R^{21} + G_L^{21}). \quad (7.1)$$

Since  $Q$  is a *global*  $SO(8)$  generator, it commutes with the full interacting Hamiltonian:  $[Q, H] = 0$ . Thus, even for  $\mu \neq 0$  the states can still be labelled by  $Q$ , which, along with all the generators  $G^{AB}$  with  $A, B = 3 \dots 8$ , remains a good quantum number. The  $SO(8)$  multiplets will of course be split by the presence of a non-zero  $\mu$ , lowering the energy of positively charged excitations and raising the negatively charged ones.

The splitting of the  $SO(8)$  multiplets can be conveniently visualized in the large- $N$  “semiconductor” picture. Of the four fermionic particle/hole excitations of the fundamental GN fermions, only the first one is charged and is shifted in energy. Specifically, employing the semiclassical notation, the excitations  $(\pm 1, 0, 0, 0)$  carry charge  $Q = \pm 2$ , and are shifted by an energy  $\Delta E_\mu = \mp 2\mu$ , as depicted schematically in Fig. 12. Provided this shift is smaller than the energy gap,  $-m < 2\mu < m$ , the *ground state* remains unaltered: The negative energy “valence” bands remain filled and the “conduction” bands empty. In terms of electrons, the ladder remains at half-filling.

Similarly, the energies of the 16 kink excitations are split into 8 with energy  $m + \mu$  and 8 with energy  $m - \mu$ . Of the 28 (two-fermion bound) states with energy  $\sqrt{3}m$ , 16 are neutral and unshifted by the chemical potential. Of the others, 6 have charge 2 and are shifted up in energy by  $2\mu$  and the other 6 down by  $-2\mu$ .

The situation is more interesting when  $2\mu > m$ . In this case, the energy of the states in the “conduction”

band for Cooper pairs drops below zero, and the ground state will be radically altered. In the large- $N$  limit the new ground state will consist of filling up the negative energy states with a Fermi-sea of Cooper pairs, as depicted in Fig. 12. For  $N = 8$  the pair excitations will *not* be describable in terms of free Fermions, but one still anticipates the general picture of a conducting sea of Cooper pairs to remain valid. Since the Fermions interact for finite  $N$ , this conducting sea will be more correctly described as a Luttinger liquid. In the limit of very low doping, however, the Cooper-pairs will be very far apart and well described in terms of hard-core Bosons or free-Fermions. In this limit, the Luttinger liquid parameters should approach those of Free fermions. It is probable that the  $N=8$  Gross-Neveu model remains integrable even in the doped case, since the states can still be labelled by the same good quantum numbers, so that exact statements about the doped Mott-insulator can be made. In the following we are less ambitious, using known results from integrability for the undoped case to infer the behavior in the very low doping limit.

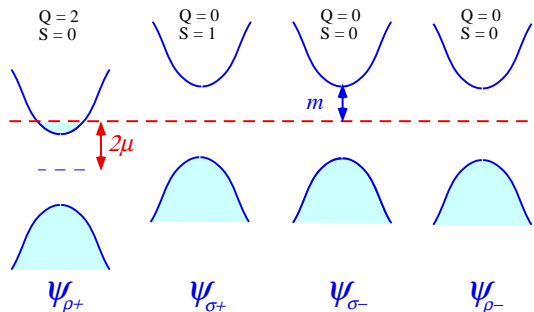


FIG. 12: Mean-field picture of the doped  $SO(8)$  GN model. Only the first band (with  $Q = 2$ ) is shifted by the chemical potential. For  $2\mu > m$ , Cooper pairs are added to the original ground state.

### A. Excitations with One pair present

When  $2\mu > m$  the energy is lowered by adding Cooper pairs to the system. Here we consider first the case  $2\mu = m + 0^+$ , so that the concentration of pairs, denoted  $x/2$ , is infinitesimal. In this limit it is sufficient to consider the properties in the presence of a *single* Cooper pair. The presence of even this one pair modifies the spectrum of other excitations – such as the spin or single-particle gaps – as we now briefly discuss.

Consider first the spin-gap, i.e. the energy of the lowest-lying spin  $s = 1$  excitation. In the undoped case, the lowest-lying triplet states are the  $\eta_{3,4,5}$  fundamental fermions, with momentum  $(\pi, \pi)$  and energy  $m$ . As known from integrability, these excitations interact via an *attractive* interaction with the other GN fermions, including the single Cooper pair present due to doping. Indeed, the binding energy is known exactly and given by  $E_b = (2 - \sqrt{3})m$ . With the single Cooper pair present,

an  $s = 1$  magnon can be added to the system into a bound state with the Cooper pair, costing a reduced energy  $m - E_b = (\sqrt{3} - 1)m$ . Thus the spin-gap at infinitesimal doping  $x = 0^+$  is reduced from the undoped value of  $m$  down to  $(\sqrt{3} - 1)m$ . There are, of course, also unbound  $s = 1$  excitations which can be created well away from the Cooper pair, with energy  $m$ . In fact, for  $x \rightarrow 0$  the energy  $m$  spin excitations will dominate the spectral weight. The spectral weight for the lower energy  $s = 1$  bound states will presumably vanish linearly with  $x$ . It is worth emphasizing that the discontinuity in the spin-gap at infinitesimal doping  $x = 0^+$  is a general feature due to the presence of a magnon/Cooper-pair bound state in the undoped Mott insulator, and is not an artifact of weak coupling. If such a bound state survives strong coupling, as suggested by numerical RG on the two-leg ladder, a discontinuity should be present.

It is also instructive to consider the energy gap for adding single electrons in the presence of the single Cooper pair. Adopting a convention where  $Q > 0$  corresponds to “hole” doping, consider the energy to add a single electron with charge  $-1$ . A single electron can be created by adding a kink excitation, for example an even kink with  $(-1, -1, -1, -1)/2$  in the semiclassical notation. When  $\mu = 0$  this costs an energy  $m$ , but is shifted *up* in energy for non-zero chemical potential:  $E_1 = m + \mu$ , as depicted in Fig. 13. When  $2\mu = m + 0^+$  and the single Cooper pair is added, the energy to add the electron can be lowered from  $E_1 = (3/2)m$  by binding the kink to the  $(1, 0, 0, 0)$  Cooper pair. This forms a charge  $Q = 1$  hole state: an odd kink with  $(1, -1, -1, -1)/2$ . The associated binding energy equals  $m$ , as follows directly from triality (at  $\mu = 0$ ). Thus, at infinitesimal (hole) doping the energy to add an electron drops by  $m$ , down to  $m/2$ . As for the case of the spin-excitations, one expects a continuum of unbound single electron excitations, at energies above  $3m/2$ .

## B. Excitations with Many pairs

For  $2\mu > m$  the “conduction band” for Cooper pairs will be partially occupied. In this case, one expects a continuum of low energy particle/hole excitations created by exciting pairs across the Fermi “surface”. For the  $SO(8)$  Gross-Neveu model the Cooper pairs will presumably interact with one another, so that the semiconductor picture of a non-interacting Fermi sea will not be quite correct. Rather, the spinless gas of Cooper pairs will presumably form an interacting Luttinger liquid. In any event, one expects a continuum of low energy excitations in the Cooper pair fluid, presumably with a linear dispersion relation. One might hope that the velocity of this mode as a function of doping  $x$  might be accessible from integrability of the doped Gross-Neveu model.

It would also be very interesting to study the energy of the spin-one excitations with *finite* doping. A

$s = 1$  magnon added to the system will interact via an attractive interaction with the sea of Cooper pairs. For infinitesimal doping ( $x = 0^+$ ) the corresponding spin-gap energy was lowered due to the formation of a magnon/Cooper-pair bound state. With many pairs present, this energy will presumably be further lowered, as depicted schematically in Fig. 12.

Finally, we consider briefly the spin one excitations at energies above threshold. These states would contribute to the spin-spectral function, accessible via inelastic neutron scattering in the doped ladder. Generally, we expect a continuum of states above threshold, corresponding for example to adding a magnon at  $(\pi, \pi)$  and simultaneously exciting multiple “particle-hole” pairs in the (Cooper-pair) Fermi-sea. This continuum should contribute to the spin-spectral function at any given momentum. For example, at momentum  $(\pi, \pi)$ , multiple particle-hole pairs with zero net momentum will contribute spectral weight at all energies above threshold. Due to this continuum of states, we do not expect any delta-functions in the energy dependence of the spin-spectral function in the doped ladder.

This expectation runs contrary to arguments put forward by Zhang for the existence of a sharp  $\pi$ -resonance in the spin-spectral function in the superconducting phase of models which exhibit an exact  $SO(5)$  symmetry. Zhang’s argument has recently been applied to the doped (power-law) superconducting phase of the two-leg ladder by Scalapino, Zhang and Hanke.<sup>44</sup> Below, we briefly reconsider Zhang’s argument for the sharp  $\pi$ -resonance, and show that in addition to  $SO(5)$  symmetry, it relies on the existence of a *condensate* in the superconducting phase. Being one-dimensional, however, a true condensate does not exist in the “superconducting” phase of the two-legged ladder. In our view, this invalidates the argument for a sharp delta-function  $\pi$ -resonance in the doped ladders, even in the presence of exact  $SO(5)$  symmetry.

Zhang’s argument for the  $\pi$ -resonance rests on the fact that the  $\pi$  operators, defined in Eq. 6.4, being global  $SO(5)$  (and  $SO(8)$ ) generators, are exact eigen-operators even with non-zero chemical potential:

$$[H_\mu, \Pi_a] = 2\mu\Pi_a, \quad (7.2)$$

where  $H_\mu = H - \mu Q$  and the subscript  $a$  labels the three components of the  $\pi$ -operators. This implies that for any eigenstate  $H_\mu|E\rangle = E|E\rangle$  with energy  $E$ , the triplet of states  $\Pi_a|E\rangle$  are also exact eigenstates, but with energy  $E + 2\mu$ , provided they are non-vanishing. Denote the exact ground state of the doped ladder with  $N$  Cooper-pairs as  $|N\rangle$ , which satisfy  $H_\mu|N\rangle = 0$ . Adding an additional Cooper-pair is accomplished with the operator  $\mathcal{O}_1^+(x) = \mathcal{O}_s(x)\psi_1^\dagger(x)$ . The zero momentum Fourier transform of this operator,  $\mathcal{O}_1^+(k = 0)$ , creates a state with  $N + 1$  pairs, which can be decomposed as,

$$\mathcal{O}_1^+(k = 0)|N\rangle = c|N + 1\rangle + \dots, \quad (7.3)$$

where the dots denote excited states with  $N + 1$  pairs present. Following Zhang, we can use the  $\pi$ -operators to rotate Cooper-pairs at zero momentum into a triplet of magnons at momentum  $(\pi, \pi)$ , since

$$[\Pi_a, \psi_1^\dagger(x)] = \sqrt{2}\eta_a(x), \quad (7.4)$$

with  $a = 3, 4, 5$ . Acting with the  $\Pi$ -operator on Eq. 7.3 and using the above commutation relation and the fact that  $\mathcal{O}_s$  commutes with  $\Pi_a$ , one obtains,

$$\mathcal{O}_a(k=0)|N\rangle = \frac{c}{\sqrt{2}}\Pi_a|N+1\rangle + \dots, \quad (7.5)$$

where  $\mathcal{O}_a(x) = \mathcal{O}_s(x)\eta_a(x)$ . The left hand side is a spin 1 triplet of states with momentum  $(\pi, \pi)$ , built by adding a magnon to the  $N$ -pair ground state. Due to the  $SO(5)$  symmetry, the states on the right side,  $\Pi_a|N+1\rangle$ , are *exact* eigenstates with energy  $2\mu$ . As argued by Zhang, the equality between the left and right sides implies that the triplet of magnons will contribute a delta-peak in the spin-spectral function at energy  $2\mu$  - the  $\pi$ -resonance.

However, this conclusion rests on the assumption of a non-vanishing overlap between  $\mathcal{O}_a|N\rangle$  and  $\Pi_a|N+1\rangle$ . But in the thermodynamic limit, the squared overlap,  $|c|^2$ , is simply the (Bose) condensate density, since

$$c = \langle N+1|\mathcal{O}_1^+(k=0)|N\rangle. \quad (7.6)$$

While non-zero in a 2d superconductor, for the two-leg ladder the condensate density is zero, and the argument for a delta-function  $\pi$ -resonance is invalid. The vanishing condensate density is a general property of 1d systems which follows from the Mermin-Wagner theorem in the thermodynamic limit. For finite  $N$  at fixed pair density, we expect  $c$  to decay like an inverse power of the system length  $L$ .

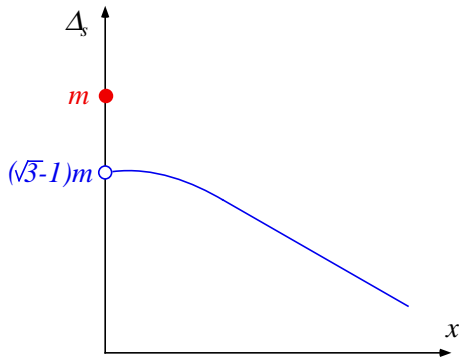


FIG. 13: Spin-gap as a function of doping  $x$ . The spin-gap is discontinuous at  $x = 0$  due to the formation of magnon-Cooper-pair bound states.

For this reason, we expect that a *finite* length  $SO(5)$ -invariant 1D model exhibits a  $\delta(\omega - 2\mu)$  peak in the spin spectral function at momentum  $(\pi, \pi)$  with weight (coefficient) decreasing as some power  $L^{-a}$ . Zhang has suggested<sup>46</sup> that the spin spectral function may have a

corresponding algebraic singularity *in frequency* in an *infinite* system. To address the fate of this finite-size peak in the thermodynamic limit, we consider now an approximate calculation of the *doped* spin-spectral function in the infinite system.

To this end, we must determine the GN operator content of the lattice spin operator. Using the techniques of Sec. IV, it is straightforward to show that the decomposition of  $S_\ell^+(x)$  contains a term

$$S_\ell^+(x) \sim (-1)^{\ell+x}\mathcal{O}_s(x)\psi_{2R}^\dagger + \dots \quad (7.7)$$

Of course, many other operators are also present, but give either negligible or identical contributions to the spectral function in the regime of interest. In the D-Mott phase, the string  $\mathcal{O}_s$  has negligible qualitative effects in correlation functions, since the bosonic fields  $\theta_a$  are all locked (i.e. only weakly fluctuating) around  $\theta_a = 0$  in that case. In the doped system, however, there is an important modification to the  $\theta_1$  field. Since the derivative of this field is just the pair density (Eq. 4.43), its average value has a mean slope  $\langle\theta_1(x)\rangle = -2\kappa_F x$ , where  $\kappa_F = \pi(1-n)/2$  is the Fermi wavevector for the sea of Cooper pairs; recall that  $1-n$  is the concentration of holes in the system. Furthermore, there will be fluctuations of  $\theta_1$  around this mean value, corresponding to the density and phase waves of the Cooper-pair fluid in the C1S0 state.

To account for both these effects, we redefine  $\theta_1(x) \rightarrow -2\kappa_F x + \theta_1(x)$ , treating the shifted (zero mean)  $\theta_1$  field as a free Bose field, as appropriate for a free Fermi or Luttinger-liquid system. The remaining three ( $\theta_2, \theta_3, \theta_4$ ) fields remain locked, and we therefore set these to zero inside the Jordan-Wigner string  $\mathcal{O}_s$ . This gives

$$S_\ell^+(x) \sim e^{i(\pi-\kappa_F)x+i\pi\ell}e^{i\theta_1/2}\psi_{2R}^\dagger. \quad (7.8)$$

As carried out for the undoped case in Sec. V, the spin spectral function can be extracted from the analytically continued Fourier transform of the imaginary time spin-spin correlation function

$$\mathcal{S}_{\ell\ell'}(x, \tau) \equiv \langle S_\ell^-(x, \tau)S_{\ell'}^+(0, 0) \rangle. \quad (7.9)$$

Using Eq. 7.8, one then finds

$$\begin{aligned} \mathcal{S}_{\ell\ell'}(x, \tau) \sim e^{-i(\pi-\kappa_F)x-i\pi(\ell-\ell')} \left\langle e^{-\frac{i}{2}(\theta_1(x, \tau) - \theta_1(0, 0))} \right. \\ \left. \times \psi_{2R}(x, \tau)\psi_{2R}^\dagger(0, 0) \right\rangle. \end{aligned} \quad (7.10)$$

To proceed, we require a calculation of the above expectation value. The simplest natural approximation, which will be our first attempt, is to decouple the charge (1) and spin (2) sectors, calculating the  $\theta_1$  correlator as appropriate for a Luttinger liquid (i.e. from a free Bose theory) and the  $\psi_2$  correlator using the “semiconductor” free-fermion operators. In particular, one finds

$$\left\langle e^{-\frac{i}{2}(\theta_1(x,\tau) - \theta_1(0,0))} \right\rangle \sim (x^2 + \tau^2)^{-K/4}, \quad (7.11)$$

where  $K$  is the Luttinger parameter of the Cooper-pair fluid;  $K = 1$  corresponds to free fermions, as is appropriate for very low dopings. Here we have set the Fermi velocity of the Cooper pair sea to one. The fundamental fermion correlator is approximately

$$\langle \psi_{2R}(x, \tau) \psi_{2R}^\dagger(0, 0) \rangle_{\text{MF}} \sim \int \frac{dp}{2\pi} e^{ipx - \epsilon_1(p)\tau} \Theta(\tau), \quad (7.12)$$

where  $\Theta$  is the Heavyside step function. To simplify Eq. 7.12, we have neglected to include the mean-field “coherence factors”. Because these are non-singular, their neglect only modifies the final result by an overall smooth momentum-dependent amplitude factor. Multiplying the two terms in Eqs. 7.11-7.12, performing the Fourier transform and analytically continuing to real frequencies gives the spin spectral function

$$A_s^{\text{MF}}(\pi - k, \pi; \omega) \sim \text{Im} \int dx dp d\tau \frac{e^{-ipx + (\omega - \epsilon_1(p+k - \kappa_F) + i\delta)\tau}}{(x^2 + \tau^2)^{K/4}} \Theta(\tau), \quad (7.13)$$

where  $\delta = 0^+$  is a positive infinitesimal. Singular behavior can only arise from the large  $x, \tau$  power-law behavior of the denominator. For large  $x$ , the oscillating exponential implies that the integral is dominated by  $p \approx 0$ , so that the dispersion  $\epsilon_1$  can be linearized around this point. Doing so, the  $p$  and  $x$  integrals can be readily performed. Up to an overall constant prefactor, one finds

$$A_s^{\text{MF}}(\pi - k, \pi; \omega) \sim \text{Im} \int_0^\infty d\tau \tau^{-K/2} e^{(\omega - \epsilon_1(k - \kappa_F) + i\delta)\tau}. \quad (7.14)$$

This integral can be related to a Gamma function by analytic continuation. Carrying this out carefully gives the final mean-field result

$$A_s^{\text{MF}}(\pi - k, \pi; \omega) \sim |\omega - \epsilon_1(k - \kappa_F)|^{-1 + \frac{K}{2}} \Theta[\omega - \epsilon_1(k - \kappa_F)]. \quad (7.15)$$

As suggested above, Eq. 7.15 indeed exhibits an algebraic singularity. For momentum  $(\pi, \pi)$ ,  $k = 0$  above, and the Fermi-level condition  $\epsilon_1(\kappa) = 2\mu$  for the Cooper-pair fluid indeed implies the singularity is located at  $\omega = 2\mu$ , identifying it with the putative “Pi resonance”. Note, however, that within this approximation identical “resonances” appear at *all* momenta, including a *lower energy one* at  $k = \kappa_F$ . Moreover, the resonance becomes more singular when the Luttinger parameter  $K$  decreases approaching a delta function as  $K \rightarrow 0$ , whereas the Pi-resonance should approach a delta function in the opposite limit of  $K \rightarrow \infty$  where the Cooper-pair fluid develops off-diagonal long-ranged order. Thus, it is unclear whether the above resonance for the 1d model has any connection with the two-dimensional Pi-resonance.

Moreover, further reflection on the nature of the mean-field approximation used above, leads us to question the validity of the singular behavior at finite frequency. While it might well be correct for the  $O(N = \infty)$  GN model, the fundamental fermions, e.g. Cooper pairs and magnons, are *strongly interacting* for the  $N = 8$  case of interest, as evidenced, e.g. by the  $O(1)$  binding energy for the mass  $\sqrt{3}m$  bound states and the degeneracy of the fundamental fermion and kink excitations in the D-Mott phase. While interactions will not significantly modify the  $\theta_1$  correlator above (since the Cooper-pair fluid remains a Luttinger liquid), they would appear to have a drastic effect upon the  $\psi_2$  Green’s function. In general, this Green’s function describes the propagation of a single massive injected particle into and interacting with a Luttinger liquid. Similar problems have been extensively studied,<sup>54</sup> and one finds that the massive particle will generally *radiate* both energy and momentum into the Luttinger liquid, decaying in the process. From such decay processes, we generally expect a finite lifetime and hence broadening of the algebraic singularity above. For large  $N$ , the interaction and hence the broadening would be small, but we see no reason for this to be the case for  $N = 8$ . Furthermore, one might naively expect that the minimum energy singularity at  $k = \kappa_F$  would survive, since it is at the bottom of the  $\psi_2$  band and thus naively has no states to decay to. The mean-field approximation, however, misses the existence of bound states, including the Cooper pair-magnon bound state which lies below the band minima at very low doping. In general, we expect that even the  $k = \kappa_F$  fundamental fermion can decay into this bound state (radiating excitations in the Luttinger liquid) in the interacting system, washing out the algebraic singularity even here.

In summary, the above argument suggests that above threshold the spin-spectral function at finite doping will be smooth as a function of energy, with no singularities. Since this conclusion is based on a number of physical arguments and approximations, we cannot rule out the possibility of some high-energy singular structure. Certainly singular behavior at  $\omega = 2\mu$  would be a remarkable phenomenon. On a much firmer standing is the spin-gap threshold energy, which is presumably a universal function of doping  $x$  for the Gross-Neveu model. One might hope that the precise functional form for this energy gap is accessible via integrability.

## ACKNOWLEDGMENTS

We are grateful to Anton Andreev, Natan Andrei, David Gross, Victor Gurarie, Charlie Kane, Andreas Ludwig, Chetan Nayak, Joe Polchinski, Hubert Saleur, Doug Scalapino and Shou-Cheng Zhang for illuminating conversations. This work has been supported by the National Science Foundation under grant Nos. PHY94-07194, DMR-9400142 and DMR-9528578.

## APPENDIX A: RG EQUATIONS

For the weakly interacting two-leg ladder with particle-hole symmetry at half-filling there are nine marginal non-chiral four fermion interactions, as discussed in detail in Section II. The leading order renormalization group (RG) flow equations for the corresponding nine interaction strengths are,

$$\dot{b}_{11}^\rho = -(b_{12}^\rho)^2 - \frac{3}{16}(b_{12}^\sigma)^2 + 4(u_{12}^\rho)^2 + \frac{3}{4}(u_{12}^\sigma)^2, \quad (\text{A1})$$

$$\dot{b}_{11}^\sigma = -2b_{12}^\rho b_{12}^\sigma - \frac{1}{2}(b_{12}^\sigma)^2 - (b_{11}^\sigma)^2 - 8u_{12}^\rho u_{12}^\sigma - 2(u_{12}^\sigma)^2, \quad (\text{A2})$$

$$\dot{b}_{12}^\rho = -2b_{11}^\rho b_{12}^\rho - \frac{3}{8}b_{11}^\sigma b_{12}^\sigma + 2b_{12}^\rho f_{12}^\rho + \frac{3}{8}b_{12}^\sigma f_{12}^\sigma + 16u_{12}^\rho u_{11}^\rho, \quad (\text{A3})$$

$$\dot{b}_{12}^\sigma = -2b_{11}^\rho b_{12}^\sigma - 2b_{12}^\rho b_{11}^\sigma - b_{12}^\sigma b_{11}^\sigma + 16u_{11}^\rho u_{12}^\sigma + 2f_{12}^\rho b_{12}^\sigma + 2b_{12}^\rho f_{12}^\sigma - b_{12}^\sigma f_{12}^\sigma, \quad (\text{A4})$$

$$\dot{f}_{12}^\rho = (b_{12}^\rho)^2 + \frac{3}{16}(b_{12}^\sigma)^2 + 16(u_{11}^\rho)^2 + 4(u_{12}^\rho)^2 + \frac{3}{4}(u_{12}^\sigma)^2, \quad (\text{A5})$$

$$\dot{f}_{12}^\sigma = 2b_{12}^\rho b_{12}^\sigma - \frac{1}{2}(b_{12}^\sigma)^2 - (f_{12}^\sigma)^2 + 8u_{12}^\rho u_{12}^\sigma - 2(u_{12}^\sigma)^2, \quad (\text{A6})$$

$$\dot{u}_{11}^\rho = 2b_{12}^\rho u_{12}^\rho + 4f_{12}^\rho u_{11}^\rho + \frac{3}{8}b_{12}^\sigma u_{12}^\sigma, \quad (\text{A7})$$

$$\dot{u}_{12}^\rho = 2b_{11}^\rho u_{12}^\rho - \frac{3}{8}b_{11}^\sigma u_{12}^\sigma + 4b_{12}^\rho u_{11}^\rho + 2f_{12}^\rho u_{12}^\rho + \frac{3}{8}f_{12}^\sigma u_{12}^\sigma, \quad (\text{A8})$$

$$\dot{u}_{12}^\sigma = -2b_{11}^\rho u_{12}^\sigma + 2b_{11}^\sigma u_{12}^\rho - b_{11}^\sigma u_{12}^\sigma + 4b_{12}^\sigma u_{11}^\rho + 2f_{12}^\rho u_{12}^\sigma + 2f_{12}^\sigma u_{12}^\rho - f_{12}^\sigma u_{12}^\sigma. \quad (\text{A9})$$

Here  $\dot{g} \equiv 2\pi v dg/dl$  with  $b = e^{dl}$  the dimensionless recaling length of the RG transformation. The last three flow equations describe the renormalization of momentum non-conserving Umklapp processes.

## APPENDIX B: GAUGE REDUNDANCY

The Bosonized sine-Gordon form for the  $SO(8)$  Gross-Neveu model appears to have a highly degenerate ground state. In terms of the four Boson fields  $\theta_a$ , the semiclassical ground states correspond to spatially uniform values chosen to minimize the potential  $V(\theta) = -g \sum_{a \neq b} \cos(\theta_a) \cos(\theta_b)$ . Solutions include  $\theta_a = 2\pi n_a$  as well as  $\theta = 2\pi n_a + \pi$  for *arbitrary* integers  $n_a$ . But as we shall see, in most situations these multiple solutions actually correspond to the same *physical* state. To see which solutions are physically equivalent, it is necessary to relate the  $\theta_a$  and their dual fields  $\varphi_a$  to the original Boson fields,  $\phi_{P_i\alpha}$ , introduced when the electron fermion

operators were bosonized. Local gauge transformations,  $\phi_{P_i\alpha} \rightarrow \phi_{P_i\alpha} + 2\pi N_{P_i\alpha}(x, \tau)$  for integer  $N_{P_i\alpha}$  leave the electron operators invariant, and so do not change the physical state. Thus, any shift in  $\theta_a$  and  $\varphi_a$  which corresponds to an *integer* shift in  $\phi_{P_i\alpha}/2\pi$  is redundant, and leaves the physical state unchanged.

To establish whether or not two different semiclassical solutions,  $\theta_a$  and  $\theta'_a$ , are actually physically equivalent we proceed as follows. For the given (spatially constant) shift  $\delta\theta_a = (\theta_a - \theta'_a)/2\pi$ , we ask whether it is possible to choose appropriate (spatially constant) shifts  $\delta\varphi_a$  so that the chiral fields  $\phi_{P_i\alpha}/2\pi$  are changed by integers. The choice for  $\delta\varphi_a$  is unconstrained, since the full interacting Hamiltonian is invariant under *arbitrary* spatially constant shifts in the four  $\varphi_a$  fields. If it is possible, then the two semiclassical solutions are physically equivalent. For physically inequivalent states, it will not be possible to choose  $\delta\varphi_a$  to give the required integer shifts.

To implement the above procedure we need an expression relating the bare chiral fields  $\phi_{P_i\alpha}$  to  $\theta_a$  and  $\varphi_a$ . This can be obtained from

$$\begin{aligned} \phi_{P_i\alpha} &= \frac{1}{4}(\varphi_{\rho+} + \alpha\varphi_{\sigma+} - q\alpha\varphi_{\sigma-} - q\varphi_{\rho-}) \\ &+ \frac{1}{4}P(\theta_{\rho+} + \alpha\theta_{\sigma+} - q\alpha\theta_{\sigma-} - q\theta_{\rho-}), \end{aligned} \quad (\text{B1})$$

where  $q = (-1)^i = 1, -1$  for bonding and anti-bonding bands respectively. For the D-Mott phase the relation between  $\theta_a, \varphi_a$  and the fields  $\theta_{\mu\pm}, \varphi_{\mu\pm}$  is given explicitly in Eq. 3.3. In the S-Mott phase, the equivalence of  $\theta_4 = \varphi_{\rho-}$  is modified to be  $\theta_4^S = \varphi_{\rho-} + \pi$ , but this  $\pi$  difference does not effect the *shifts*  $\delta\theta_a$  between *different* semiclassical states. Thus the ground state degeneracies in the D-Mott and S-Mott phases must necessarily be the same. In subsection B.1 below we show that both of these phases have unique ground states. It is necessary to consider the SP and CDW phases separately (in subsection B.2 below), since there is a non-trivial modification in the relation between  $\theta_a, \varphi_a$  and the fields  $\theta_{\mu\pm}, \varphi_{\mu\pm}$ . As we shall show, in these latter two phases the ground state is *two-fold* degenerate - corresponding physically to the spontaneous breaking of a discrete parity symmetry (see Section VI).

### 1. D-Mott and S-Mott phases

In the D-Mott and S-Mott phases, shifts in the fields  $\theta_a$  and  $\varphi_a$  induce shifts in the chiral fields,  $\delta\phi_{P_i\alpha}$ , of the general form

$$\delta\phi_{P_i\alpha} = \frac{1}{4}P(\mathbf{A}_P)_{ab}\delta\theta_b + \frac{1}{4}(\mathbf{A}_P)_{ab}\delta\varphi_b, \quad (\text{B2})$$

where  $a = 1 \uparrow, 1 \downarrow, 2 \uparrow, 2 \downarrow$  labels the band and spin indices and  $b = 1, \dots, 4$  labels the four flavors of the sine-Gordon bosons. Here and below, all shifts will be measured in units of  $2\pi$ , so that for example  $\delta\phi = (\phi - \phi')/2\pi$ .

The matrices  $\mathbf{A}_P$  can be explicitly constructed by using Eqs. B1, 3.3,

$$(\mathbf{A}_P)_{ab} = \begin{pmatrix} 1 & 1 & 1 & P \\ 1 & -1 & -1 & P \\ 1 & 1 & -1 & -P \\ 1 & -1 & 1 & -P \end{pmatrix}. \quad (\text{B3})$$

It will be convenient to separate out the two contributions coming from the shifts in  $\theta_a$  and  $\phi_a$ , respectively, by defining

$$\delta\Theta_{Pa} = P(\mathbf{A}_P)^{ab}\delta\theta_b, \quad \delta\Phi_{Pa} = (\mathbf{A}_P)^{ab}\delta\varphi_b. \quad (\text{B4})$$

Comparing two semiclassical solutions,  $\theta_a$  and  $\theta'_a$ , determines the shifts  $\delta\Theta_{Pa}$ . These two solutions are physically equivalent, provided shifts  $\delta\varphi_a$  can be chosen so that the following eight constraint equations are satisfied,

$$\Theta_{Pa} + \delta\Phi_{Pa} = 4N_{Pa}, \quad (\text{B5})$$

with *integer*  $N_{Pa}$ . In this case, all eight shifts  $\delta\phi_{Pi\alpha}$  are integer, and the electron fields are left unchanged.

Since the four shifts,  $\delta\varphi_a$ , determine *both* right and left vectors,  $\delta\Phi_{Ra}, \delta\Phi_{La}$ , these two vectors are not independent, and similarly for the  $\theta$  shifts. Indeed one can see that,

$$\delta\Phi_{Ra} = \frac{1}{2}(\mathbf{M})_{ab}\delta\Phi_{Lb}, \quad (\text{B6})$$

$$\delta\Theta_{Ra} = -\frac{1}{2}(\mathbf{M})_{ab}\delta\Theta_{Lb}, \quad (\text{B7})$$

with  $\mathbf{M} = 2\mathbf{A}_R\mathbf{A}_L^{-1}$  or,

$$(\mathbf{M})_{ab} = \begin{pmatrix} 1 & -1 & 1 & 1 \\ -1 & 1 & 1 & 1 \\ 1 & 1 & 1 & -1 \\ 1 & 1 & -1 & 1 \end{pmatrix}. \quad (\text{B8})$$

We can now use the eight constraint equations to eliminate  $\delta\Phi$  and arrive at four equations for  $\delta\Theta$ . To this end, upon multiplying by  $\mathbf{M}$  on the left sector of Eq. B5, one obtains  $\delta\Phi_{Ra} - \delta\Theta_{Ra} = 4(\mathbf{M})_{ab}N_{La}$ . Upon combining with the right sector of Eq. B5 one obtains,

$$\delta\Theta_{Ra} = 2N_{Ra} - (\mathbf{M})_{ab}N_{Lb}. \quad (\text{B9})$$

Two semiclassical solutions (which determine  $\delta\Theta_{Ra}$ ) are then physically equivalent provided these four equations have solutions for *integer*  $N_{Pa}$ .

All of the semiclassical solutions take the form  $\theta_a = 2n_a\pi$  or  $\theta_a = (2n_a + 1)\pi$  with arbitrary integers  $n_a$ . It is straightforward to show that for *any* two of these solutions the difference  $\delta\theta_a$  corresponds to  $\delta\Theta_{Ra}$  which are either even integer for all  $a = 1, \dots, 4$  or all odd integers. When they are even integers, Eq. B9 can be solved for integer  $N_{Ra}$  by taking  $N_{La} = 0$ . For odd integer  $\delta\Theta_{Ra}$  a solution with integer  $N_{Ra}$  is also possible by taking, for example,  $N_{La} = \delta_{a1}$ .

We have thereby established the physical equivalence between all of the semiclassical solutions. This implies that the D-Mott and S-Mott ground states are unique.

## 2. SP and CDW phases

In the SP and CDW phases, the relation between  $\theta_a, \varphi_a$  and  $\theta_{\mu\pm}, \varphi_{\mu\pm}$  are changed, so the above conclusions are modified. In particular, one has

$$\theta_3^{SP} = \varphi_{\sigma-}, \quad \varphi_3^{SP} = \theta_{\sigma-}, \quad (\text{B10})$$

in the SP phase and  $\theta_3^{CDW} = \theta_3^{SP} + \pi$ ,  $\varphi_3^{CDW} = \theta_3^{SP}$  in the CDW phase. Because the Boson fields are defined differently, the matrix  $\mathbf{A}_P$  which relates the two sets of fields in Eq. B2 is modified. The appropriate matrix in this case, denoted  $\tilde{\mathbf{A}}_P$ , is given by,

$$(\tilde{\mathbf{A}}_P)_{ab} = \begin{pmatrix} 1 & 1 & P & P \\ 1 & -1 & -P & P \\ 1 & 1 & -P & -P \\ 1 & -1 & P & -P \end{pmatrix}. \quad (\text{B11})$$

Notice that  $\tilde{\mathbf{A}}_R = \mathbf{A}_R$ , although the left matrices differ in the third column. Similarly, the matrix  $\mathbf{M}$  is also modified, becoming

$$(\tilde{\mathbf{M}})_{ab} = \begin{pmatrix} 0 & 0 & 2 & 0 \\ 0 & 0 & 0 & 2 \\ 2 & 0 & 0 & 0 \\ 0 & 2 & 0 & 0 \end{pmatrix}. \quad (\text{B12})$$

Physical equivalence between two semiclassical solutions for the SP or CDW phases is, once again, established by finding a solution of Eq. B9 with integer  $N_{Pi\alpha}$ , except with  $\tilde{\mathbf{M}}$  replacing  $\mathbf{M}$ . As before, the difference between any two of the semiclassical solutions leads to either even integer or odd integer  $\delta\Theta_{Ra}$ . For even integer  $\delta\Theta_{Ra}$  a solution is again possible by taking  $N_{La} = 0$  and choosing appropriate integers for  $N_{Ra}$ . However, a solution in the integers is *not* possible for two semiclassical solutions differing by an odd integer shift vector  $\delta\Theta_{Ra}$  (since  $\tilde{\mathbf{M}}_{ab}N_{Lb}$  is always odd). Two such semiclassical solutions would thus correspond to physically distinct phases.

The fact that the ground state is actually two-fold degenerate can be established as follows. Consider two specific semiclassical solutions,  $\theta_a^1 = 0$  and  $\theta_a^2 = 2\pi\delta_{a1}$ . One can readily show that the shift vector,  $\delta\Theta_a^{12}$ , connecting these two states is an odd integer vector, so that these two states are physically distinct. Next consider an arbitrary third semiclassical solution,  $\theta_a^3$ . If the relative shift vector between the first and third solutions,  $\delta\Theta_a^{13}$  is even then the physical states are equivalent. If, on the other hand,  $\delta\Theta_a^{13}$  is an odd integer, then  $\delta\Theta_a^{23}$  is necessarily even, and the second and third solutions describe the same physical state. It is thus clear that there are only two physically distinct ground states in the SP and CDW phases. As discussed in Section VII this two-fold degeneracy corresponds to a spontaneous breaking of a discrete parity symmetry.



## APPENDIX C: GAMMA MATRICES AND SPINOR REPRESENTATIONS

In this appendix, we discuss some technical details of gamma matrices and spinor representations of  $SO(5)$ . In general, there are two types of representations for  $SO(N)$ . The first are tensors, which transform like products of vectors. Irreducible representations are then found by taking symmetric and anti-symmetric combinations (Young tableaux). However, to describe how (complex) fermions transform under rotations, the second representation, the spinor one, is necessary. It has already been used in constructing invariants in Sec. VI, but here we review the mathematics in somewhat more technical detail, in order to allow the reader to perform concrete calculations if he or she so desires. To explain the spinor representation, let us introduce a set of  $N$  generalized Dirac matrices which obey the Clifford algebra,

$$\{\Gamma^A, \Gamma^B\} = 2\delta_{AB}, \quad (C1)$$

where  $A, B = 1, 2, \dots, N$ . We then construct the  $N(N-1)/2$  generators defined as commutators between all pairs of these Dirac matrices,

$$\Gamma^{AB} = \frac{i}{4}[\Gamma^A, \Gamma^B]. \quad (C2)$$

It is easy to show that these generators satisfy the  $SO(N)$  commutation relations

$$[\Gamma^{AB}, \Gamma^{CD}] = i(\delta_{AD}\Gamma^{BC} - \delta_{AC}\Gamma^{BD} - \delta_{BD}\Gamma^{AC} + \delta_{BC}\Gamma^{AD}). \quad (C3)$$

For  $N = 5$ , we choose a specific set of matrices to represent the  $SO(5)$  group. The minimum dimension of a set of five matrices which satisfy the Clifford algebra is  $4 \times 4$ . Our particular choice is

$$\Gamma^1 = \begin{pmatrix} 0 & i\sigma_y \\ -i\sigma_y & 0 \end{pmatrix} \Gamma^2 = \begin{pmatrix} 0 & \sigma_y \\ \sigma_y & 0 \end{pmatrix} \Gamma^{3,4,5} = \begin{pmatrix} -\sigma & 0 \\ 0 & -\sigma^* \end{pmatrix}. \quad (C4)$$

A useful property of the spinor representation is its ‘‘reality’’. This means that the conjugate representation  $-(\Gamma^{ab})^*$  also obeys the algebra, and is equivalent under a unitary transformation to the original representation. This follows because it is always possible to find a matrix  $R$  which satisfies the properties

$$R^2 = -1, \quad R^{-1} = R^\dagger = -R, \\ R^{-1}\Gamma^{AB}R = -(\Gamma^{AB})^*, \quad R^{-1}\Gamma^A R = (\Gamma^A)^*. \quad (C5)$$

For  $N = 5$  with our particular choice of Dirac matrices in Eq. C4, the matrix  $R$  is simply

$$R = \begin{pmatrix} 0 & \mathbf{1} \\ -\mathbf{1} & 0 \end{pmatrix}, \quad (C6)$$

where  $\mathbf{1}$  is the two by two identity matrix. The matrix  $R$  is useful in constructing irreducible representations of  $SO(5)$ .

As we have seen in Sec. VI, these abstract matrices can be elevated to physical operators by sandwiching them between two *spinors*. The useful details are already given in the text of Sec. VI. Here we provide some reasoning and motivation for the choice of spinor taken there. For convenience, we copy the spinor definition from Eq. 6.7:

$$\Psi(\mathbf{k}) = \begin{pmatrix} a_\alpha(\mathbf{k}) \\ \phi_{\mathbf{k}} a_\alpha^\dagger(-\mathbf{k} + \mathbf{N}) \end{pmatrix}, \quad (C7)$$

where  $\mathbf{N} = (\pi, \pi)$ . Here  $\phi_{\mathbf{k}}$  is a complex function with absolute value one, chosen by Rabello et. al.<sup>53</sup> to have D-wave symmetry in two-dimensions. As discussed in Section VI, this factor plays no role in the case of the two-leg ladder, and can be set to unity. At first blush, the particular choice of spinor appears rather arbitrary. It is not, for several reasons. At half filling, the system is particle-hole symmetric. For every hole excitation at momentum  $\mathbf{k}$  created by  $a(\mathbf{k})$ , there is a particle excitation counterpart at momentum  $\mathbf{k} - \mathbf{N}$  created by  $a^\dagger(\mathbf{k} - \mathbf{N})$ . Parity symmetry implies there is also a particle excitation at the opposite momentum  $-\mathbf{k} + \mathbf{N}$ . Because these excitations occur symmetrically, they are chosen as upper and lower components in the spinor. The use of the parity symmetry is not essential. However, it is rather convenient for later analysis in weak coupling because, by such a construction, all components have the same chirality, i.e. act on the same side of the Fermi surface. Since the four-components spinor  $\Psi(\mathbf{k})$  contains excitations at both  $\mathbf{k}$  and  $-\mathbf{k} + \mathbf{N}$ , the momentum  $\mathbf{k}$  is only allowed to run over half of the Brillouin zone. The halved region in momentum space is also known as the folded Brillouin zone (shown in Fig. 9). Finally, one would like the spinor to obey canonical anti-commutation relations so that it annihilates or creates fermionic excitations. This is the origin of the constraint on  $\phi_{\mathbf{k}}$ : direct calculation verifies that, provided  $|\phi_{\mathbf{k}}|^2 = 1$ , the canonical anti-commutation relation is satisfied,

$$\{\Psi_a(\mathbf{k}), \Psi_b^\dagger(\mathbf{k}')\} = (2\pi)^d \delta_{ab} \delta(\mathbf{k} - \mathbf{k}'). \quad (C8)$$

Further straightforward algebra demonstrates that when the spinor satisfies canonical anti-commutators, the currents in Eqs. 6.14-6.18 satisfy appropriate Kac-Moody algebras. This exercise, which we do not reproduce here, verifies that these currents are indeed  $SO(5)$  scalars, vectors, and tensors, as indicated in Sec. VI.

We conclude this appendix by obtaining expressions which relate the 28  $SO(5)$  currents defined in Sec. VI, to the 28  $SO(8)$  currents,  $G_p^{AB}$ , introduced in Sec. IV. These relations can be determined by bosonizing the  $SO(5)$  currents, rewriting in terms of the GN bosons  $\theta_a$  and  $\varphi_a$  and the Klein factors, refermionizing, and finally changing from Dirac to Majorana fermions. For example,

$$\begin{aligned}\mathcal{J}_P^{21} &= \frac{1}{2\pi} \partial_x \phi_{P\rho+} = \psi_{P\rho+}^\dagger \psi_{P\rho+} \\ &= i\eta_{P2}\eta_{P1} = G_P^{21}.\end{aligned}\quad (\text{C9})$$

The general relations can be conveniently presented in the following form:

$$G_P^{AB} = \begin{bmatrix} \mathbf{T}_P & -\mathbf{V}_P^t \\ \mathbf{V}_P & \mathbf{S}_P \end{bmatrix}_{AB}.\quad (\text{C10})$$

The  $5 \times 5$  anti-symmetric tensor matrix  $\mathbf{T}_P^{AB} = \mathcal{J}_P^{AB}$  for  $A \neq B$  and it is zero for  $A = B$ . The  $3 \times 5$  vector matrix is

$$\mathbf{V}_P^{CB} = \frac{1}{2} \begin{pmatrix} \mathcal{J}_P^B \\ -\text{Im}\mathcal{I}_P^B \\ \text{PRe}\mathcal{I}_P^B \end{pmatrix}_C.\quad (\text{C11})$$

Finally, the  $3 \times 3$  anti-symmetric scalar matrix is

$$\mathbf{S}_P = -\frac{1}{2} \begin{pmatrix} 0 & & \\ \text{Re}\mathcal{I}_P & 0 & \\ \text{PIm}\mathcal{I}_P & \text{P}\mathcal{J}_P & 0 \end{pmatrix}.\quad (\text{C12})$$

#### APPENDIX D: $SO(5)$ CURRENTS IN $SU(2) \times U(1)$ AND $SO(8)$ NOTATION

In Section VI the most general set of  $SO(5)$  invariant interactions for the weak coupling two-leg ladder were expressed as products of right and left moving  $SO(5)$  currents, see Eq. 6.20. Here we re-express these five interactions in terms of charge and spin currents with lower  $U(1) \times SU(2)$  symmetry, which were introduced in Section II. The products of  $SO(5)$  scalar, vector, and tensor currents are re-expressed as

$$\mathcal{J}_R \mathcal{J}_L = (J_{R11} - J_{R22} - 2)(J_{L11} - J_{L22} - 2),\quad (\text{D1})$$

$$\begin{aligned}\mathcal{J}_R^A \mathcal{J}_L^A &= 4(\mathbf{J}_{R11} - \mathbf{J}_{R22})(\mathbf{J}_{L11} - \mathbf{J}_{L22}) \\ &\quad + 2(I_{R12}^\dagger I_{L21} + I_{L21}^\dagger I_{R12}),\end{aligned}\quad (\text{D2})$$

$$\begin{aligned}\mathcal{J}_R^{AB} \mathcal{J}_L^{AB} &= \frac{1}{2}(J_{R11} + J_{R22} - 2)(J_{L11} + J_{L22} - 2) \\ &\quad + 2(\mathbf{J}_{R11} + \mathbf{J}_{R22})(\mathbf{J}_{L11} + \mathbf{J}_{L22}) \\ &\quad - 4(I_{R12}^\dagger \mathbf{I}_{L21} + I_{L21}^\dagger \mathbf{I}_{R12}).\end{aligned}\quad (\text{D3})$$

Notice that these three interactions conserve the number of particles in each band. The remaining two  $SO(5)$  invariant interactions, involving anomalous scalars and vectors, scatter particles from one band to the other. In terms of the  $U(1) \times SU(2)$  charge and spin currents, they are

$$\mathcal{I}_R \mathcal{I}_L + \mathcal{I}_R^\dagger \mathcal{I}_L^\dagger = 4(J_{R21} J_{L21} + J_{R12} J_{L12}),\quad (\text{D4})$$

$$\begin{aligned}\mathcal{I}_R^A \mathcal{I}_L^A + \mathcal{I}_R^{A\dagger} \mathcal{I}_L^{A\dagger} &= 16(\mathbf{J}_{R21} \mathbf{J}_{L21} + \mathbf{J}_{R12} \mathbf{J}_{L12}) \\ &\quad - 2(I_{R11}^\dagger I_{L22} + I_{R22}^\dagger I_{L11}) \\ &\quad + I_{L11}^\dagger I_{R22} + I_{L22}^\dagger I_{R11}.\end{aligned}\quad (\text{D5})$$

For a given set of five  $SO(5)$  invariant interaction parameters, these operator identities enable us to obtain the corresponding values of the nine forward, backward and Umklapp scattering amplitudes;

$$b_{11}^\rho = g_s + \frac{1}{2}g_t, \quad b_{11}^\sigma = -4g_v - 2g_t,\quad (\text{D6})$$

$$b_{12}^\rho = 4h_s, \quad b_{12}^\sigma = -16h_v,\quad (\text{D7})$$

$$f_{12}^\rho = -g_s + \frac{1}{2}g_t, \quad f_{12}^\sigma = 4g_v - 2g_t,\quad (\text{D8})$$

$$u_{11}^\rho = -2h_v, \quad u_{12}^\rho = g_v, \quad u_{12}^\sigma = 2g_t.\quad (\text{D9})$$

From these, and the nine RG flow equations in Appendix A, one can obtain a closed set of five RG flow equations for the five  $SO(5)$  invariant coupling constants, given explicitly in Appendix E.

It is also instructive to re-express the five  $SO(5)$  invariant interactions in terms of the  $SO(8)$  currents - specifically the 28  $SO(8)$  generators  $G^{AB} = i\eta_A \eta_B$ , comprising the vector (fundamental) representation of  $SO(8)$ . For the first three  $SO(5)$  interactions one finds,

$$\mathcal{J}_R \mathcal{J}_L = -4G_R^{78} G_L^{78},\quad (\text{D10})$$

$$\mathcal{J}_R^A \mathcal{J}_L^A = 4 \sum_{A=1}^5 G_R^{A6} G_L^{A6},\quad (\text{D11})$$

$$\mathcal{J}_R^{AB} \mathcal{J}_L^{AB} = \sum_{A,B=1}^5 G_R^{AB} G_L^{AB}.\quad (\text{D12})$$

As expected, these expressions show that  $G^{78}, G^{A6}$  and  $G^{AB}$  (for  $A, B = 1, \dots, 5$ ) transform under  $SO(5)$  rotations as scalar, vector and (rank two) tensor, respectively. The remaining two anomalous  $SO(5)$  invariant interactions can similarly be re-expressed as,

$$\mathcal{I}_R \mathcal{I}_L + \mathcal{I}_R^\dagger \mathcal{I}_L^\dagger = 8(G_R^{67} G_L^{67} + G_R^{68} G_L^{68}),\quad (\text{D13})$$

$$\mathcal{I}_R^A \mathcal{I}_L^A + \mathcal{I}_R^{A\dagger} \mathcal{I}_L^{A\dagger} = -8 \sum_{A=1}^5 (G_R^{A7} G_L^{A7} + G_R^{A8} G_L^{A8}).\quad (\text{D14})$$

It is clear that  $G^{67,68}$  and  $G^{A7,A8}$  transform as  $SO(5)$  scalars and vectors, respectively.

#### APPENDIX E: $SO(5)$ RG EQUATIONS

For the weakly interacting two-leg ladder at half-filling, requiring  $SO(5)$  symmetry reduces the number of marginal four-fermion interactions from nine down to five. Due to symmetry, one expects the RG flow equations to close in the manifold of  $SO(5)$  invariant models. This closure can be demonstrated explicitly by combining the expressions obtained in Appendix D which specify the five dimensional  $SO(5)$  invariant manifold, with the general RG flow equations in Appendix A. When re-expressed in terms of the  $SO(5)$  couplings, the nine RG flow equations are seen to be redundant - only 5 are independent. Thus confined to the  $SO(5)$  invariant manifold, the set of independent RG flow equations can be written,

$$\dot{g}_s = -16h_s^2 - 80h_v^2, \quad (\text{E1})$$

$$\dot{g}_v = 8g_v g_t - 32h_s h_v, \quad (\text{E2})$$

$$\dot{g}_t = 8g_v^2 + 6g_t^2 + 64h_v^2, \quad (\text{E3})$$

$$\dot{h}_s = -4g_s h_s - 20g_v h_v, \quad (\text{E4})$$

$$\dot{h}_v = -4g_v h_s - 4g_s h_v + 8g_t h_v. \quad (\text{E5})$$

<sup>1</sup> J. Bednorz and K. Muller, Z. Phys. B **64**, 188 (1986).

<sup>2</sup> P. Anderson, Science **235**, 1196 (1987).

<sup>3</sup> E. Dagotto, J. Riera, and D. Scalapino, Phys. Rev. B **45**, 5744 (1992).

<sup>4</sup> T. M. Rice, S. Gopalan, and M. Sigrist, Europhys. Lett. **23**, 445 (1993).

<sup>5</sup> In one dimension, strong quantum fluctuations prohibit true long-range order. Nevertheless, many 1d Mott insulators, including e.g. the half-filled 1d Hubbard model, develop instead power-law magnetic correlations and still maintain low-energy magnon modes. Such systems are thus close counterparts of higher-dimensional systems with broken spin-rotational invariance.

<sup>6</sup> B. Levi, Phys. Today **49**, 17 (1996).

<sup>7</sup> B. Batlogg and V. Emery, Nature **382**, 20 (1996).

<sup>8</sup> N. Ong, Science **273**, 321 (1996).

<sup>9</sup> H. Schulz, T. Ziman, and D. Poilblanc, in *Magnetic Systems with Competing Interactions*, edited by H. Diep (World Scientific Publishing, Singapore, 1994).

<sup>10</sup> For a review, see E. Dagotto and T. Rice, Science **271**, 618 (1996); and references therein.

<sup>11</sup> H. J. Schulz, Phys. Rev. B **34**, 6372 (1986).

<sup>12</sup> S. White, R. Noack, and D. Scalapino, Phys. Rev. Lett. **73**, 886 (1994).

<sup>13</sup> R. Noack, S. White, and D. Scalapino, Phys. Rev. Lett. **73**, 882 (1994).

<sup>14</sup> R. Noack, S. White, and D. Scalapino, Europhys. Lett. **30**, 163 (1995).

<sup>15</sup> C. Hayward and D. Poilblanc, Phys. Rev. B **53**, 11721 (1996).

<sup>16</sup> K. Sano, J. Phys. Society of Japan **65**, 1146 (1996).

<sup>17</sup> M. Troyer, H. Tsunetsugu, and T. Rice, Phys. Rev. B **53**, 251 (1996).

<sup>18</sup> L. Balents and M. P. A. Fisher, Phys. Rev. B **53**, 12133 (1996).

<sup>19</sup> H. H. Lin, L. Balents, and M. P. A. Fisher, Phys. Rev. B **56**, 6569 (1997).

<sup>20</sup> M. Fabrizio, Phys. Rev. B **48**, 15838 (1993).

<sup>21</sup> H. J. Schulz, Phys. Rev. B **53**, R2959 (1996).

<sup>22</sup> H. J. Schulz, Phys. Rev. Lett. **77**, 2790 (1996).

<sup>23</sup> N. Nagaosa, Solid State Comm. **94**, 495 (1995).

<sup>24</sup> A. Finkel'stein and A. Larkin, Phys. Rev. B **47**, 10461 (1993).

<sup>25</sup> K. Kuroki and H. Aoki, Phys. Rev. Lett. **72**, 2947 (1994).

<sup>26</sup> M. Azuma, Z. Hiroi, M. Takano, K. Ishida and Y. Kitaoka, Phys. Rev. Lett. **73**, 3463 (1994).

<sup>27</sup> K. Ishida, Y. Kitaoka, K. Asayama, M. Azuma, Z. Hiroi and M. Takano, J. Phys. Soc. Jpn **63**, 3222 (1994).

<sup>28</sup> K. Kojima, A. Keren, G. M. Luke, B. Nachumi, W. D. Wu, Y. J. Uemure, M. Azuma, and M. Takano, Phys. Rev. Lett. **74**, 2812 (1995).

<sup>29</sup> M. Uehara, T. Nagata, J. Akimitsu, H. Takahashi, N. Mori and K. Kinoshita, J. Phys. Soc. Jpn **65**, 2764 (1996).

<sup>30</sup> M. Isobe, J. Q. Li, Y. Matsui, T. Ohta, M. Onoda, F. Izumi, S. Nakano, T. Matsumoto, H. Hayakawa, E. Takayama-Muromachi, Physica C **282**, 811 (1997).

<sup>31</sup> T. Ebbesen, Phys. Today **49**, 26 (1996).

<sup>32</sup> L. Balents and M. P. A. Fisher, Phys. Rev. B **55**, 11973 (1997).

<sup>33</sup> Y. Krotov, D. H. Lee, and G. Louie, Phys. Rev. Lett. **78**, 4245 (1997).

<sup>34</sup> H. H. Lin, cond-mat/9709166 (unpublished).

<sup>35</sup> V. Emery, in *Highly conducting one-dimensional solids*, edited by J. Devreese, R. Evrard, and V. Van Doren (Plenum Press, New York, 1979), p. 247.

<sup>36</sup> D. Gross and A. Neveu, Phys. Rev. D **10**, 3235 (1974).

<sup>37</sup> A. Zamolodchikov and A. Zamolodchikov, Annals Phys. **120**, 253 (1979).

<sup>38</sup> R. Shankar and E. Witten, Nucl. Phys. B **141**, 349 (1978).

<sup>39</sup> M. Karowski and H. Thun, Nucl. Phys. B **190**, 61 (1981).

<sup>40</sup> R. Dashen, B. Hasslacher, and A. Neveu, Phys. Rev. D **12**, 2443 (1975).

<sup>41</sup> S. C. Zhang, Science **275**, 1089 (1997).

<sup>42</sup> R. Shankar, Phys. Lett. **92B**, 333 (1980).

<sup>43</sup> R. Shankar, Phys. Rev. Lett. **46**, 379 (1981).

<sup>44</sup> D. Scalapino, S. C. Zhang, and W. Hanke, cond-mat/9711117 (unpublished).

<sup>45</sup> D. Scalapino and S. White, private communication.

<sup>46</sup> S.-C. Zhang, private communication.

<sup>47</sup> R. Shankar, Acta Phys. Polonica B **26**, 1835 (1995).

<sup>48</sup> T. Giamarchi, Physica B **230-232**, 975 (1997).

<sup>49</sup> K. Damle and S. Sachdev, cond-mat/9711014 (unpublished).

<sup>50</sup> D. Shelton and D. Senechal, cond-mat/9710251 (unpublished).

<sup>51</sup> E. Arrigoni and W. Hanke, preprint (unpublished).

<sup>52</sup> C. Henley, cond-mat/9707275 (unpublished).

<sup>53</sup> S. Rabello, H. Kohno, E. Demler, and S. C. Zhang, cond-mat/9707027 (unpublished).

<sup>54</sup> See, e.g. A. H. C. Neto and M. P. A. Fisher, Phys. Rev. B **53**, 9713 (1996); and references therein.